Published for SISSA by Springer

Received: May 17, 2018
Revised: November 11, 2018
Accepted: November 18, 2018
Published: November 29, 2018

Anatomy of $b \to c\,\tau\,\nu$ anomalies

Aleksandr Azatov,[a,d] **Debjyoti Bardhan,**[b] **Diptimoy Ghosh,**[c,d] **Francesco Sgarlata**[a,d] **and Elena Venturini**[a,d]

[a] *SISSA International School for Advanced Studies, Via Bonomea 265, 34136, Trieste, Italy*
[b] *Department of Physics, Ben-Gurion University, Beer-Sheva 8410501, Israel*
[c] *International Centre for Theoretical Physics, Strada Costiera 11, 34014 Trieste, Italy*
[d] *INFN Trieste, Via Bonomea 265, 34136, Trieste, Italy*

E-mail: aleksandr.azatov@sissa.it, bardhan@post.bgu.ac.il, dghosh@ictp.it, francesco.sgarlata@sissa.it, eventuri@sissa.it

Abstract: In recent times, one of the strongest hints of Physics Beyond the Standard Model (BSM) has been the anomaly in the ratios R_D and R_{D^*} measured in the charged current decays of B-mesons. In this work, we perform a comprehensive analysis of these decay modes, first in a model independent way and subsequently, in the context of composite Higgs models. We discuss in depth as to how linearly realised $\mathrm{SU(2)_L} \times \mathrm{U(1)_Y}$ symmetry imposes severe constraint on the various scenarios because of correlations with other $\Delta F = 1$ processes and $Z\,\tau\,\tau$ and $Z\,\nu\,\nu$ couplings. In the composite Higgs paradigm with partial compositeness, we show that, irrespective of the flavour structure of the composite sector, constraints from $\Delta F = 2$ processes bring the compositeness scale down to $\sim 650\,\mathrm{GeV}$ which is in tension with electroweak precision observables. In the presence of composite leptoquarks, the situation improves only marginally (a factor of $\sqrt{2}$ in the compositeness scale), thus making the new states soon discoverable by direct searches at the LHC. We also comment on the possible explanation of the R_{K,K^*} anomalies within the composite Higgs framework.

Keywords: Beyond Standard Model, Heavy Quark Physics, Technicolor and Composite Models

ArXiv ePrint: 1805.03209

https://doi.org/10.1007/JHEP11(2018)187

JHEP11(2018)187

Contents

1 Introduction 1

2 Operators for $b \to c\,\ell\,\nu$ decay 2

3 Explaining R_D and R_{D^*} 4
- 3.1 Vector and axial-vector operators 4
- 3.2 Scalar and pseudo-scalar operators 4
- 3.3 Tensor operators 6
- 3.4 Combination of tensor, scalar and pseudo-scalar operators 7
- 3.5 Distinguishing the various explanations 8

4 Linearly realised $\mathbf{SU(2)_L \times U(1)_Y}$ gauge invariance 8
- 4.1 List of operators 9
- 4.2 Correspondence with section 2 10
- 4.3 Correlations 13

5 Going beyond the dimension-6 analysis: partial compositeness 17
- 5.1 Two-site Lagrangian 18
  - 5.1.1 Fermion masses 18
  - 5.1.2 Vector fields 20
- 5.2 R_{D,D^*} from the composite electroweak resonances 21
- 5.3 Leptoquark contribution 24

6 R_{K,K^*} anomalies 26

7 Summary and outlook 28

A Decay width of the B_c meson 29

B Form factors for $B_c \to J/\psi$ and $B_c \to \eta_c$ decay processes 31
- B.1 Vector and axial-vector form-factors 31
  - B.1.1 $B_c \to \eta_c$ 31
  - B.1.2 $B_c \to J/\psi$ 32
- B.2 Tensor form-factors 32
  - B.2.1 $B_c \to \eta_c$ 32
  - B.2.2 $B_c \to J/\psi$ 34

C Formulae for calculating branching ratios 35
- C.1 Analytic formulas for $B \to D$ decay 36
- C.2 Semi-numerical formulas for R_D 37
- C.3 Analytic formulas for $B \to D^*$ decay 37
- C.4 Semi-numerical formulas for R_{D^*} 39
- C.5 Semi-numerical formulas for R_{η_c} 39
- C.6 Semi-numerical formulas for $R_{J/\psi}$ 40
- C.7 Combination of vector and scalar operators 40

JHEP11(2018)187

D From the gauge to the mass eigenstates 41

E Mixing of $[C_{lq}^{(3,1)}]'$ and $[C_{\phi l}^{(3,1)}]'$ 44

F Constraints from Z interactions with fermions 45

1 Introduction

The Standard Model (SM) of particle physics has been remarkably successful in explaining almost all the measurements made till date in accelerator-based experiments, ranging from a few GeV in centre-of-mass energy to a few hundred GeV. However, deviations from the SM expectations approximately at the $2\sigma - 4\sigma$ level have shown up in a number of recent measurements involving semi-leptonic B-meson decays, both in charged current and neutral current channels.

In this work, we focus mainly on the analysis of the charged current anomalies,[1] namely R_D and R_{D^*} defined in the following way

$$R_{D^{(*)}} = \frac{\mathcal{B}\left(B \to D^{(*)}\,\tau\,\nu\right)}{\mathcal{B}\left(B \to D^{(*)}\,\ell_0\,\nu\right)}\,, \tag{1.1}$$

where the ℓ_0 stands for either e or μ. The experimental results as well as the SM predictions for R_D and R_{D^*} are summarised in table 1. We also show two other relevant recent measurements, which are however rather imprecise at the moment — the τ polarisation, $P_\tau(D^*)$, in the decay $B \to D^{(*)}\,\tau\,\nu$, and $R_{J/\psi}$, a ratio similar to eq. (1.1) for the decay $B_c \to J/\psi\,\tau\,\nu$. It can be seen from table 1 that a successful explanation of the R_{D,D^*} anomalies requires a new physics (NP) contribution of the order of at least 10 - 20% of the SM contribution to the branching ratio. As the SM contribution is generated at the tree level by $W^\pm$ boson exchange, this is a rather large effect. Such a large effect puts any NP explanation under strong pressure arising from experimental measurements of other $\Delta F = 1$ and $\Delta F = 2$ processes, electroweak precision observables and direct searches at the LHC.

In the first part of this work (sections 2–4), we provide a comprehensive analysis of the possible explanations of these anomalies in as model independent way as possible. We discuss the various implications of (linearly realised) $\mathrm{SU}(2) \times \mathrm{U}(1)$ symmetry. In particular, we focus on the correlations among the observables which could be used in the future to decipher the physics behind these anomalies.

Some of the results which are presented in this part already exist in the literature in some form or another. While we try to perform the analysis in a comprehensive and systematic way, and present our results within a unified language, we will explicitly point out to the existing literature wherever appropriate.

[1] While the statistical significance of these experimental results is not yet large enough to claim a discovery, we will call them 'anomalies' by common usage of the word.

JHEP11(2018)187

Observable	SM prediction	Measurement
R_D	0.300 ± 0.008 [1] 0.299 ± 0.011 [2] 0.299 ± 0.003 [4]	0.407 ± 0.046 [3]
R_{D^*}	0.252 ± 0.003 [5] 0.260 ± 0.008 [6]	0.304 ± 0.015 [3]
$P_\tau(D^*)$	-0.47 ± 0.04 [6]	$-0.38 \pm 0.51(\text{stat.})\,^{+0.21}_{-0.16}(\text{syst.})$ [7, 8]
$R_{J/\psi}$	0.290	0.71 ± 0.25 [9]

Table 1. Observables, their SM predictions and the experimentally measured values. The experimental averages for R_D and R_{D^*} shown in the third column are based on [7, 10–15]. The SM prediction of $R_{J/\psi}$ is based on the form-factors given in [16], see appendix B for more details. As the $B_c \to J/\psi$ form-factors are not very reliably known, we do not show any uncertainty for $R_{J/\psi}$. However, it is expected to be similar to that of R_{D^*}.

In the second part of the paper (section 5), we apply these results to composite Higgs models with partial compositeness. An explanation of the flavour anomalies within this framework has received a lot of attention in the recent past [17–28]. However, this scenario, motivated by the Higgs mass naturalness problem, generically predicts flavour violating effects which are often too large to be compatible with experimetal measurements. This can be partially cured by introducing additional flavour symmetries suppressing the undesirable flavour violating effects [17, 20, 24]. In this work, instead of explicitly relying on flavour symmetries, we take an agnostic approach and rely only on the correlations among the various flavour violating observables coming from partial compositness. Interestingly, even without making any assumption on the flavour structure of the composite sector, we are able to find strong correlations between $\Delta F = 1$ and $\Delta F = 2$ observables leading to an upper bound on the scale of compositeness.

2 Operators for $b \to c\,\ell\,\nu$ decay

The relevant Lagrangian for the quark level process $b \to c\,\ell\,\nu$ can be written as,

$$\mathcal{L}_{\text{eff}}^{b\to c\,\ell\,\nu} = \mathcal{L}_{\text{eff}}^{b\to c\,\ell\,\nu}|_{\text{SM}} - \sum \frac{g_i^{cb\ell\nu}}{\Lambda^2}\mathcal{O}_i^{cb\ell\nu} + \text{h.c.} + \ldots \quad (\ell = \tau, \mu, \text{e}) \tag{2.1}$$

where the ellipses refer to terms which are suppressed by additional factors of $(\frac{\partial}{\Lambda})^2$. As $(\frac{\partial}{\Lambda})^2 \sim (\frac{M_B}{\Lambda})^2$ for the processes we are interested in, these ellipses are completely negligible for new physics (NP) scales heavier than the weak scale. Here,

$$\mathcal{L}_{\text{eff}}^{b\to c\,\ell\,\nu}|_{\text{SM}} = -\frac{2G_F V_{cb}}{\sqrt{2}}\left(\mathcal{O}_{\text{VL}}^{cb\ell\nu} - \mathcal{O}_{\text{AL}}^{cb\ell\nu}\right), \tag{2.2}$$

JHEP11(2018)187

and the definition of the operators are

$$\begin{aligned}
\mathcal{O}_{\rm VL}^{cb\ell\nu} &= [\bar{c}\,\gamma^\mu\, b][\bar{\ell}\,\gamma_\mu\, P_L\,\nu] & \mathcal{O}_{\rm VR}^{cb\ell\nu} &= [\bar{c}\,\gamma^\mu\, b][\bar{\ell}\,\gamma_\mu\, P_R\,\nu] \\
\mathcal{O}_{\rm AL}^{cb\ell\nu} &= [\bar{c}\,\gamma^\mu\,\gamma_5\, b][\bar{\ell}\,\gamma_\mu\, P_L\,\nu] & \mathcal{O}_{\rm AR}^{cb\ell\nu} &= [\bar{c}\,\gamma^\mu\,\gamma_5\, b][\bar{\ell}\,\gamma_\mu\, P_R\,\nu] \\
\mathcal{O}_{\rm SL}^{cb\ell\nu} &= [\bar{c}\, b][\bar{\ell}\, P_L\,\nu] & \mathcal{O}_{\rm SR}^{cb\ell\nu} &= [\bar{c}\, b][\bar{\ell}\, P_R\,\nu] \\
\mathcal{O}_{\rm PL}^{cb\ell\nu} &= [\bar{c}\,\gamma_5\, b][[\bar{\ell}\, P_L\,\nu] & \mathcal{O}_{\rm PR}^{cb\ell\nu} &= [\bar{c}\,\gamma_5\, b][[\bar{\ell}\, P_R\,\nu] \\
\mathcal{O}_{\rm TL}^{cb\ell\nu} &= [\bar{c}\,\sigma^{\mu\nu}\, b][\bar{\ell}\,\sigma_{\mu\nu}\, P_L\,\nu] & \mathcal{O}_{\rm TR}^{cb\ell\nu} &= [\bar{c}\,\sigma^{\mu\nu}\, b][\bar{\ell}\,\sigma_{\mu\nu}\, P_R\,\nu]\,.
\end{aligned} \tag{2.3}$$

Note that the operators in the right hand side of eq. (2.3) (referred to as right-chiral operators below) involve right-chiral neutrinos. In this work, we assume that light right-chiral neutrinos do not exist in nature.[2] Moreover, even in their presence, the operators involving them do not interfere with those involving left-chiral neutrinos (and hence not to the SM operators). This means, by naive power counting, that in order to explain the experimental data by the right-chiral operators, the required NP scale of these operators have to be lower than that for the left-chiral operators.

For notational convenience, we will normalise the new WCs by

$$\frac{2G_F V_{cb}}{\sqrt{2}} = \frac{1}{\Lambda_{\rm SM}^2} \approx \frac{1}{(1.2\,\text{TeV})^2}\,. \tag{2.4}$$

Thus, we have

$$\begin{aligned}
\mathcal{L}_{\rm eff}^{b\to c\,\ell\,\nu} &= \mathcal{L}_{\rm eff}^{b\to c\,\ell\,\nu}|_{\rm SM} - \sum \frac{g_i^{cb\ell\nu}}{\Lambda^2}\mathcal{O}_i^{cb\ell\nu} + \text{h.c.} \\
&= -\frac{2G_F V_{cb}}{\sqrt{2}} \sum C_i^{cb\ell\nu}\mathcal{O}_i^{cb\ell\nu} + \text{h.c.}
\end{aligned} \tag{2.5}$$

where,

$$\frac{g_{\rm VL}^{cb\ell\nu}}{\Lambda^2} = \frac{2G_F V_{cb}}{\sqrt{2}}(C_{\rm VL}^{cb\ell\nu} - 1), \quad \frac{g_{\rm AL}^{cb\ell\nu}}{\Lambda^2} = \frac{2G_F V_{cb}}{\sqrt{2}}(C_{\rm AL}^{cb\ell\nu} + 1), \quad \frac{g_{\rm SL,PL,TL}^{cb\ell\nu}}{\Lambda^2} = \frac{2G_F V_{cb}}{\sqrt{2}} C_{\rm SL,PL,TL}^{cb\ell\nu}.$$

In the SM, $C_{\rm VL}^{cb\ell\nu} = 1, C_{\rm AL}^{cb\ell\nu} = -1$.

Although there are five operators with left-chiral neutrinos, not all of them contribute to both R_D and R_{D^*}. This is because the following matrix elements vanish identically:

$$\langle D(p_D, M_D)|\bar{c}\gamma^\mu\gamma_5 b|B(p_B, M_B)\rangle = 0\,, \tag{2.6}$$

$$\langle D(p_D, M_D)|\bar{c}\gamma_5 b|B(p_B, M_B)\rangle = 0\,, \tag{2.7}$$

$$\langle D^*(p_{D^*}, M_{D^*}, \epsilon_{D^*})|\bar{c}b|B(p_B, M_B)\rangle = 0\,. \tag{2.8}$$

Thus, the operators $\mathcal{O}_{\rm AL}^{cb\ell\nu}$ and $\mathcal{O}_{\rm PL}^{cb\ell\nu}$ do not contribute to R_D, and similarly, the operator $\mathcal{O}_{\rm SL}^{cb\ell\nu}$ does not contribute to R_{D^*}.

In appendix C, we provide approximate semi-numerical formulas for R_D and R_{D^*} in terms of the Wilson coefficients.

[2] See [29, 30] for some recent proposals where the anomalies are explained by operators with right-handed neutrinos.

JHEP11(2018)187

3 Explaining R_D and R_{D^*}

In this section, we systematically study the possible role of various dimension-6 operators in explaining the R_D and R_{D^*} anomalies. As mentioned before, some of the results that will be shown in this section are not new, and already exist in the literature in some form or another [31–42]. Our aim would be to offer a coherent picture to the readers and add some important insights and aspects to the discussion.

For the calculation of R_D we have used the vector and scalar form factors from [2, 43] and tensor form factors from [44, 45]. As lattice QCD results at nonzero recoil are not yet available for $B \to D^*$, we have used the HQET form factors parametrized by [46] with the following numerical values of the relevant parameters [47, 48]

$$\begin{aligned} &R_1(1) = 1.406 \pm 0.033,\ R_2(1) = 0.853 \pm 0.020,\ \rho^2_{D^*} = 1.207 \pm 0.026 \\ &h_{A_1}(1) = 0.906 \pm 0.013\,. \end{aligned} \tag{3.1}$$

In view of the absence of lattice calculations, to be conservative, we use two times larger uncertainties than those quoted above.

For state-of-the-art $B \to D^*$ form-factors we refer the readers to [49] (see also [50]). It should be noted that, since we have not used the state-of-the-art form-factors, our results for the allowed values of the Wilson Coefficients are correct only up to sub-leading terms in $\Lambda/m_{b,c}$.

3.1 Vector and axial-vector operators

Here we consider only the operators $\mathcal{O}^\tau_{\rm VL}$ and $\mathcal{O}^\tau_{\rm AL}$, and investigate whether they are capable of explaining R_D and R_{D^*} anomalies simultaneously. We also comment on the compatibility with the recent measurement of $R_{J/\psi}$.

In figure 1, we show the regions in the $C^\tau_{\rm VL}$-$C^\tau_{\rm AL}$ plane that satisfy the experimental data on R_D, R_{D^*} and $R_{J/\psi}$ within 1σ. Note that the uncertainties in the form-factors have been carefully taken into account in obtaining the various allowed regions. However, the semi-numerical formulas given in the previous section can be used to qualitatively understand the results. It can be seen that there is an overlap region (the overlap between the red and green bands) that successfully explains both R_D and R_{D^*}. This overlap region is outside the 1σ experimental measurement of $R_{J/\psi}$, but consistent with $R_{J/\psi}$ at $\approx 1.5\,\sigma$.

It is interesting that $C^\tau_{\rm VL} = -C^\tau_{\rm AL} \approx 1.1$ falls in the overlap region mentioned above. As we will see in the next section, the relation $C^\tau_{\rm VL} = -C^\tau_{\rm AL}$ is expected if $\mathrm{SU(2)_L} \times \mathrm{U(1)_Y}$ gauge invariance in linearly realised at the dimension-6 level. Note that the vector and axial-vector operators do not have anomalous dimensions if only QCD interactions are considered (see, for example, appendix-E of [51] and also [52]). Hence, we take $C^\tau_{\rm VL,AL}(\Lambda) = C^\tau_{\rm VL,AL}(m_b)$.

3.2 Scalar and pseudo-scalar operators

Here we consider the scalar and pseudo-scalar operators, $\mathcal{O}^\tau_{\rm SL}$ and $\mathcal{O}^\tau_{\rm PL}$ respectively. In the left panel of figure 2, we show the parameter space that satisfies the individual experimental

JHEP11(2018)187

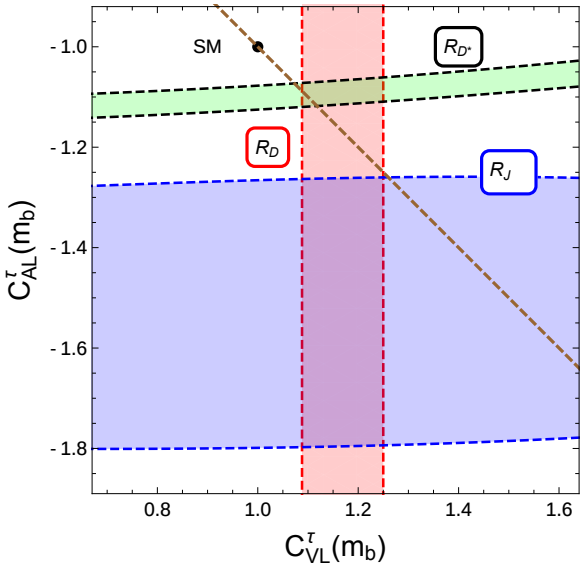

Figure 1. The vertical red band corresponds to the values of $C^\tau_{\rm VL}$ that satisfy the experimental measurement of R_D within 1σ. Similarly, the green (blue) region corresponds to the values of $C^\tau_{\rm VL}$ and $C^\tau_{\rm AL}$ that satisfy the experimental measurement of R_{D^*} ($R_{J/\psi}$) within 1σ. All the WCs are defines at the m_b scale. The oblique dashed line is the locus of the equation $C^\tau_{\rm VL} = -C^\tau_{\rm AL}$.

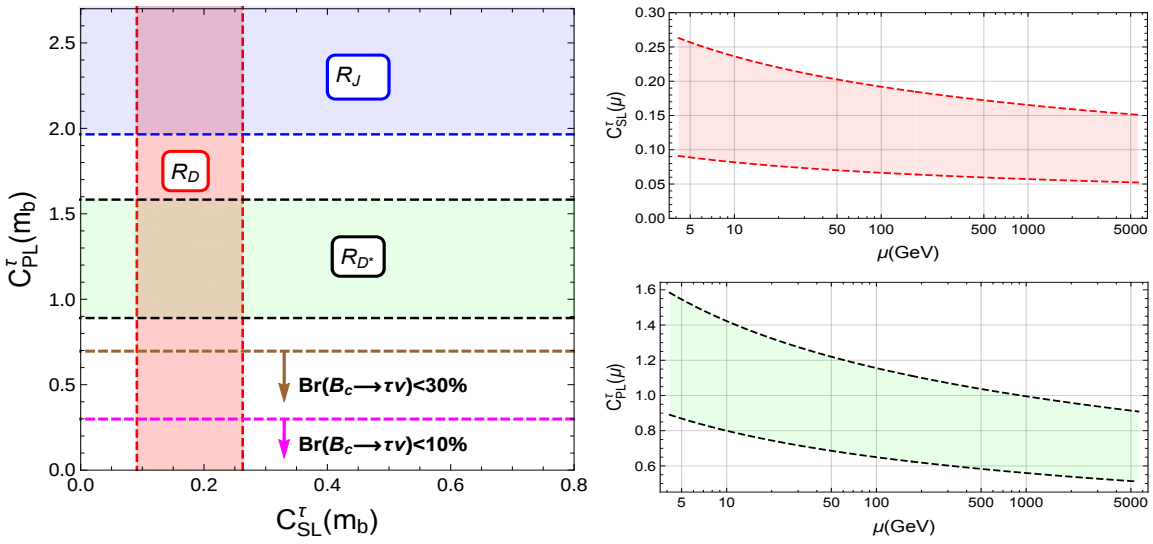

Figure 2. *Left panel*: the red and green (blue) bands correspond to the values of $C^\tau_{\rm SL}$ and $C^\tau_{\rm PL}$ that satisfy the experimental measurement of R_D and R_{D^*} ($R_{J/\psi}$) within 1σ respectively. The values of $C^\tau_{\rm PL}$ that correspond to ${\rm Br}(B_c \to \tau\nu) < 30\%$ and $< 10\%$ are also shown. *Right panel*: renormalisation group running of the WCs $C^\tau_{\rm SL}$ and $C^\tau_{\rm PL}$.

data on R_D, R_{D^*} and $R_{J/\psi}$ within 1σ. As discussed before, while the operator $\mathcal{O}^\tau_{\rm SL}$ contributes to R_D only, the operator $\mathcal{O}^\tau_{\rm PL}$ contributes only to R_{D^*}. This explains the vertical and horizontal nature of the allowed regions for R_D and R_{D^*} respectively.

JHEP11(2018)187

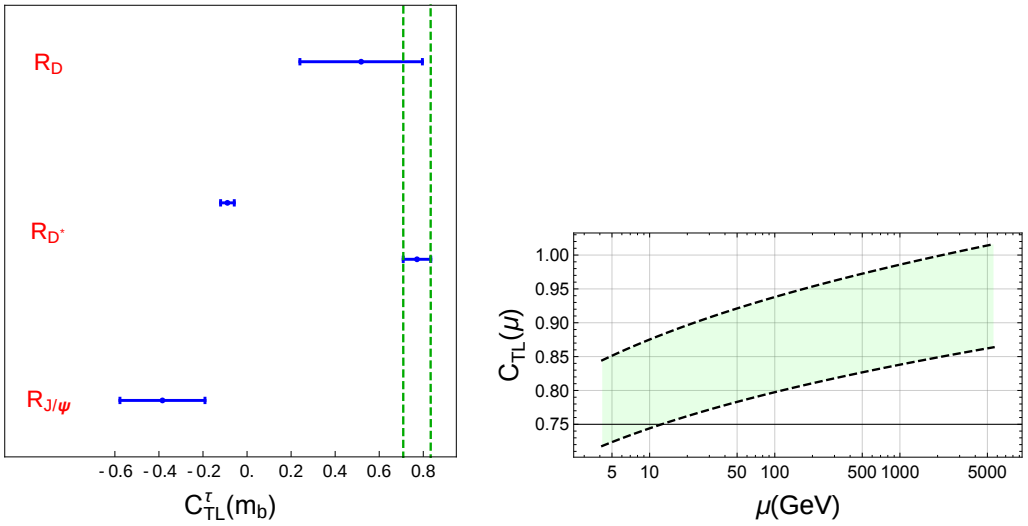

Figure 3. *Left panel*: the horizontal lines correspond to the values of $C^{\tau}_{\rm TL}$ that satisfy the experimental measurement of R_D, R_{D^*} and $R_{J/\psi}$ within 1σ. The green band corresponds to values of $C^{\tau}_{\rm TL}$ that explains R_D and R_{D^*} simultaneously. *Right panel*: renormalisation group running of $C^{\tau}_{\rm TL}$.

Note that the operator $\mathcal{O}^{\tau}_{\rm PL}$ directly contributes to the decay $B_c \to \tau\nu$ also (refer to appendix A for more details). The regions below the two horizontal dashed lines correspond to $\mathrm{Br}(B_c \to \tau\nu) < 30\%$ and $< 10\%$, which were claimed to be the indirect experimental upper bounds by the authors of [53] and [54] respectively. Thus, an explanation of R_{D^*} by the operator $\mathcal{O}^{\tau}_{\rm PL}$ is in serious tension with the upper bound on $\mathrm{Br}(B_c \to \tau\nu)$.

The right panel of figure 2 shows the renormalisation group (RG) running (considering only QCD interactions) of the WCs $C^{\tau}_{\rm SL}$ and $C^{\tau}_{\rm PL}$ from the m_b scale to 5 TeV using the following equation [51],

$$C(m_b) = \left[\frac{\alpha_s(m_t)}{\alpha_s(m_b)}\right]^{\frac{\gamma}{2\beta_0^{(5)}}} \left[\frac{\alpha_s(\Lambda)}{\alpha_s(m_t)}\right]^{\frac{\gamma}{2\beta_0^{(6)}}} C(\Lambda)\,, \tag{3.2}$$

where, $\gamma = -8$. The values at the m_b scale are taken from the allowed bands in the left panel.

3.3 Tensor operators

We now turn to the discussion of the tensor operator. In figure 3, we show the allowed values of $C^{\tau}_{\rm TL}$ that are consistent with the 1σ experimental measurements of R_D, R_{D^*} and $R_{J/\psi}$. The values enclosed by the green vertical dashed lines correspond to simultaneous explanation of R_D and R_{D^*} anomalies. Note however that the prediction for $R_{J/\psi}$ in this $C^{\tau}_{\rm TL}$ region is $\approx 0.17 - 0.23$, which is below the SM prediction and quite far from the current experimental central value. The RG running of $C^{\tau}_{\rm TL}$ is shown in the right panel of figure 3 (using eq. (3.2) with $\gamma = 8/3$ [51]) where the initial values of $C^{\tau}_{\rm TL}$ at the m_b scale correspond to the range enclosed by the two vertical dashed lines in the left panel.

Note that the tensor operator does not contribute to the decay $B_c \to \tau\nu$ because the matrix element $\langle 0|\bar{c}\,\sigma^{\mu\nu}\,b|\bar{B}_c\rangle$ identically vanishes. Hence, there is no constraint on $C^{\tau}_{\rm TL}$ from the process $B_c \to \tau\nu$.

JHEP11(2018)187

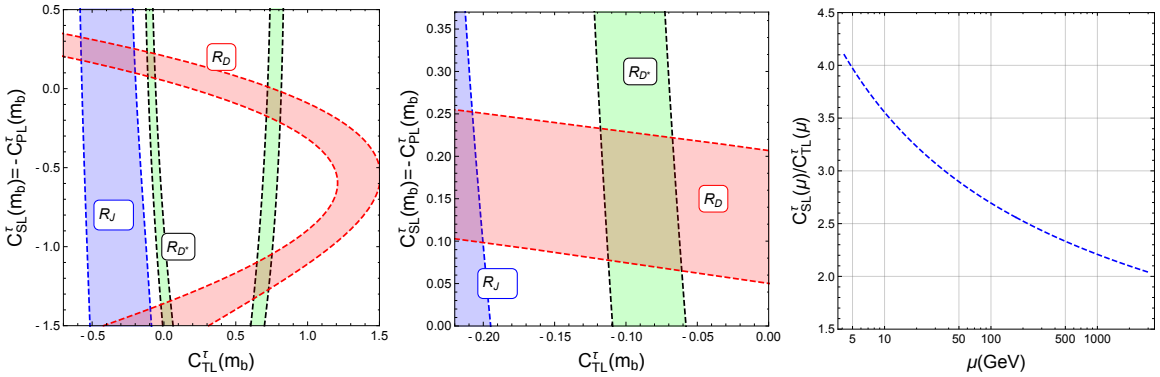

Figure 4. The red and green (blue) shaded regions in the left panel correspond to the values of $C^{\tau}_{\rm SL} = -C^{\tau}_{\rm PL}$ and $C^{\tau}_{\rm TL}$ that satisfy the experimental measurement of R_D and R_{D^*} ($R_{J/\psi}$) within 1σ respectively. The small overlap of the red and green regions for positive (negative) values of $C^{\tau}_{\rm SL}$ ($C^{\tau}_{\rm TL}$) is magnified separately in the middle panel. The right panel shows the RG evolution of the coupling ratio $C^{\tau}_{\rm SL}/C^{\tau}_{\rm TL}$ assuming $C^{\tau}_{\rm SL}/C^{\tau}_{\rm TL} = 2$ at 3 TeV. See text for more details.

3.4 Combination of tensor, scalar and pseudo-scalar operators

In this section, we consider the scenario in which the scalar, pseudo-scalar and tensor operators are present simultaneously.[3] In the upper left panel of figure 4, we show the various allowed regions in the $C^{\tau}_{\rm TL}$-$C^{\tau}_{\rm SL}$ plane assuming the relation $C^{\tau}_{\rm SL} = -C^{\tau}_{\rm PL}$. From the upper panel of figure 4, it can be seen that a simultaneous explanation of the R_D and R_{D^*} anomalies requires $C^{\tau}_{\rm SL}(m_b) = -C^{\tau}_{\rm PL}(m_b) \in [0.08, 0.23]$ and $C^{\tau}_{\rm TL}(m_b) \in [-0.11, -0.06]$ (the small overlap of the red and green regions for positive values of $C^{\tau}_{\rm SL}$ and negative values of $C^{\tau}_{\rm TL}$). We are ignoring the overlap regions with $C^{\tau}_{\rm PL} > 1$ because of the bound from $\mathrm{Br}(B_c \to \tau\nu)$. There is also an overlap region enclosing $C^{\tau}_{\rm SL} = -C^{\tau}_{\rm PL} = 0$ and for non-zero $C^{\tau}_{\rm TL}$ which corresponds to the tensor solution discussed in the previous section.

We would like to comment in passing that there exist scalar leptoquark models that generate the operator $(\bar{c}P_L\nu)\,(\bar{\tau}P_L b)$ at the matching scale[4] Λ, see e.g., [55]. This operator can be written in terms of the operators in eq. (2.3) after performing the Fierz transformation,[5]

$$(\bar{c}P_L\nu)\,(\bar{\tau}P_L b) = -\frac{1}{8}\left[2(\mathcal{O}^{\tau}_{\rm SL} - \mathcal{O}^{\tau}_{\rm PL}) + \mathcal{O}^{\tau}_{\rm TL}\right]. \tag{3.3}$$

[3]The combination of vector and scalar operators is discussed in appendix C.7.

[4]This operator arises from a $\mathrm{SU(2)_L} \times \mathrm{U(1)_Y}$ gauge invariant operator $\left(\bar{l}^k u'\right)\epsilon_{jk}\left(\bar{q}'^j e'\right)$ which, by using Fierz transformation, gives

$$\left(\bar{l}^k u'\right)\epsilon_{jk}\left(\bar{q}'^j e'\right) = -\frac{1}{8}\left[4\left(\bar{l}'^j e'\right)\epsilon_{jk}\left(\bar{q}'^k u'\right) + \left(\bar{l}'^j \sigma_{\mu\nu} e'\right)\epsilon_{jk}\left(\bar{q}'^k \sigma^{\mu\nu} u'\right)\right].$$

See section 4 below for the notations.

[5]Note that vector leptoquarks, after Fierz transformation, generate vector operators only in the basis of section 2. A scenario with vector leptoquarks will be discussed in section 5.3.

JHEP11(2018)187

Thus, at the matching scale one gets

$$C^{\tau}_{\rm SL}(\Lambda) = -C^{\tau}_{\rm PL}(\Lambda) = 2C^{\tau}_{\rm TL}(\Lambda)\,. \tag{3.4}$$

This was our motivation to consider $C^{\tau}_{\rm SL} = -C^{\tau}_{\rm PL}$ in figure 4. The ratio $C^{\tau}_{\rm SL}/C^{\tau}_{\rm TL}$, however, increases with the decreasing RG scale as shown in the right panel of figure 4. Assuming $C^{\tau}_{\rm SL}(\Lambda)/C^{\tau}_{\rm TL}(\Lambda) = 2$ for $\Lambda = 3\,\text{TeV}$, we get $C^{\tau}_{\rm SL}(m_b)/C^{\tau}_{\rm TL}(m_b) \approx 4$.

Note that, in the above discussion we have considered only real values of the Wilson coefficients. Allowing for complex Wilson coefficients may lead to new possibilities, see for example [56].

3.5 Distinguishing the various explanations

In the previous subsections we saw that simultaneous explanations of the R_D and R_{D^*} anomalies are possible by

1. a combination of vector and axial-vector operators (the overlap of red and green regions in figure 1)
2. a combination of scalar and pseudo-scalar operators (the overlap of red and green regions in figure 2)
3. tensor operator only (the region between the two dashed vertical lines in figure 3)
4. a combination of scalar, pseudo-scalar and tensor operators (the overlap of red and green regions in figure 4, in particular, the region with positive values of $C^{\tau}_{\rm SL}$ and negative values of $C^{\tau}_{\rm TL}$.)

The second solution is quite strongly disfavoured by the existing indirect upper bound on the branching ratio of $B_c \to \tau\nu$. So we ignore it here. We also ignore the scenario with a combination of vector and scalar operators because of the reason mentioned in the last paragraph of section C.7.

We now very briefly comment on the possibility of distinguishing the three possible solutions 1), 3) and 4) by measuring the τ-polarisation ($P_\tau(D^*)$), forward-backward asymmetry ($\mathcal{A}_{\rm FB}(D^*)$) and more interestingly, $R_{J/\psi}$. In figure 5, we plot the predictions for $P_\tau(D^*)$, $\mathcal{A}_{\rm FB}(D^*)$ and $R_{J/\psi}$ for values of the WCs that correspond to various simultaneous solutions of R_D and R_{D^*} anomalies.

It can be seen that it is indeed possible to discriminate the three solutions by measuring $P_\tau(D^*)$, $\mathcal{A}_{\rm FB}(D^*)$ and $R_{J/\psi}$. In fact, as can be seen from the right panel of figure 5, $R_{J/\psi}$ can be a very good discriminating observable between the solutions 1) and 3). Of course, with more data, various kinematical distributions can also be used to discriminate the different Lorentz structures [31, 39, 42, 57–61].

4 Linearly realised $\mathbf{SU(2)_L \times U(1)_Y}$ gauge invariance

In the previous sections, we considered operators which were manifestly $\text{SU}(3) \times \text{U}(1)_{\rm em}$ invariant, but invariance under the full electroweak group was not demanded. We investigate the consequences of $\text{SU}(2)_{\rm L} \times \text{U}(1)_{\rm Y}$ invariance in this section.

JHEP11(2018)187

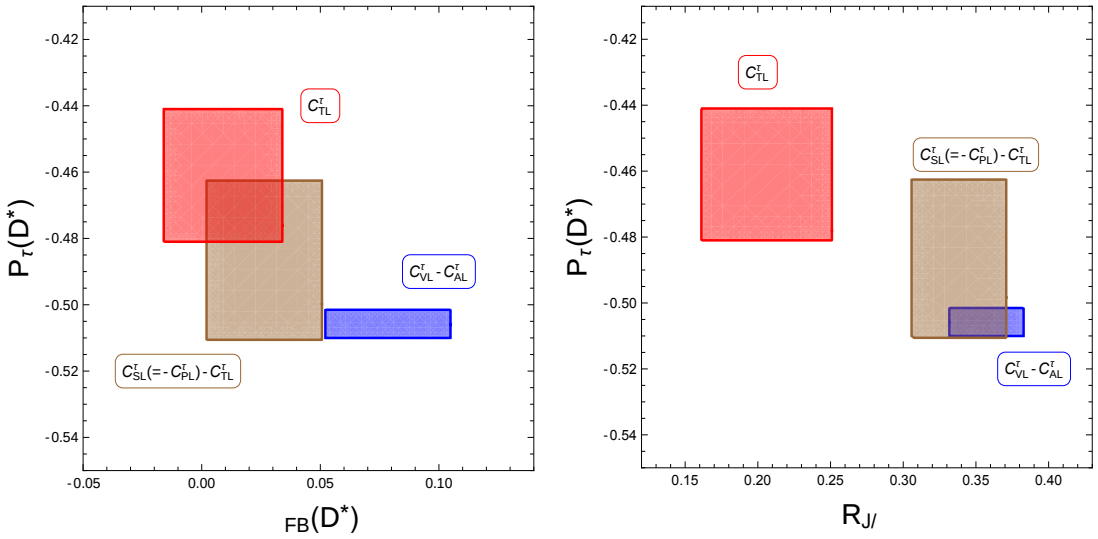

Figure 5. Predictions for $P_\tau(D^*)$, $\mathcal{A}_{\rm FB}(D^*)$ and $R_{J/\psi}$ for values of the WCs that correspond to various simultaneous solutions of R_D and R_{D^*} anomalies. See text for more details.

4.1 List of operators

The SU(3) $\times$ SU(2)$_{\rm L}$ $\times$ U(1)$_{\rm Y}$ invariant dimension-6 operators that lead to $b \to c\,\tau\,\nu$ decay are given by (using the same notation as in [62]; the primes represent the fact that the operators and couplings are written in the gauge basis)

$$\mathcal{L}^{\rm dim6} = -\frac{1}{\Lambda^2}\sum_{p'r's't'}\Big\{[C_{lq}^{(3)}]'_{p'r's't'}\left(\bar{l}'_{p'}\gamma_\mu\sigma^I l'_{r'}\right)\left(\bar{q}'_{s'}\gamma^\mu\sigma^I q'_{t'}\right)+\text{h.c.} \tag{4.1}$$

$$+[C_{ledq}]'_{p'r's't'}\left(\bar{l}'^{j}_{p'}e'_{r'}\right)\left(\bar{d}'_{s'}q'^{j}_{t'}\right)+\text{h.c.} \tag{4.2}$$

$$+[C_{lequ}^{(1)}]'_{p'r's't'}\left(\bar{l}'^{j}_{p'}e'_{r'}\right)\epsilon_{jk}\left(\bar{q}'^{k}_{s'}u'_{t'}\right)+\text{h.c.} \tag{4.3}$$

$$+[C_{lequ}^{(3)}]'_{p'r's't'}\left(\bar{l}'^{j}_{p'}\sigma_{\mu\nu}e'_{r'}\right)\epsilon_{jk}\left(\bar{q}'^{k}_{s'}\sigma^{\mu\nu}u'_{t'}\right)+\text{h.c.} \tag{4.4}$$

$$+[C_{\phi l}^{(3)}]'_{p'r'}\left(\phi^\dagger i\overleftrightarrow{D}^I_\mu\phi\right)\left(\bar{l}'_{p'}\,\sigma^I\gamma^\mu\,l'_{r'}\right)+\text{h.c.} \tag{4.5}$$

$$+[C_{\phi q}^{(3)}]'_{p'r'}\left(\phi^\dagger i\overleftrightarrow{D}^I_\mu\phi\right)\left(\bar{q}'_{p'}\,\sigma^I\gamma^\mu\,q'_{r'}\right)+\text{h.c.} \tag{4.6}$$

$$+[C_{\phi ud}]'_{p'r'}\left(\phi^j\epsilon_{jk}\,i(D_\mu\phi)^k\right)\left(\bar{u}'_{p'}\gamma^\mu d'_{r'}\right)+\text{h.c.}\Big\} \tag{4.7}$$

where, ϵ_{ij} is antisymmetric with $\epsilon_{12}=+1$, and

$$\phi^\dagger i\overleftrightarrow{D}^I_\mu\phi = i\left(\phi^\dagger\sigma^I D_\mu\phi-(D_\mu\phi)^\dagger\sigma^I\phi\right) \tag{4.8}$$

$$D_\mu\phi=\left(\partial_\mu+ig_2\frac{\sigma^I}{2}W^I_\mu+ig_1Y_\phi B_\mu\right)\phi\ ,Y_\phi=\frac{1}{2}\,. \tag{4.9}$$

(Note that, the operator structure $\left(\bar{l}'^{j}_{p'}\sigma_{\mu\nu}e'_{r'}\right)\left(\bar{d}'_{s'}\sigma^{\mu\nu}q'^{ij}_{t'}\right)$ vanishes algebraically.)

JHEP11(2018)187

The operators $[\mathcal{O}^{(3)}_{\phi q}]_{p'r'}$ and $[\mathcal{O}_{\phi ud}]_{p'r'}$ modify the charged current vertex of the quarks, in particular, the one of our interest $\bar{c}bW$. However, this affects both the $b \to c\,\tau\,\nu$ and $b \to c\,\ell_0\,\nu$ decays in the same way. Consequently, the operators $[\mathcal{O}^{(3)}_{\phi q}]_{p'r'}$ and $[\mathcal{O}_{\phi ud}]_{p'r'}$ are not relevant for the explanation of the R_D and R_{D^*} anomalies, and we will ignore them in the rest of the paper.

It can be seen from eq. (4.1) and eq. (4.5) that the operators only involve left chiral fields. Consequently, these operators only lead to V-A interactions. We stress that it is not true in general that linearly realised $\mathrm{SU(2)_L} \times \mathrm{U(1)_Y}$ gauge invariance forbids V+A operators at the dimension-6 level. For example, the operator in eq. (4.7) generates V+A operator, but, as mentioned before, it does not lead to lepton non-universality at the dimension-6 level. This is an important consequence of linearly realised $\mathrm{SU(2)_L} \times \mathrm{U(1)_Y}$ gauge invariance.

Note however that at the dimension-8 level, the operator $(\mathcal{O}^{\tau}_{\mathrm{VL}} + \mathcal{O}^{\tau}_{\mathrm{AL}})$ with the possibility of lepton non-universality can be generated. For example, consider the operator

$$\mathcal{O}^{8}_{\mathrm{RL}} = \frac{1}{\Lambda^4}\left(\bar{l}'_{p'}\phi\right)\gamma_\mu\left(l'_{r'}\phi\right)\left(\bar{u}'_{s'}\gamma^\mu d'_{t'}\right) \tag{4.10}$$

where the objects inside each of the parenthesis are constructed as SU(2) singlets. After electroweak symmetry breaking, this operator generates the following interaction term

$$\frac{v^2}{\Lambda^2}\,\frac{1}{\Lambda^2}\,[\bar{\ell}\,\gamma_\mu\,P_L\,\nu][\bar{c}\,\gamma^\mu\,P_R\,b] \tag{4.11}$$

with right handed current in the quark sector. We will however ignore dimension-8 operators in the rest of this paper.

4.2 Correspondence with section 2

We now expand the various SU(2) structures in order to relate the WCs of the $\mathrm{SU(2)_L} \times \mathrm{U(1)_Y}$ invariant operators to those in section 2:

$$\begin{aligned}\left(\bar{l}'_{p'}\gamma_\mu\sigma^I l'_{r'}\right)\left(\bar{q}'_{s'}\gamma^\mu\sigma^I q'_{t'}\right) = {}& \left(\bar{\nu}'_{p'}\gamma^\mu P_L\nu'_{r'}\right)\left(\bar{u}'_{s'}\gamma_\mu P_L u'_{t'}\right) + \left(\bar{e}'_{p'}\gamma^\mu P_L e'_{r'}\right)\left(\bar{d}'_{s'}\gamma_\mu P_L d'_{t'}\right) \\ & - \left(\bar{e}'_{p'}\gamma^\mu P_L e'_{r'}\right)\left(\bar{u}'_{s'}\gamma_\mu P_L u'_{t'}\right) - \left(\bar{\nu}'_{p'}\gamma^\mu P_L\nu'_{r'}\right)\left(\bar{d}'_{s'}\gamma_\mu P_L d'_{t'}\right) \\ & + 2\left(\bar{\nu}'_{p'}\gamma^\mu P_L e'_{r'}\right)\left(\bar{d}'_{s'}\gamma_\mu P_L u'_{t'}\right) + 2\left(\bar{e}'_{p'}\gamma^\mu P_L\nu'_{r'}\right)\left(\bar{u}'_{s'}\gamma_\mu P_L d'_{t'}\right)\end{aligned} \tag{4.12}$$

$$\begin{aligned}\left(\phi^\dagger i\overleftrightarrow{D}^I_\mu\phi\right)\left(\bar{l}'_{p'}\,\sigma^I\gamma^\mu\,l'_{r'}\right) = {}& \Bigg[-\frac{1}{2}\frac{g_2}{\cos\theta_W}Z_\mu\left(\overline{\nu'}_{p'}\gamma^\mu P_L\nu'_{r'}\right) + \frac{1}{2}\frac{g_2}{\cos\theta_W}Z_\mu\left(\overline{e'}_{p'}\gamma^\mu P_L e'_{r'}\right) \\ & - \frac{g_2}{\sqrt{2}}W^+_\mu\left(\overline{\nu'}_{p'}\gamma^\mu P_L e'_{r'}\right) - \frac{g_2}{\sqrt{2}}W^-_\mu\left(\overline{e'}_{p'}\gamma^\mu P_L\nu'_{r'}\right)\Bigg]\left(v^2+2vh+h^2\right).\end{aligned} \tag{4.13}$$

The scalar and tensor operators can be decomposed similarly. It is clear that, as a consequence of the manifest $\mathrm{SU(2)_L} \times \mathrm{U(1)_Y}$ gauge invariance, the operators relevant for the explanation of the R_D and R_{D^*} anomalies get related to other operators, in particular, to operators that give rise to neutral current decays. However, in order to understand these correlations more concretely, we have to first rotate the fields from the gauge to the mass eigenstates.

JHEP11(2018)187

From the gauge to the mass eigenstates. We introduce the following mixing matrices which relate the gauge and mass eigenstates

$$\begin{aligned}(e_{L,R})_{r'} &= (V^e_{L,R})_{r'r}(e_{L,R})_r, \quad (\nu_{L,R})_{r'} = (V^\nu_{L,R})_{r'r}(\nu_{L,R})_r\,,\\ (u_{L,R})_{r'} &= (V^u_{L,R})_{r'r}(u_{L,R})_r, \quad (d_{L,R})_{r'} = (V^d_{L,R})_{r'r}(d_{L,R})_r\end{aligned} \tag{4.14}$$

The CKM and PMNS matrices are defined as

$$V_{\rm CKM} = (V^u_L)^\dagger V^d_L, \quad V_{\rm PMNS} = (V^\nu_L)^\dagger V^e_L\,. \tag{4.15}$$

Using the above definition of the mixing matrices, we get (see appendix D)

$$\begin{aligned}\Delta C^{cb\tau\nu_3}_{\rm VL} &= \frac{\Lambda^2_{\rm SM}}{\Lambda^2}\left[[\tilde{C}^{(3)e\nu ud}_{lq}]_{3323} + \left([\tilde{C}^{(3)\nu edu}_{lq}]_{3332}\right)^*\right]\\ &\quad - \frac{\Lambda^2_{\rm SM}}{\Lambda^2}\left[[\tilde{C}^{(3)e\nu}_{\phi l}]_{33} + \left([\tilde{C}^{(3)\nu e}_{\phi l}]_{33}\right)^*\right]V_{cb} \qquad (4.16)\\ \Delta C^{cb\tau\nu_3}_{\rm AL} &= -\Delta C^{cb\tau\nu_\tau}_{\rm VL} \qquad (4.17)\end{aligned}$$

Similar relations can also be found for the scalar and tensor operators, see appendix D. The $[\tilde{C}]$ couplings are related to the $[C]'$ couplings of section 4.1 by appropriate mixing matrices. For example,

$$\sum_{p',r',s',t'} [C^{(3)}_{lq}]'_{p'r's't'}(V^\nu_L)^\dagger_{pp'}(V^\nu_L)_{r'r}(V^u_L)^\dagger_{ss'}(V^u_L)_{t't} \equiv [\tilde{C}^{(3)\nu\nu uu}_{lq}]_{prst} \tag{4.18}$$

see appendix D for more details.

Note that the operator $\left(\phi^\dagger i\overleftrightarrow{D}^I_\mu\phi\right)\left(\bar{l}'_{p'}\,\sigma^I\gamma^\mu\,l'_{r'}\right)$ modifies the leptonic charged and neutral current vertices of W and Z bosons respectively (see eq. (4.13)). So in order to explain the $R_{D^{(*)}}$ data by this operator, lepton non-universality has to be introduced at these vertices. However, a strong bound on such lepton non-universality exists from LEP [63]:

$$\frac{{\rm Br}(W^+\to\tau^+\nu)}{[{\rm Br}(W^+\to\mu^+\nu)+{\rm Br}(W^+\to e^+\nu)]/2} = 1.077\pm 0.026\,. \tag{4.19}$$

This means that the branching ratio of $W^+\to\tau^+\nu$ can exceed that of $W^+\to\mu^+\nu$ or $W^+\to e^+\nu$ at most by 10.3% at 1σ. Thus the correction to the $W\tau\nu$ vertex can at most be 5% of the SM, assuming that the $W\bar{\mu}\nu$ and $W\bar{e}\nu$ vertices have no NP. This gives (using eq. (4.13) and appendix D)[6]

$$-\left[\left([\tilde{C}^{(3)e\nu}_{\phi l}] + [\tilde{C}^{(3)\nu e}_{\phi l}]^\dagger\right)_{33}\right]\frac{v^2}{\Lambda^2} \lesssim 0.05\,, \tag{4.21}$$

[6]The SM couplings are defined by

$$\mathcal{L}^{\rm SM}_{W\tau\nu} = -\frac{g_2}{\sqrt{2}}g^\tau_W\left(W^-_\mu\,\bar{\tau}\gamma^\mu P_L\nu_\tau + W^+_\mu\bar{\nu}_\tau\gamma^\mu P_L\tau\right), \tag{4.20}$$

where $g^\tau_W = 1$. Any deviation from the SM will be denoted by Δg^τ_W.

JHEP11(2018)187

which, from the second line of eq. (4.16), implies

$$\Delta C^{\tau}_{\rm VL} = -\Delta C^{\tau}_{\rm AL} < 0.05\,, \tag{4.22}$$

where we have used $v^2 = 1/(\sqrt{2}G_F) = \Lambda^2_{\rm SM}V_{cb} \approx (246\ \text{GeV})^2$.

As we saw in section 3.1, $\Delta C^{\tau}_{\rm VL} = -\Delta C^{\tau}_{\rm AL} < 0.05$ is not enough to explain the $R_{D^{(*)}}$ data within their $1\,\sigma$ experimental ranges. Moreover, as can be seen from eq. (4.16), contribution of this operator to the WCs $C^{\tau}_{\rm VL} = -C^{\tau}_{\rm AL}$ is suppressed by V_{cb} compared to the other contribution. This operator also modifies the $Z_\mu \bar{\tau}\gamma^\mu P_L \tau$ coupling, and the modification is given by[7]

$$\Delta g^{\tau}_L = \frac{1}{2}\left[\left([\tilde{C}^{(3)e\nu}_{\phi l}] + [\tilde{C}^{(3)\nu e}_{\phi l}]^\dagger\right) V_{\rm PMNS}\right]_{33}\frac{v^2}{\Lambda^2}\ ,\ \Delta g^{\tau}_R = 0. \tag{4.24}$$

Using the experimental constraint from LEP [64], and assuming that there is no NP in the decays to light leptons, we get[8]

$$|\Delta g^{\tau}_L| \lesssim 6\times 10^{-4}, \quad \Rightarrow \left|\left([\tilde{C}^{(3)e\nu}_{\phi l}] + [\tilde{C}^{(3)\nu e}_{\phi l}]^\dagger\right)_{33}\right| \lesssim 0.02\left(\frac{\Lambda^2}{\text{TeV}^2}\right) \tag{4.25}$$

$$\Rightarrow \Delta C^{\tau}_{\rm VL} \lesssim 0.001\,. \tag{4.26}$$

Similarly,

$$\Delta g^{\nu}_L = -\frac{1}{2}\left[V_{\rm PMNS}\left([\tilde{C}^{(3)e\nu}_{\phi l}] + [\tilde{C}^{(3)\nu e}_{\phi l}]^\dagger\right)V^\dagger_{\rm PMNS}\right]_{33}\frac{v^2}{\Lambda^2} \tag{4.27}$$

which should be compared with the experimental constraint [64]

$$|\Delta g^{\nu}_L| \lesssim 1.2\times 10^{-3}\,. \tag{4.28}$$

Given these constraints, it is clear that the operator $\mathcal{O}^{(3)}_{\phi l}$ alone is unable to explain the R_{D,D^*} data. We will thus not consider this operator anymore in this work. Before closing this section, we would like to mention that a much stronger indirect constraint (compared to eq. (4.21)) on the $W\tau\nu$ coupling can be obtained from measurements of leptonic tau decays assuming that no other four-fermion operator that can either contribute to $\tau \to e\,\nu\,\bar{\nu}$ or $\mu \to e\,\nu\,\bar{\nu}$ exists [65]. Assuming no NP in the $W\mu\,\nu$ vertex, this gives,

$$-0.4\times 10^{-3} \lesssim -\left[\left([\tilde{C}^{(3)e\nu}_{\phi l}] + [\tilde{C}^{(3)\nu e}_{\phi l}]^\dagger\right)_{33}\right]\frac{v^2}{\Lambda^2} \lesssim 2.6\times 10^{-3}\ . \tag{4.29}$$

[7] We define the SM couplings to be

$$\mathcal{L}^{\rm SM}_{Z\tau\tau} = -\frac{g_2}{\cos\theta_W} Z_\mu\left(g^{\tau}_L \bar{\tau}\gamma^\mu P_L\tau + g^{\tau}_R\bar{\tau}\gamma^\mu P_R\tau\right)\,, \tag{4.23}$$

where $g^{\tau}_L = -1/2 + \sin^2\theta_W \approx -0.27$ and $g^{\tau}_R = \sin^2\theta_W \approx 0.23$. The vector and axial-vector couplings are defined by $g^{\tau}_{V,A} = g^{\tau}_L \pm g^{\tau}_R$.

[8] Here we have assumed $(V_{\rm PMNS})_{33} = 1$. However, given the strong experimental constraints, our results will not change if correct values of $(V_{\rm PMNS})_{13}$ and $(V_{\rm PMNS})_{23}$ are used.

JHEP11(2018)187

4.3 Correlations

The linearly realised SU(3) × SU(2)$_{\rm L}$ × U(1)$_{\rm Y}$ symmetry leads to various correlations among the flavour violating neutral and charged current observables. To start with, we assume that only the operator(s) that is (are) needed for the explanation of the R_{D,D^*} anomalies is (are) present. In particular, we consider the operator of eq. (4.1) and investigate the correlations arising from it. We will not consider the scalar and tensor operators anymore because, as discussed in the previous sections, an explanation of R_{D,D^*} anomalies by scalar (or a combination of scalar and tensor) operators is strongly disfavoured by the upper bound on $\mathrm{Br}(B_c \to \tau\,\nu)$, and it is rather difficult to generate only the tensor operator.

Without loss of generality, we now go to a basis where the left-chiral down quarks and left-chiral charged leptons are in the mass basis. This amounts to setting

$$V_L^e = \mathbb{1}_{3\times 3}\,, \qquad V_L^d = \mathbb{1}_{3\times 3}\,. \tag{4.30}$$

It should be emphasised that we are not making any assumption here by going to a particular basis. This just means that our primed WCs of section 4.1 are defined in this basis. In this basis, we have

$$V_{\rm CKM} = V_L^{u\dagger}\,, \qquad V_{\rm PMNS} = V_L^{\nu\dagger}\,. \tag{4.31}$$

Let us first consider the contribution to the operator $(\bar\tau\gamma^\mu P_L\nu)(\bar c\gamma_\mu P_L b)$. From eq. (D.1) and (D.2), one can read off the coefficient of this operator. For simplicity, we assume that the NP Wilson coefficients, $[C_{lq}^{(3)}]'_{p'r's't'}$, are diagonal in the Lepton flavours. We get

$$-2\left([\tilde C_{lq}^{(3)e\nu ud}]_{3r23} + ([\tilde C_{lq}^{(3)\nu edu}]_{r332})^*\right)(\bar\tau\gamma^\mu P_L\nu_r)\,(\bar c\gamma_\mu P_L b) \tag{4.32}$$

$$\begin{aligned}&= -2\Big(([C_{lq}^{(3)}]'_{3313} + ([C_{lq}^{(3)}]'_{3331})^*)V_{cd} + ([C_{lq}^{(3)}]'_{3323} + ([C_{lq}^{(3)}]'_{3332})^*)V_{cs}\\ &\quad + ([C_{lq}^{(3)}]'_{3333} + ([C_{lq}^{(3)}]'_{3333})^*)V_{cb}\Big) \times [V_{\rm PMNS}^\dagger]_{3r}\,(\bar\tau\gamma^\mu P_L\nu_r)\,(\bar c\gamma_\mu P_L b)\end{aligned} \tag{4.33}$$

Note that $\nu_{L\tau} = [V_{\rm PMNS}^\dagger]_{3r}\,\nu_{L\,r}$, $\nu_{L\tau}$ being the τ-flavour neutrino. As we discussed in the previous sections, in order to explain the anomalies at the $1\,\sigma$ level, the coefficient of the operator $(\bar\tau\gamma^\mu P_L\nu_\tau)\,(\bar c\gamma_\mu P_L b)$ in eq. (4.33) should at least be ~ 0.16 for a NP scale $\Lambda = \Lambda_{\rm SM}$. This gives,

$$\begin{aligned}&([C_{lq}^{(3)}]'_{3313} + ([C_{lq}^{(3)}]'_{3331})^*)V_{cd} + ([C_{lq}^{(3)}]'_{3323} + ([C_{lq}^{(3)}]'_{3332})^*)V_{cs} + ([C_{lq}^{(3)}]'_{3333} + ([C_{lq}^{(3)}]'_{3333})^*)V_{cb}\\ &\qquad \gtrsim 0.06\left(\frac{\Lambda^2}{\mathrm{TeV}^2}\right).\end{aligned} \tag{4.34}$$

We would now like to understand whether this condition is consistent with the other measurements of B meson decays. We first consider the decay $B \to K^*\bar\nu\nu$, or in other words, the operator $(\bar\nu\gamma^\mu P_L\nu)\,(\bar s\gamma_\mu P_L b)$. Contribution to this operator is given by

$$\left([C_{lq}^{(3)}]'_{p'r'23} + [C_{lq}^{(3)}]'^*_{r'p'32}\right)(\bar\nu_{p'}\gamma^\mu P_L\nu_{r'})\,(\bar s\gamma_\mu P_L b)\,. \tag{4.35}$$

JHEP11(2018)187

Experimental bound on $\mathrm{Br}(B^0 \to K^{*0}\bar{\nu}\nu)$ [66] then requires the Wilson coefficients to satisfy (the SM prediction is taken from [67]),

$$-0.005 \left(\frac{\Lambda^2}{\mathrm{TeV}^2}\right) \lesssim [C_{lq}^{(3)}]'_{3323} + [C_{lq}^{(3)}]'^*_{3332} \leq 0.025 \left(\frac{\Lambda^2}{\mathrm{TeV}^2}\right). \tag{4.36}$$

The first term on the left hand side of eq. (4.34) contributes to $b \to d\,\bar{\nu}\,\nu$ processes. Using the experimental bound on the $\mathrm{Br}(B^0 \to \pi^0\bar{\nu}\,\nu)$ [66] and the corresponding SM prediction from [68], we obtain

$$-0.018 \left(\frac{\Lambda^2}{\mathrm{TeV}^2}\right) \lesssim [C_{lq}^{(3)}]'_{3313} + [C_{lq}^{(3)}]'^*_{3331} \lesssim 0.023 \left(\frac{\Lambda^2}{\mathrm{TeV}^2}\right). \tag{4.37}$$

The same coupling can also be constrained by measurement of $\mathrm{Br}(B_u \to \tau\,\nu_\tau)$. Assuming the maximum allowed value of $\mathrm{Br}(B_u \to \tau\,\nu_\tau)$ to be twice that of the SM [69] and, in the absence of cancellations (see eq. (4.50) below), we get

$$-0.15 \left(\frac{\Lambda^2}{\mathrm{TeV}^2}\right) \lesssim [C_{lq}^{(3)}]'_{3313} + [C_{lq}^{(3)}]'^*_{3331} \lesssim 0.025 \left(\frac{\Lambda^2}{\mathrm{TeV}^2}\right). \tag{4.38}$$

Thus, the maximum contribution from the first two terms of eq. (4.34) subject to the constraints in eqs. (4.36) and (4.37) is $\approx 0.03\,(\Lambda^2/\mathrm{TeV}^2)$. This requires

$$([C_{lq}^{(3)}]'_{3333} + [C_{lq}^{(3)}]'^*_{3333})V_{cb} \gtrsim 0.03 \left(\frac{\Lambda^2}{\mathrm{TeV}^2}\right). \tag{4.39}$$

See also [70] for a related discussion. We now investigate whether the coupling $([C_{lq}^{(3)}]'_{3333} + [C_{lq}^{(3)}]'^*_{3333})$ is constrained by other measurements. First of all, notice that the coefficient of the operator $(\bar{\tau}\gamma^\mu P_L \tau)\left(\bar{b}\gamma_\mu P_L b\right)$ is given by

$$[\tilde{C}_{lq}^{(3)eedd}]_{3333} + ([\tilde{C}_{lq}^{(3)eedd}]_{3333})^* = [C_{lq}^{(3)}]'_{3333} + ([C_{lq}^{(3)}]'_{3333})^*. \tag{4.40}$$

Direct searches of processes involving two τ leptons in the final state constrain this coupling weakly [71]:

$$\left|[C_{lq}^{(3)}]'_{3333} + ([C_{lq}^{(3)}]'_{3333})^*\right| < 2.6 \left(\frac{\Lambda^2}{\mathrm{TeV}^2}\right). \tag{4.41}$$

Moreover, as we show below, the same coupling also appears in the coefficient of the operator $(\bar{\tau}\gamma^\mu P_L \tau)\,(\bar{t}\gamma_\mu P_L t)$. From eq. (D.1) and (D.2) we get, for the coefficient of this operator,

$$\left[\tilde{C}_{lq}^{(3)eeuu}\right]_{3333} + \left[\tilde{C}_{lq}^{(3)eeuu}\right]^*_{3333} \tag{4.42}$$

where,

$$\begin{aligned}
\left[\tilde{C}_{lq}^{(3)eeuu}\right]_{3333} &= \left[C_{lq}^{(3)}\right]'_{p'r's't'} (V_L^e)^\dagger_{3p'} (V_L^e)_{r'3} (V_L^u)^\dagger_{3s'} (V_L^u)_{t'3} \\
&= \left[C_{lq}^{(3)}\right]'_{3333} |V_{tb}|^2 + \left[C_{lq}^{(3)}\right]'_{3323} V_{ts}V_{tb}^* + \left[C_{lq}^{(3)}\right]'_{3332} V_{tb}V_{ts}^* \\
&\quad + \left[C_{lq}^{(3)}\right]'_{3311} |V_{td}|^2 + \left[C_{lq}^{(3)}\right]'_{3313} V_{td}V_{tb}^* + \left[C_{lq}^{(3)}\right]'_{3331} V_{tb}V_{td}^* \\
&\quad + \left[C_{lq}^{(3)}\right]'_{3322} |V_{ts}|^2 + \left[C_{lq}^{(3)}\right]'_{3312} V_{td}V_{cb}^* + \left[C_{lq}^{(3)}\right]'_{3321} V_{cb}V_{td}^*.
\end{aligned} \tag{4.43}$$

JHEP11(2018)187

The 2nd, 3rd, 5th and 6th terms in eq. (4.43) are small because of eqs. (4.36) and (4.37). All the other terms which are of the form $[C_{lq}^{(3)}]'_{33ij}$, $i,j=1,2$ are constrained by direct searches of $\tau\,\tau$ final state (taking into account the enhancement of the di-jet $\to \tau\tau$ cross-section compared to that of $\bar{b}\,b \to \tau^+\,\tau^-$ due to larger parton distribution functions, we get bounds which are stronger than eq. (4.41) by a factor of ~ 2 for $([C_{lq}^{(3)}]'_{3322} + \text{c.c})$ to a factor of ~ 8 for $([C_{lq}^{(3)}]'_{3311} + \text{c.c})$). Thus, the only term which remains is of the form

$$\left(\left[C_{lq}^{(3)}\right]'_{3333} + \left[C_{lq}^{(3)}\right]'^{*}_{3333}\right)|V_{tb}|^2\,. \tag{4.44}$$

This term, once the top quarks in the operator $(\bar{\tau}\gamma^\mu P_L\tau)\,(\bar{t}\gamma_\mu P_L t)$ form a loop and are attached to Z, contributes to Δg_L^τ [72]. As Δg_L^τ is very strongly constrained, see eq. (4.25), this provides a stringent constraint on the coupling of eq. (4.44). Indeed, from eq. (E.9) in appendix E, we find

$$\left|[C_{lq}^{(3)}]'_{3333} + [C_{lq}^{(3)}]'^{*}_{3333}\right| \lesssim \frac{0.017}{V_{cb}}\left(\frac{\Lambda}{\text{TeV}}\right)^2 \frac{1}{1+0.6\log\frac{\Lambda}{\text{TeV}}}\,, \tag{4.45}$$

which clearly rules out the possibility of explaining R_{D,D^*} anomalies by this term, unless there are other contributions to the modifications of the Z couplings making it compatible with the experimental observations.

It is worth mentioning that in our discussion so far we have made the assumption that no other operator is present except the one required for the R_{D,D^*} anomaly. The presence of other operator(s) can however help evade some of these constraints [73]. For example, one possibility is to assume the presence of the singlet operator

$$\mathcal{L}^{\text{dim6}} \supset -\frac{1}{\Lambda^2}\sum_{p'r's't'}[C_{lq}^{(1)}]'_{p'r's't'}\left(\bar{l}'_{p'}\gamma_\mu l'_{r'}\right)\left(\bar{q}'_{s'}\gamma^\mu q'_{t'}\right) + \text{h.c.} \tag{4.46}$$

which, for appropriate values of the WC, can cancel the large contribution from the triplet operator both in $b \to s\,\bar{\nu}\,\nu$ [73] and Δg_L^τ [72, 74]. However, NP contributions to Δg_L^τ, Δg_L^ν and Δg_W^τ cannot be cancelled simultaneously. This can be understood in the following way. Note that, while the operator $[\mathcal{O}_{lq}^{(3)}]'$ generates the operator $[\mathcal{O}_{\phi l}^{(3)}]'$ (and not $[\mathcal{O}_{\phi l}^{(1)}]'$) through RG running, the operator $[\mathcal{O}_{lq}^{(1)}]'$ generates the operator $[\mathcal{O}_{\phi l}^{(1)}]'$ (and not $[\mathcal{O}_{\phi l}^{(3)}]'$). The operator $[\mathcal{O}_{\phi l}^{(3)}]'$ contributes to Δg_L^τ and Δg_L^ν with opposite signs (see eq. (4.13))while $[\mathcal{O}_{\phi l}^{(1)}]'$ contributes to them with the same sign. Thus, taking into account constraints from Δg_L^ν, Δg_L^τ and Δg_W^τ, we get (see appendix E for details)

$$\left|[C_{lq}^{(3,1)}]'_{3333} + [C_{lq}^{(3,1)}]'^{*}_{3333}\right| \lesssim \frac{0.025}{V_{cb}}\left(\frac{\Lambda}{\text{TeV}}\right)^2 \frac{1}{1+0.6\log\frac{\Lambda}{\text{TeV}}}\,. \tag{4.47}$$

JHEP11(2018)187

This makes the explanation of the R_{D,D^*} anomalies by the third term of eq. (4.34) impossible even in the presence of the operator of eq. (4.46). This leaves us with two possibilities:

I. The anomaly is explained by the second term in eq. (4.34). The tension with the $\mathrm{Br}(B^0 \to K^{*0}\bar{\nu}\nu)$ in eq. (4.36) is assumed to be cured by cancellation against the contribution of the operator in eq. (4.46). However, in this case, the flavour structure of the BSM sector must be such that the last term of eq. (4.34) is smaller than the second by at least factor of ~ 3.

II. The other possibility is to assume the presence of appropriate UV contribution at the matching scale that takes care of the $\Delta g_L^{\tau,\nu}$ constraints. In this case, one can explain the anomalies by the third term of eq. (4.34) alone.

As we will see in section 5.2 and 5.3, where we study the explanation of the $R_{D,D*}$ anomalies within the partial compositeness framework, elements of both the above mechanisms can in principle be present there.

Before concluding this section, we would like to comment on a few observables which do not provide relevant constraints at this moment, but may become important in the future.

- $b \to s\tau\tau$ transition. The coefficient of the operator $(\bar{\tau}\gamma^\mu P_L \tau)\,(\bar{s}\gamma_\mu P_L b)$ is given by

$$-([C_{lq}^{(3)}]'_{3323} + ([C_{lq}^{(3)}]'^{*}_{3332})\,. \tag{4.48}$$

  Now we assume that we are in scenario (I) where $B \to K^*\bar{\nu}\nu$ transition is cancelled by the singlet operator, and eq. (4.34) is saturated by the second term. Then, in the standard notation, we get for the WCs, $\Delta C_9^\tau = -\Delta C_{10}^\tau = -35$, with the corresponding Lagrangian:

$$\mathcal{L}_{b\to s\tau\tau} = -35\,\frac{4G_F}{\sqrt{2}}\,V_{tb}V_{ts}^*\,\frac{\alpha_{em}}{4\pi}\,[\bar{\tau}\gamma^\mu(1-\gamma_5)\tau][\bar{s}\gamma_\mu P_L b]\,. \tag{4.49}$$

  giving rise to large enhancement in $B_s \to \tau^+\tau^-$ (by a factor of ~ 50 compared to the SM in the branching fraction) and $B \to K/K^*\tau^+\tau^-$ decays (by a factor of $\sim 60\,(\text{for}\,K), 75\,(\text{for}\,K^*)$ compared to the SM in the branching fraction). It is interesting to note that large enhancement in $\mathrm{Br}(B_s \to \tau^+\tau^-)$ was also proposed as a possible solution to the like-sign di-muon charge asymmetry observed in one of the experiments in Tevatron [75, 76].

- $b \to u\tau\nu$ transition. In this case, the operator $(\bar{\tau}\gamma^\mu P_L \nu)\,(\bar{u}\gamma_\mu P_L b)$ is generated with the Wilson coefficient:

$$\begin{aligned}
&-\left(2[\tilde{C}_{lq}^{(3)e\nu ud}]_{3r13} + 2([\tilde{C}_{lq}^{(3)\nu edu}]_{r331})^*\right)(\bar{\tau}\gamma^\mu P_L \nu_r)\,(\bar{u}\gamma_\mu P_L b)\\
&= -2\left(([C_{lq}^{(3)}]'_{3313} + ([C_{lq}^{(3)}]'_{3331})^*)V_{ud} + ([C_{lq}^{(3)}]'_{3323} + ([C_{lq}^{(3)}]'_{3332})^*)V_{us}\right.\\
&\quad \left. + ([C_{lq}^{(3)}]'_{3333} + ([C_{lq}^{(3)}]'_{3333})^*)V_{ub}\right) \times (\bar{\tau}\gamma^\mu P_L \nu_\tau)\,(\bar{u}\gamma_\mu P_L b)
\end{aligned} \tag{4.50}$$

  where, we have again used $\nu_{L\tau} = [V_L^\nu]_{3r}\nu_r$, and assumed that the NP Wilson coefficients, $[C_{lq}^{(3)}]'_{p'r's't'}$, are diagonal in the Lepton flavours. Assuming that we have

JHEP11(2018)187

both singlet and triplet operators, the $b \to s(d)\nu\nu$ transitions do not lead to any constraints. Then, if the second (third) term in eq. (4.34) is responsible for R_{D,D^*} anomalies (i.e., saturates the inequality), we get

$$\mathcal{L}_{b\to u\tau\nu} \approx -0.2(0.1)\,\frac{4G_F}{\sqrt{2}}\,V_{ub}\,(\bar{\tau}\gamma^\mu P_L\nu_\tau)\,(\bar{u}\gamma_\mu P_L b)\ , \tag{4.51}$$

which leads to approximately 45% (20%) increase in $\mathrm{Br}(B_u \to \tau\,\nu_\tau)$. Instead, if one assumes that the first term in eq. (4.34) is responsible for R_{D,D^*} anomalies and saturates the inequality, the corresponding NP coupling for $b \to u\tau\nu$ becomes,

$$\mathcal{L}_{b\to u\tau\nu} \approx -4\,\frac{4G_F}{\sqrt{2}}\,V_{ub}\,(\bar{\tau}\gamma^\mu P_L\nu_\tau)\,(\bar{u}\gamma_\mu P_L b)\ , \tag{4.52}$$

which is obviously ruled out by experiment. Thus, even in the presence of cancellation in $b \to d\,\bar{\nu}\,\nu$, an explanation of R_{D,D^*} by the first term in eq. (4.34) seems very unlikely.

Similar analysis can also be done for the scalar, pseudo-scalar and tensor operators. Since the scalar and pseudo-scalar operators alone cannot explain the anomalies because of the strong constraint from $B_c \to \tau\nu$ (see section 3.2), we do not discuss them anymore. The tensor operator, $[C^{(3)}_{lequ}]'_{p'r's't'}\left(\bar{l}'^{j}_{p'}\sigma^{\mu\nu}e'_{r'}\right)\epsilon_{jk}\left(\bar{q}'^{k}_{s'}\sigma_{\mu\nu}u'_{t'}\right)$, on the other hand, is not affected by the process $B_c \to \tau\nu$, and generates, along with the charged current operator which is relevant for $R_{D^{(*)}}$, also neutral current operators involving up-type quarks.

5 Going beyond the dimension-6 analysis: partial compositeness

In the previous section, we illustrated that some other processes e.g., $B \to K^*\nu\,\nu$, $Z\,\tau\,\tau$ and $Z\,\nu\,\nu$ couplings can provide stringent restrictions on the possible explanations of R_D and R_{D^*} anomalies. It would be interesting also to study the correlations with the various $\Delta F = 2$ observables where the constraints on NP are particularly strong. Such an analysis requires specific assumptions on the underlying UV theory, or some power-counting rules. As we discussed before, explanations for the R_D and R_{D^*} anomalies call for NP close to the TeV scale, which is also expected for the naturalness of the Higgs mass. This coincidence of scales advocates for the speculation of a common origin of these two seemingly unrelated phenomena. This motivates us to consider the Composite Higgs paradigm [77], and, in particular, the models where fermion masses are generated via the Partial Compositeness (PC) mechanism [78]. In fact, recently there has been a lot of effort invested in analysing the B-meson anomalies within this framework [19–21, 24–27], all of which, however, focusses on specific models. A novel feature of our study would instead be to carry out the analysis in the EFT language, emphasising the correlations among the various observables. In particular, our aim would be to identify the key features that these models should possess in order to satisfy the experimental data. Our main results will be independent of the concrete realisation of PC, and are thus expected to be quite generic.

JHEP11(2018)187

5.1 Two-site Lagrangian

In this subsection we will briefly sketch the minimal Composite Higgs construction (for the details see the orginal paper [79] and reviews [80, 81]) and the familiar reader can directly proceed to the subsection 5.2. The global symmetry breaking pattern is taken as follows:

$$\text{MCHM} : \mathrm{U}(1)_{\mathrm{X}} \times \mathrm{SU}(3) \times \mathrm{SO}(5) \to \mathrm{U}(1)_{\mathrm{X}} \times \mathrm{SU}(3) \times \mathrm{SU}(2)_{\mathrm{L}} \times \mathrm{SU}(2)_{\mathrm{R}}. \tag{5.1}$$

We will study the phenomenology within effective field theory approach, using so called two site model [82]. The model consists of two sectors: the composite sector invariant under $\mathrm{SO}(5) \times \mathrm{SU}(3) \times \mathrm{U}(1)_{\mathrm{X}}$ and the elementary sector invariant under $\mathrm{SU}(2) \times \mathrm{SU}(3) \times \mathrm{U}(1)_{\mathrm{Y}}$. The SM gauge symmetry is identified with the diagonal subgroup, where the "composite hypercharge" generator is defined as follows

$$T_Y = T_X + T_R^3. \tag{5.2}$$

The Higgs boson appears as the Goldstone boson of the spontaneous symmetry breaking SO(5)/SO(4). We will use the CCWZ formalism [83, 84] to parametrise the nonlinearly realised symmetry SO(5)/SO(4) for the composite sector (in our discussion we will follow closely the notations of [85]). Then the Higgs boson appears inside the usual Goldstone boson matrix U which in the unitary gauge is equal to:

$$U = e^{i\Pi(x)} = \begin{pmatrix} \mathbb{1}_{3\times 3} & & \\ & \cos\frac{h}{f} & \sin\frac{h}{f} \\ & -\sin\frac{h}{f} & \cos\frac{h}{f} \end{pmatrix}, \tag{5.3}$$

where h is the Higgs boson and the f is the scale of the global symmetry breaking. It is customary to define two covariant derivatives (Maurer-Cartan 1-form)

$$-iU^\dagger D_\mu U = d_\mu^{\hat{a}} T^{\hat{a}} + E_\mu^a T^a = d_\mu + E_\mu \tag{5.4}$$

decomposing it along the broken $T^{\hat{a}}$ and unbroken T^a generators. The Higgs kinetic term and the mass of the gauge terms come from the two derivative term of the chiral Lagrangian

$$\frac{f^2}{4} Tr(d_\mu d^\mu) = \frac{1}{2}(\partial_\mu h)^2 + \frac{1}{2}\left(2m_W^2 W_\mu^+ W_\mu^- + m_Z^2 Z_\mu Z^\mu\right)\sin^2\frac{h}{f}. \tag{5.5}$$

5.1.1 Fermion masses

Let us proceed to the fermion mass generation. For concreteness we consider the model where the composite fields appear as a fiveplets of SO(5), i.e. MCHM5 model [79]. However we will show explicitly that our results depend only mildly on this assumption and practically do not change for the other fermion embeddings. The fivepletes after the SO(5)/SO(4) breaking can be decomposed as a fourplet of SO(4) and a singlet. The fourplet of SO(4) has in its turn two $\mathrm{SU}(2)_{\mathrm{L}}$ doublets: one with the standard model quantum numbers denoted as $\mathcal{O}_{\mathbf{SM}}$,[9] and another one $\mathcal{O}_{\mathbf{EX}}$, where the doublets are related by $\mathrm{SU}(2)_{\mathrm{R}}$ transformations.

[9] We intend that it has the same quantum numbers as the elementary doublet under the $\mathrm{SU}(3)\times\mathrm{SU}(2)_{\mathrm{L}}\times\mathrm{U}(1)_{\mathrm{Y}}$ subgroup.

JHEP11(2018)187

	$\mathrm{SU}(3)^{\mathrm{co}}$	$\mathrm{SU}(2)^{\mathrm{co}}_L$	$\mathrm{SU}(2)^{\mathrm{co}}_R$	$\mathrm{U}(1)^{\mathrm{co}}_X$
$\tilde{\mathcal{O}}_{q_1}$	**3**	**2**	**2**	2/3
$\tilde{\mathcal{O}}_{q_2}$	**3**	**2**	**2**	−1/3
$\tilde{\mathcal{O}}_u$	**3**	**1**	**1**	2/3
$\tilde{\mathcal{O}}_d$	**3**	**1**	**1**	−1/3
$\tilde{\mathcal{O}}_{\ell_1}$	**1**	**2**	**2**	0
$\tilde{\mathcal{O}}_{\ell_2}$	**1**	**2**	**2**	−1
$\tilde{\mathcal{O}}_e$	**1**	**1**	**1**	−1

	$\mathrm{SU}(3)^{\mathrm{el}}$	$\mathrm{SU}(2)^{\mathrm{el}}_L$	$\mathrm{U}(1)_Y{}^{\mathrm{el}}$
$\tilde{q}_L$	**3**	**2**	1/6
$\tilde{u}_R$	**3**	**1**	2/3
$\tilde{d}_R$	**3**	**1**	−1/3
$\tilde{\ell}_L$	**1**	**2**	−1/2
$\tilde{e}_R$	**1**	**1**	−1
$\tilde{\nu}_R$	**1**	**1**	0

Table 2. Group representations and charges of the fermion composite resonances and elementary fields.

The singlet operators are denoted as $\tilde{\mathcal{O}}_{u,d,e}$ and the full spectrum is

$$\tilde{\mathcal{O}}_{q_1} = \left(\tilde{\mathcal{O}}^{q_1}_{\mathbf{EX}}\,\tilde{\mathcal{O}}^{q_1}_{\mathbf{SM}}\right), \quad \tilde{\mathcal{O}}^{q_1}_{\mathbf{SM}} = \begin{pmatrix} U \\ D \end{pmatrix}, \qquad \tilde{\mathcal{O}}^{q_1}_{\mathbf{EX}} = \begin{pmatrix} \chi_{5/3} \\ \chi_{2/3} \end{pmatrix}$$
$$\text{5-plet} \quad \Psi_{q_1} = \left(\tilde{\mathcal{O}}_{q_1}, \tilde{\mathcal{O}}_u\right) \tag{5.6}$$

$$\tilde{\mathcal{O}}_{q_2} = \left(\tilde{\mathcal{O}}^{q_2}_{\mathbf{SM}}\,\tilde{\mathcal{O}}^{q_2}_{\mathbf{EX}}\right), \quad \tilde{\mathcal{O}}^{q_2}_{\mathbf{SM}} = \begin{pmatrix} U' \\ D' \end{pmatrix}, \qquad \tilde{\mathcal{O}}^{q_2}_{\mathbf{EX}} = \begin{pmatrix} \chi_{-1/3} \\ \chi_{-4/3} \end{pmatrix}$$
$$\text{5-plet} \quad \Psi_{q_2} = \left(\tilde{\mathcal{O}}_{q_2}, \tilde{\mathcal{O}}_d\right) \tag{5.7}$$

$$\tilde{\mathcal{O}}_{\ell_1} = \left(\tilde{\mathcal{O}}^{\ell_1}_{\mathbf{EX}}\,\tilde{\mathcal{O}}^{\ell_1}_{\mathbf{SM}}\right), \quad \tilde{\mathcal{O}}^{\ell_1}_{\mathbf{SM}} = \begin{pmatrix} N \\ E \end{pmatrix}, \qquad \tilde{\mathcal{O}}^{\ell_1}_{\mathbf{EX}} = \begin{pmatrix} \chi_{+1} \\ \chi_0 \end{pmatrix}$$
$$\text{5-plet} \quad \Psi_{l_1} = \left(\tilde{\mathcal{O}}_{l_1}, \tilde{\mathcal{O}}_N\right) \tag{5.8}$$

$$\tilde{\mathcal{O}}_{\ell_2} = \left(\tilde{\mathcal{O}}^{\ell_2}_{\mathbf{SM}}\,\tilde{\mathcal{O}}^{\ell_2}_{\mathbf{EX}}\right), \quad \tilde{\mathcal{O}}^{\ell_2}_{\mathbf{SM}} = \begin{pmatrix} N' \\ E' \end{pmatrix}, \qquad \tilde{\mathcal{O}}^{\ell_2}_{\mathbf{EX}} = \begin{pmatrix} \chi_{-1} \\ \chi_{-2} \end{pmatrix}$$
$$\text{5-plet} \quad \Psi_{l_2} = \left(\tilde{\mathcal{O}}_{l_2}, \tilde{\mathcal{O}}_e\right) \tag{5.9}$$

where the charges of the components of a $\mathrm{SU}(2)_{\mathrm{R}}$ doublet $\tilde{\mathcal{O}} = \left(\tilde{\mathcal{O}}_1, \tilde{\mathcal{O}}_2\right)$ under T^3_R are equal to $+\frac{1}{2}$ and $-\frac{1}{2}$ respectively. The elementary fields are denoted as $\tilde{q}_L$, $\tilde{l}_L$, $\tilde{u}_R$, $\tilde{d}_R$, $\tilde{e}_R$. Each field is a 3-vector in the flavour generation space and the subscript of χ field indicates its electric charge.

The elementary $\mathrm{SU}(2)_{\mathrm{L}}$ doublet $\tilde{q}_L$ is embedded in the incomplete fiveplet of SO(5). Thus, the group representations and charges of the fermion states are depicted in table 2. Note that we have two composite doublets $\tilde{\mathcal{O}}^{q_1}_{\mathbf{SM}}$ and $\tilde{\mathcal{O}}^{q_2}_{\mathbf{SM}}$ which have the same quantum numbers under the SM gauge group; similarly for the leptons.

JHEP11(2018)187

The symmetries of the composite sector are broken explicitly to the diagonal subgroup by the mixing with the elementary sector, which is given by:

$$\begin{aligned}\mathcal{L}_{\text{flavour}} = \lambda_q M_* \bar{\tilde{q}}_L U(h)\Psi_{q_1} + \tilde{\lambda}_q M_* \bar{\tilde{q}}_L U(h)\Psi_{q_2} + \lambda_u M_* \bar{\tilde{u}}_R U(h)\Psi_{q_1} + \lambda_d M_* \bar{\tilde{d}}_R \Psi_{q_2} \\ + \lambda_l M_* \bar{\tilde{l}}_L U(h)\Psi_{l_1} + \tilde{\lambda}_l M_* \bar{\tilde{l}}_L U(h)\Psi_{l_2} + \lambda_e M_* \bar{\tilde{e}}_R U(h)\Psi_{l_2}\end{aligned} \tag{5.10}$$

where the SM doublets where uplifted to incomplete 5-plets as follows:

$$\begin{aligned}\lambda_q \tilde{q}_L &\equiv \lambda_q \left[(0, q_L), 0\right] \\ \tilde{\lambda}_q \tilde{q}_L &\equiv \tilde{\lambda}_q \left[(q_L, 0), 0\right],\end{aligned} \tag{5.11}$$

where we put zeros in all the missing components and $(q_L, 0)$ singles out the SO(4) multiplet. Note also that symmetries of the model allow us to further split λ_q mixing into two independent parameters

$$\lambda_q \bar{\tilde{q}}_L U(h)\Psi_{q_1} \to \begin{cases} \left[\lambda_q^{(4)} \bar{\tilde{q}}_L\right]_I U(h)_{Ii} \left[\mathcal{O}_{q_1}\right]_i, \text{ where } I = 1, \dots 5, \quad i = 1, \dots 4 \\ \left[\lambda_q^{(1)} \bar{\tilde{q}}_L\right]_I U(h)_{I5} \mathcal{O}_u \end{cases}, \tag{5.12}$$

where the sum over repeating indices is understood. Let us look at the fermion spectrum before EWSSB. Due to the mixing λ we will have one massless SM state and one heavy field with the mass $M_*(1+\lambda)/\sqrt{1+\lambda^2}$, which becomes M_* in the limit $\lambda \ll 1$. This leads to the mixing between the elementary and composite states which can be described by the mixing angles defined as follows:

$$\begin{pmatrix} \tilde{\psi} \\ \tilde{\mathcal{O}} \end{pmatrix} = \begin{pmatrix} \cos\theta_\psi & -\sin\theta_\psi \\ \sin\theta_\psi & \cos\theta_\psi \end{pmatrix} \begin{pmatrix} \psi' \\ \mathcal{O} \end{pmatrix} \tag{5.13}$$

with

$$\sin\theta_\psi \equiv \hat{s} = \frac{\lambda}{\sqrt{1+\lambda^2}}, \qquad \cos\theta_\psi \equiv \hat{c} = \frac{1}{\sqrt{1+\lambda^2}}, \tag{5.14}$$

where $\hat{s}, \hat{c}$ are the sine and cosine of the corresponding mixing angles. Then the SM Yukawa coupling will scale as

$$y_{u,d} \sim \frac{s_{q_{1,2}} s_{u,d} M_*}{f}. \tag{5.15}$$

5.1.2 Vector fields

We are interested in the interactions between the SM fermions and the composite vector fields. We will follow the vector formalism [85] (see for example the ref. [86] for the comparison of various formalisms) for a spin-1 fields where it is assumed that the vector fields transform non-homogeneously

$$\tilde{\rho}_\mu \to \mathcal{H}\tilde{\rho}_\mu \mathcal{H}^\dagger - i\mathcal{H}\partial_\mu \mathcal{H}^\dagger, \tag{5.16}$$

where $\mathcal{H}$ is unbroken subgroup (SO(4)) transformation. Then the following interactions are allowed by the CCWZ symmetries:

$$\mathcal{L}^{\text{vec}} = -\frac{1}{4g_*^2}\tilde{\rho}^a_{\mu\nu}\tilde{\rho}_a^{\mu\nu} + \frac{M_*^2}{2g_*^2}(\tilde{\rho}^a_\mu - E^a_\mu)^2 + \dots \tag{5.17}$$

JHEP11(2018)187

where g_* is a strength of interactions between the composite fields and we have ignored the higher derivative terms. The Lagrangian eq. (5.17) in the limit of vanishing Higgs vev reduces to

$$\mathcal{L}_{\rm vec} = -\frac{1}{4}\tilde{\rho}^a_{\mu\nu}\tilde{\rho}^{\mu\nu}_a + \frac{M_*^2}{2}\tilde{\rho}^a_\mu\tilde{\rho}^\mu_a - M_*^2\frac{g_{el}}{g_*}\tilde{\rho}^a_\mu A^\mu_a + \frac{M_*^2}{2}\frac{g_{el}^2}{g_*^2}A^a_\mu A^\mu_a, \tag{5.18}$$

where A^μ_a are the elementary vector fields. The interaction between $\tilde{\rho}$ and the composite fermions can be deduced from the symmetries

$$\mathcal{L}_{ferm} = \bar{\Psi}\gamma^\mu\left(i\partial_\mu + g_*\tilde{\rho}_\mu\right)\Psi, \tag{5.19}$$

where $\tilde{\rho}_\mu = \tilde{\rho}^a_\mu T^{\rm co}_a$and $T^{\rm co}_a$ are the generators of the global symmetry group of the composite sector.[10] In order to get mass eigenstates vectors, a diagonalisation of the matrix of masses and mixing is needed

$$\begin{pmatrix} A_\mu \\ \tilde{\rho}_\mu \end{pmatrix} \to \begin{pmatrix} \cos\theta & -\sin\theta \\ \sin\theta & \cos\theta \end{pmatrix}\begin{pmatrix} A^{SM}_\mu \\ \rho_\mu \end{pmatrix}, \qquad \cos\theta = \frac{g_*}{\sqrt{g_*^2+g_{el}^2}} \tag{5.20}$$

where $\tilde{\rho}_\mu$ is an eigenstate with mass of $M_*\sqrt{1+g_{el}^2/g_*^2}$ and the orthogonal A^{SM}_μ is the massless state, that is identified with the SM gauge boson. Rotating to the mass eigenstate basis we get

$$\bar{\psi'}_i\left[\sqrt{g_*^2-g^2}\left[\hat{s}^\dagger T^{\rm co}_a\hat{s}\right]^i_j - \frac{g^2}{\sqrt{g_*^2-g^2}}\left[\hat{c}^\dagger T^{\rm el}_a\hat{c}\right]^i_j\right]\gamma^\mu\psi'^j\rho^a_\mu\,, \tag{5.21}$$

where the first term comes from the mixing of the elementary and composite fermions and the second term corresponds to the mixing between composite and elementary vector bosons (eq. (5.20)). In this paper we are mainly interested in the flavour non universal and flavour violating effects, so the contribution of the last term will be subleading since $g_* \gg g$ and the non-universalities in $\hat{c} \sim 1 - \hat{s}^2/2$ have an extra $\hat{s}$ supression. Note that the eq. (5.21) is a generic prediction of the partial compositness and the various fermion embeddings lead only to the generators $T^a_{\rm co}$ for the different group representations.

5.2 R_{D,D^*} from the composite electroweak resonances

We are interested in the dimension-6 four-fermion operators. These operators are generated by the exchange of the composite vector resonances. Using the eq. (5.21) and assuming $g_* \gg g$ we can see that the these operators at the dimension-6 level schematically take the form

$$\frac{g_*^2}{M_*^2}\left[\bar{\psi'}\,\hat{s}^\dagger T^{\rm co}_a\hat{s}\,\gamma^\mu\psi'\right]\left[\bar{\psi'}\,\hat{s}^\dagger T^{\rm co}_a\hat{s}\,\gamma_\mu\psi'\right]. \tag{5.22}$$

Our aim would now be to understand the correlations among the flavour-changing $\Delta F = 2$ operators and those that contribute to the $R_{D^{(*)}}$ anomalies. The effective Lagrangian for the $\Delta F = 2$ transitions can be written as

$$\mathcal{L}_{\Delta F=2} = -{\rm const}\times\frac{g_*^2}{M_*^2}\left(\bar{\psi}_{i\,L}\left[V_L^{d\dagger}\hat{s}_q^\dagger\hat{s}_q V_L^d\right]^i_{\ j}\gamma^\mu\,\psi_{j\,L}\right)^2, \tag{5.23}$$

[10] Of course, we can have different values of g_* for SU(3), SO(5) and U(1)$_X$ parts of the global group.

JHEP11(2018)187

where V_L^d is the rotation matrix for the left-handed quarks defined in eq. (4.15) and the constant in front for the case of MCHM5 is equal to

$$\text{const} = \frac{M_*^2}{2g_*^2}\left(\frac{1}{3}\frac{g_{*3}^2}{M_{*3}^2} + \frac{1}{2}\frac{g_{*2}^2}{M_{*2}^2} + \frac{4}{9}\frac{g_{*X}^2}{M_{*X}^2}\right) . \tag{5.24}$$

The first term inside the parenthesis corresponds to the contribution of the composite gluon, the second to the $\mathrm{SU(2)_{L,R}}$ triplets and the third to $\mathrm{U(1)_X}$ vector bosons (the number 4/9 is fixed by the $\mathrm{U}(1)_X$ charge assignment of the up-like multiplet $\tilde{O}_{q_1}$, see eq. (5.6)). Experimental data on $\bar{K}$-K, $\bar{B}_d$-B_d and $\bar{B}_s$-B_s mixings give the following constraints,[11]

$$\left|\left[V_L^{d\dagger}\hat{s}_q^\dagger\hat{s}_q V_L^d\right]^i{}_j\right| \lesssim \frac{(M_*/\text{TeV})}{g_*\sqrt{\text{const}}} \begin{cases} 10^{-3}\,, \text{ from } \bar{K}\text{-}K \text{ mixing, i.e., } i=1, j=2 \text{ [87]} \\ 1.1\times 10^{-3}\,, \text{ from } \bar{B}_d\text{-}B_d \text{ mixing, i.e., } i=1, j=3 \text{ [88]} \\ 4\times 10^{-3}\,, \text{ from } \bar{B}_s\text{-}B_s \text{ mixing, i.e., } i=2, j=3 \text{ [88]}, \end{cases} \tag{5.25}$$

where the numerical values are obtained by running the couplings to the scale M_*. Keeping the above constraints from $\Delta F = 2$ processes in mind, we now look at the $b \to c\tau\nu$ transitions. We assume that the NP contribution arises from the exchange of a composite vector field which is a triplet of $\mathrm{SU(2)_L}$. This generates the interaction Lagrangian

$$\begin{aligned} \mathcal{L}_{b\to c\,\tau\,\nu} &= -\frac{g_{*2}^2}{2M_{*2}^2}\left(\bar{\tau}_L\left[V_L^{e\dagger}\hat{s}_l{}^\dagger\hat{s}_l V_L^{\nu\dagger}\right]^3{}_3\,\gamma^\mu\,\nu_{\tau L}\right)\left(\bar{c}_L\left[V_L^{u\dagger}\hat{s_q}{}^\dagger\hat{s_q}V_L^d\right]^2{}_3\,\gamma^\mu\,b_L\right) \\ &= -\frac{g_*^2}{2M_*^2}\left(\bar{\tau}_L\left[V_L^{e\dagger}\hat{s}_l{}^\dagger\hat{s}_l V_L^{\nu}\right]^3{}_3\,\gamma^\mu\,\nu_{\tau L}\right)\left(\bar{c}_L\left[V_{\text{CKM}}V_L^{d\dagger}\hat{s_q}{}^\dagger\hat{s_q}V_L^d\right]^2{}_3\,\gamma^\mu\,b_L\right) , \end{aligned} \tag{5.26}$$

where we have assumed $g_{*2} = g_*, M_{*2} = M_*$ and the roational matrices are defined in eq. (4.15). If we decide to remain agnostic about the leptonic sector, we can still use the loose upper bound

$$\left|\left[V_L^{e\dagger}\hat{s}_l{}^\dagger\hat{s}_l V_L^{\nu}\right]^3{}_3\right| < 1 \tag{5.27}$$

which is satisfied even for maximal possible τ compositeness. Thus, for the explanation of R_D and R_{D^*} anomalies at the $1\,\sigma$ level, we need

$$\left[V_{\text{CKM}}V_L^{d\dagger}\hat{s_q}{}^\dagger\hat{s_q}V_L^d\right]^2{}_3 \gtrsim 0.2\left(\frac{M_*/g_*}{\text{TeV}}\right)^2 , \tag{5.28}$$

where the numerical factor 0.2 corresponds to $\Delta C_{\text{VL}}^\tau = -\Delta C_{\text{AL}}^\tau = 0.08$ (see figure 1). Expanding eq. (5.28), we get

$$\begin{aligned} &V_{cd}\left[V_L^{d\dagger}\hat{s_q}{}^\dagger\hat{s_q}V_L^d\right]^1{}_3 + V_{cs}\left[V_L^{d\dagger}\hat{s_q}{}^\dagger\hat{s_q}V_L^d\right]^2{}_3 + V_{cb}\left[V_L^{d\dagger}\hat{s_q}{}^\dagger\hat{s_q}V_L^d\right]^3{}_3 \gtrsim 0.2\left(\frac{M_*/g_*}{\text{TeV}}\right)^2 \\ \implies &|V_{cd}|\left|\left[V_L^{d\dagger}\hat{s_q}{}^\dagger\hat{s_q}V_L^d\right]^1{}_3\right| + |V_{cs}|\left|\left[V_L^{d\dagger}\hat{s_q}{}^\dagger\hat{s_q}V_L^d\right]^2{}_3\right| + |V_{cb}|\left|\left[V_L^{d\dagger}\hat{s_q}{}^\dagger\hat{s_q}V_L^d\right]^3{}_3\right| \gtrsim 0.2\left(\frac{M_*/g_*}{\text{TeV}}\right)^2 \end{aligned}$$

[11] Here, we have assumed that only one $\Delta F = 2$ operator (the operator Q_1 in the basis of [87]) is generated. In principle, other operator(s) may also be generated at the matching scale, and cancel part of the contribution from Q_1. However, barring large accidental cancellations, our results should always hold.

JHEP11(2018)187

Using the upper bounds on $\left|\left[V_L^{d\dagger}\hat{s_q}^\dagger\hat{s_q}V_L^d\right]^1_{\ 3}\right|$ and $\left|\left[V_L^{d\dagger}\hat{s_q}^\dagger\hat{s_q}V_L^d\right]^2_{\ 3}\right|$ from eq. (5.25) and the trivial inequality $\left|\left[V^{d\dagger}\hat{s_q}^\dagger\hat{s_q}V^d\right]^3_{\ 3}\right| \leq 1$, we now get

$$1.1\times10^{-3}\,|V_{cd}|\,\frac{(M_*/\text{TeV})}{g_*\sqrt{\text{const}}}+4\times10^{-3}\,|V_{cs}|\,\frac{(M_*/\text{TeV})}{g_*\sqrt{\text{const}}}+|V_{cb}|\gtrsim 0.2\left(\frac{M_*/\text{TeV}}{g_*}\right)^2 \tag{5.29}$$

As the first two terms are negligibly small compared to the third term (for small $(M_*/\text{TeV})/g_*$) on the left hand side, we finally get

$$M_*/g_* \lesssim\ 0.45\,\text{TeV} \tag{5.30}$$

Note that partial compositeness automatically selects the scenario (II) (see discussion after eq. (4.47)) for fitting the R_{D,D^*} anomalies. This solution, as mentioned in section 4.3, requires the presence of additional UV contributions to protect $g_L^{\tau,\nu}$ couplings of the Z boson. In the appendix F, we explicitly show how this can be achieved. Interestingly, the generated operators automatically satisfy the condition of scenario (I) due to the SO(4) structure of the model.

We would like to make a few comments here regarding the robustness of this result and its applicability to the various models employing partial compositeness. The only assumption that we have made in deriving the eq. (5.30) is that the charged current operator (see eq. (5.26)) is generated by a vector field, which is a triplet of electroweak $\text{SU}(2)_\text{L}$. The rest of the discussion is completely model independent and applies to various embeddings of the SM fermions into the composite multiplets, choices of the off-diagonal elementary-composite mixing parameters $\hat{s}$, and is practically independent of the mass of the composite gluon and the mass of the $\text{U}(1)_\text{X}$ vector. It should also be emphasised that we have been completely agnostic of the dynamics that allows the model under consideration to satisfy the constraints from $\Delta F = 2$ processes namely, those given in eq. (5.25). For example, in anarchic partial compositness, where the left-handed quark mixing parameters scale as the CKM matrix elements

$$[\hat{s}_q]_i \sim V_{ti} \tag{5.31}$$

these bounds are roughly $M_* \gtrsim 10$–$20\,\text{TeV}$ [89, 90],[12] which is a too high scale to explain the R_D and R_{D^*} anomalies. However the scale of the compositeness can be lowered and made consistent with the $R_{D^{(*)}}$ anomalies by invoking additional flavour symmetries, for example U(2) [17, 91, 92]. Interestingly the bounds from the direct searches at the LHC [93, 94] on the composite partners of the top quarks are still in the range of $M_* \gtrsim 1.2\,\text{TeV}$, making them consistent with the requirement of eq. (5.30)

The constraint in eq. (5.30), in general, can pose serious difficulties with the electroweak precision observables and measurement of Higgs's couplings to electroweak vector bosons. Indeed the constraints from electroweak precision tests [95–97] require the scale of

[12]The strongest constraint in this case comes from the ϵ_K bound.

JHEP11(2018)187

compositeness to be $\gtrsim 1.2\,\text{TeV}$ in order to satisfy the data at 2σ level. At the same time the mass of the vector resonance is related to the scale of compositeness, f, as

$$M_*^2 = a_\rho g_*^2 f^2, \tag{5.32}$$

where a_ρ is a number of $\mathcal{O}(1)$. In an explicit two-site construction, $a_\rho = 1/\sqrt{2}$ (see for example [81]) so that the compositeness scale is constrained to $f \lesssim 0.64\,\text{TeV}$. This is incompatible with the bound from electroweak precision measurements mentioned above. It may however be possible to accommodate the electroweak precision observables by additional UV contributions, see for example, [98–100].

The tension with meson mixing data makes it interesting to think of other possibilities of enhancing the contributions to R_D and R_{D^*} without modifying the $\Delta F = 2$ observables considerably. This can be partially achieved in scenarios with composite vector leptoquarks which we discuss in the next section.

5.3 Leptoquark contribution

The composite vector leptoquark scenario in connection to the B meson anomalies was first proposed in [17, 20, 24]. In this construction, the global symmetry of the composite sector is extended from SO(5) × SU(3) (where SU(3) is weakly gauged later and becomes the SU(3) of QCD) to SO(5) × SU(4). The composite gluon, which is an octet of SU(3), lies inside the **15** dimensional adjoint of SU(4) and is accompanied by two SU(3) triplets $\mathbf{3} + \bar{\mathbf{3}}$ ($\tilde{V}_{(3,1)_{\frac{2}{3}}} + \tilde{V}^*_{(\bar{3},1)_{-\frac{2}{3}}}$) and a singlet ($\tilde{B}_{(1,1)_0}$), where the subscripts of vectors indicate the representations under the $\text{SU}(3) \times \text{SU}(2)_L \times \text{U}(1)_Y$ subgroup. The hypercharge is given by the following combination of group generators: $Y = \sqrt{\frac{2}{3}} T_{15} + T^3_R + X$ and under the SM gauge group these fields. The Lagrangian is the same as in section 5.1, apart from the presence of $\tilde{V}_{(3,1)_{\frac{2}{3}}}$ and $\tilde{B}_{(1,1)_0}$ vector bosons. In particular, in the composite sector, leptoquarks couple to fermion currents in which there are quark and lepton resonances. Indeed, from eq. (5.19) one gets also the interaction

$$\frac{g_*}{\sqrt{2}} \tilde{V}_\mu \overline{\tilde{\mathcal{O}}}^q_{SM} \gamma^\mu \tilde{\mathcal{O}}^l_{SM} \tag{5.33}$$

where g_* is the strong coupling for the SU(4) of the composite sector. This interaction after integrating out the heavy fermions reduces to

$$\frac{g_*}{\sqrt{2}} \bar{\psi}'_q \left[\hat{s_q}^\dagger \hat{s}_l \right] \gamma^\mu \psi'_l \tilde{V}_\mu \,. \tag{5.34}$$

Here we focus only on the relevant interaction term for R_{D,D^*} anomalies,

$$\mathcal{L}_{LQ} = -g_* \left(\bar{q}'_{L\,i} \left[\hat{s}^\dagger_q \hat{s}_l \right]^i_{\ j} \gamma_\mu \, l'_{L\,j} \right) V^\mu_{LQ} \,. \tag{5.35}$$

Moving to the mass basis the effective Lagrangian for the $b \to c\,\tau\,\nu$ processes can now be written as,

$$\begin{aligned} \mathcal{L}_{b\to c\,\tau\,\nu} &= -\frac{g_*^2}{2M_*^2} \left(\bar{c}_L \left[V_{\text{CKM}} V_L^{d\dagger} \hat{s_q}^\dagger \hat{s}_l V_L^\nu \right]^2_{\ 3} \gamma^\mu \, \nu_{\tau L} \right) \left(\bar{\tau}_L \left[V_L^{e\dagger} \hat{s_l}^\dagger \hat{s_q} V_L^d \right]^3_{\ 3} \gamma^\mu \, b_L \right) \\ &\overset{\text{Fierz}}{=} -\frac{g_*^2}{2M_*^2} \left[V_{\text{CKM}} V_L^{d\dagger} \hat{s_q}^\dagger \hat{s}_l V_L^\nu \right]^2_{\ 3} \left[V_L^{e\dagger} \hat{s_l}^\dagger \hat{s_q} V_L^d \right]^3_{\ 3} \left(\bar{c}_L \, \gamma^\mu \, b_L \right) \left(\bar{\tau}_L \, \gamma^\mu \, \nu_{\tau L} \right) . \end{aligned} \tag{5.36}$$

JHEP11(2018)187

In order to find the upper bound on the coefficient of the operator $(\bar{c}_L\,\gamma^\mu\,b_L)\,(\bar{\tau}_L\,\gamma^\mu\,\nu_{\tau L})$, we need to find an upper bound on $\left[V_{\rm CKM}V_L^{d\dagger}\hat{s_q}^\dagger\hat{s}_l V_L^\nu\right]^2_{\ 3}$ consistent with the data on B meson mixing. As before, we have used the trivial inequality $\left[V_L^{e\dagger}\hat{s}_l{}^\dagger\hat{s}_q V_L^d\right]^3_{\ 3}\leq 1$.

Without loss of generality, we now go to the basis of elementary and composite fields in which the lepton compositeness matrix has the following form:

$$\hat{s}_l=\begin{pmatrix}*&0&0\\*&*&0\\*&*&*\end{pmatrix}\,, \tag{5.37}$$

where $*$ stands for non-zero entry. We now assume that only the third family of leptons has a strong mixing with the composite sector i.e. only $(\hat{s}_l)_{33}\sim 1$ and the rest of the elements are much smaller. In this case, the WC in eq. (5.36) is controlled by,

$$\left[V_{\rm CKM}V_L^{d\dagger}\hat{s_q}^\dagger\right]^2_{\ 3}=V_{cd}\left[V_L^{d\dagger}\hat{s_q}^\dagger\right]^1_{\ 3}+V_{cs}\left[V_L^{d\dagger}\hat{s_q}^\dagger\right]^2_{\ 3}+V_{cb}\left[V_L^{d\dagger}\hat{s_q}^\dagger\right]^3_{\ 3}\,. \tag{5.38}$$

Our aim now is to understand how big $\left[V_{\rm CKM}V_L^{d\dagger}\hat{s_q}^\dagger\right]^2_{\ 3}$ can be, consistently with an almost diagonal $\left[V_L^{d\dagger}\hat{s_q}^\dagger\hat{s}_q V_L^d\right]$ (as the off-diagonal elements are constrained to be $\lesssim 10^{-3}$, see eq. (5.25)). Similar to the leptonic elementary-composite mixing matrix $\hat{s}_l$, we can also make $\hat{s}_q$ triangular by suitable field redefinitions of the elementary fields. Thus, without loss of generality, we can write,

$$\hat{s}_q=\begin{pmatrix}s_{11}&0&0\\s_{21}&s_{22}&0\\s_{31}&s_{32}&s_{33}\end{pmatrix}\,, \tag{5.39}$$

Let us now consider the special case where only the third generation quark mixes strongly with the composite sector so that,

$$s_{33}\gg s_{ij},\quad i\text{ or }j\neq 3\,, \tag{5.40}$$

In this case, while $[V_L^{d\dagger}\hat{s_q}^\dagger]^3_{\ 3}$ can be close to unity, the other terms in eq. (5.38), in order to be consistent with a diagonal $\left[V_L^{d\dagger}\hat{s_q}^\dagger\hat{s}_q V_L^d\right]$, must scale as

$$\left[V_L^{d\dagger}\hat{s_q}^\dagger\right]^1_{\ 3}\sim\frac{s_{31}(s_{ij})^2}{(s_{33})^2},\quad \left[V_L^{d\dagger}\hat{s_q}^\dagger\right]^2_{\ 3}\sim\frac{s_{32}(s_{ij})^2}{(s_{33})^2}\,. \tag{5.41}$$

It can be noticed that these elements have an additional suppression of (s_{ij}/s_{33}) compared to the naive expectation. This renders the contributions of the first two terms of eq. (5.38) subdominant. Thus, adding the contribution of the electroweak triplet from eq. (5.29), for the explanation of R_{D,D^*} anomalies at the $1\,\sigma$ level, we must have

$$\begin{aligned}2V_{cb}&\gtrsim 0.2\left(\frac{M_*/g_*}{\rm TeV}\right)^2\\ \implies M_*/g_*&\lesssim 0.63\,{\rm TeV}\,,\end{aligned} \tag{5.42}$$

JHEP11(2018)187

where we have assumed that the electroweak triplet and the leptoquarks have the same mass and coupling. Hence, the role of leptoquarks is just to double the contribution to R_{D,D^*} without worsening the other low energy observables. This increase of the upper bound on the scale of compositeness by a factor of $\sqrt{2}$ helps ameliorate the constraints from S and T parameters which are now in agreement at almost $2\,\sigma$ level.[13]

It is worth emphasising that the result of eq. (5.42) was derived assuming the hierarchical nature (see eq. (5.40)) of the mixing matrix $\hat{s}_q$ and the constraint of eq. (5.42) can be relaxed if this assumption is not valid. For example, if we assume that the matrix $\hat{s_q}$ is not hierarchical but unitary, then $\left[V_L^{d\dagger}\hat{s_q}^\dagger\right]$ is again unitary and $\left[V_L^{d\dagger}\hat{s_q}^\dagger\hat{s_q}V_L^{d}\right]$ is automatically diagonal. However, this only implies that

$$\left(\left[V_L^{d\dagger}\hat{s_q}^\dagger\right]^1_{\ 3}\right)^2+\left(\left[V_L^{d\dagger}\hat{s_q}^\dagger\right]^2_{\ 3}\right)^2+\left(\left[V_L^{d\dagger}\hat{s_q}^\dagger\right]^3_{\ 3}\right)^2=1\,. \tag{5.43}$$

Now, choosing $\left[V_L^{d\dagger}\hat{s_q}^\dagger\right]^2_{\ 3}\sim 1$ and the other two elements to be very small, we get from eq. (5.38) that $\left[V_{\rm CKM}V_L^{d\dagger}\hat{s_q}^\dagger\right]^2_{\ 3}\sim 1$. In this case, eq. (5.42) gets modified to

$$\begin{aligned}(1+V_{cb})&\gtrsim 0.2\left(\frac{M_*/g_*}{\rm TeV}\right)^2\\ \to M_*/g_*&\lesssim 2.28\,{\rm TeV}\,.\end{aligned} \tag{5.44}$$

This very conspired scenario could be realised in U(3) symmetric models [92, 101] where $\hat{s}_q\propto \mathbb{1}_{3\times 3}$. Indeed, if $\left[V_{\rm CKM}V_L^{d\dagger}\hat{s_q}^\dagger\right]^2_{\ 3}\sim 1$, the constraint on the composite scale becomes that of eq. (5.44). However in this case [92] we have to face the constraints from the modification of the Z decays to hadrons requiring (see table 4 of [92])

$$M_*\gtrsim 6\sqrt{g_*}{\rm TeV}, \tag{5.45}$$

for the composite fermions masses. Assuming the vector fields are at the same scale, fitting the anomalies becomes practically impossible.

6 R_{K,K^*} anomalies

In this section, we investigate very briefly whether the R_{K,K^*} anomalies can be explained within the composite Higgs framework (see [18–22, 24–28, 102] for related discussion). It is known that the discrepancy of the experimental data on R_K and R_{K^*} with the SM expectations can be alleviated by the following operator [103–108][14]

$$\mathcal{L}_{b\to s\mu\mu}=-\frac{1}{\Lambda^2}\,(\bar{s}\gamma_\mu P_L\,b)(\bar{\mu}\gamma^\mu P_L\,\mu)\,, \tag{6.1}$$

with $1/\Lambda^2\gtrsim 1/(38\,{\rm TeV})^2$ at the $1\,\sigma$ level.

[13] Note that if we assume $\frac{g_{*4}}{M_{*4}}>\frac{g_{*2}}{M_{*2}}$ i.e., smaller masses of the SU(4) resonances than those of the SO(4) fields, we can be in the situation where the composite leptoquark contribution dominates in R_{D,D^*} and the tension with electroweak precision observables can be relaxed even further.

[14] Actually, the experimental value of $R_{K^*}^{\rm Low}$ cannot be explained simultaneously with R_K and $R_{K^*}^{\rm Central}$ by this operator (see, for example, the upper left panel of figure 6 in [108]), and either additional light fields [108] or tensor operators [109] are required.

JHEP11(2018)187

In models with partial compositeness, such an operator can be generated by the exchange of either a neutral Z' vector boson or a vector leptoquark. We examine the flavour structures of these two cases and identify the features that can explain the data.

***Z′* contribution.** Following the analysis of section 5.2, neutral composite bosons $\rho^3_{L,R}, \rho_X$ will generate

$$\frac{g_{*2}^2}{2M_{*2}^2}\left(\bar{s}\,[V_L^{d\,\dagger}\hat{s}_q^\dagger\hat{s}_q V_L^d]^2{}_3\gamma_\mu P_L\, b\right)\left(\bar{\mu}\,[V_L^{e\,\dagger}\hat{s}_l^\dagger\hat{s}_l V_L^e]^2{}_2\gamma^\mu P_L\,\mu\right) \tag{6.2}$$

which, after implementing the $\bar{B}_s$-B_s mixing constraint from eq. (5.25), gives (assuming $V_L^e = \mathbb{1}$ and diagonal $\hat{s}_l$),

$$\frac{g_*}{(M_*/\text{TeV})}\frac{1}{\sqrt{\text{const}}}\,s_\mu^2 \gtrsim 0.35, \tag{6.3}$$

for the explanation of the R_{K,K^*} anomaly, where 'const' is defined in eq. (5.24) and $g_{*,2} = g_*$, $M_{*,2} = M_*$. This inevitably requires large muon compositeness. Let us compare our results with the discussion in the previous two sections 5.2 and 5.3. Constraints from $\Delta F = 2$ processes require an almost diagonal $\left[V_L^{d\dagger}\hat{s}^\dagger\hat{s}V_L^d\right]$ matrix, which forces the operator in eq. (6.2) to be small as well. However, note that if $\left[V_L^{d\dagger}\hat{s}^\dagger\hat{s}V_L^d\right]_{23} = \epsilon$ (ϵ being some small parameter), $\Delta F = 2$ observables scale as ϵ^2 and R_K as ϵ. It is precisely this extra power of ϵ suppression that can make the explanation for the two measurements consistent [20].

Leptoquark contribution. The flavour structure in this case is different from the Z' contribution and the relevant operator in given by

$$\frac{g_*^2}{M_*^2}\left(\bar{s}\,[V_L^{d\,\dagger}\hat{s}_q^\dagger\hat{s}_l V_L^e]^2{}_2\gamma_\mu P_L\,\mu\right)\left(\bar{\mu}\,[V_L^{e\,\dagger}\hat{s}_l^\dagger\hat{s}_q V_L^d]^2{}_3\gamma^\mu P_L\, b\right)\,, \tag{6.4}$$

In this case correlations with the other low energy measurements are less strict and as an illustration we will consider two extreme scenarios (for simplicity we will assume diagonal $\hat{s}_{l,q}$)

- *Flavour trivial lepton sector.* In this case we assume $V_L^e = \mathbb{1}$ and this obviously evades all the constraints from LFV processes like $\tau \to 3\mu$. In such a scenario, the main constraint comes from B_s mixing. Using the bound from eq. (5.25), we get

$$s_\mu \geq 0.1(\text{const})^{1/8}\left(\frac{M_*/\text{TeV}}{g_*}\right)^{3/4}, \tag{6.5}$$

  where $s_{s,b}$ are equal to the maximal possible values allowed by the $\bar{B}_s - B_s$ mixing. Interestingly, even in this case the bound becomes less strict compared to the one obtained for the Z' contribution (see eq. (6.3)). However, the scale of the muon compositeness must still be quite high.

JHEP11(2018)187

- *Flavour trivial down quarks* [24]. If we assume $V_L^d = \mathbb{1}$, R_K can be generated solely by the leptoquark contribution and Z' mediated diagrams vanish. Interestingly, we can correlate the R_K with the flavour violating τ decay $\tau \to 3\mu$ arising from the operator:

$$\text{const} \times \frac{g_*^2}{M_*^2}\left(\bar{\tau}\left[V_L^{e\dagger}\hat{s}_l^\dagger \hat{s}_l V_L^e\right]_2^3 \gamma_\mu P_L \mu\right)\left(\bar{\mu}\left[V_L^{e\dagger}\hat{s}_l^\dagger \hat{s}_l V_L^e\right]_2^2 \gamma_\mu P_L \mu\right) \tag{6.6}$$

where now

$$\text{const} = \frac{1}{2}\frac{M_*^2}{g_*^2}\left(\frac{g_*^2}{2M_{*2}^2} + \frac{3g_{*3}^2}{8M_{*3}^2} + \frac{g_{*X}^2}{4M_{*X}^2}\right), \tag{6.7}$$

comes from the contributions of the $\rho_L^3, \rho_R^3, \rho_X$ and $\rho_{T_{15}}$ and we have assumed that the λ_l mixing is the dominant one (see appendix F). Assuming that the mixing with the first generation is small, we focus only on the $\mu - \tau$ rotations with the mixing angle θ. The experimental bound on $\tau \to 3\mu$ [110] gives

$$\frac{\text{const}}{2}\frac{g_*^2}{M_*^2} s_\tau^2 \sin 2\theta \left[\cos^2\theta s_\mu^2 + \sin^2\theta s_\tau^2\right] \leq \frac{4\times 10^{-3}}{\text{TeV}^2} \tag{6.8}$$

If the angle θ is small, say $\theta \sim s_\mu/s_\tau \ll 1$, then the upper bound on the muon compositeness becomes

$$s_\mu s_\tau^{1/3} \leq 0.1\,(\text{const})^{-1/3}\left(\frac{M_*/\text{TeV}}{g_*}\right)^{2/3}. \tag{6.9}$$

On the other hand, the bound on R_K implies

$$s_s s_b s_\mu s_\tau \sin 2\theta \geq 10^{-3}\left(\frac{M_*/\text{TeV}}{g_*}\right)^2 \tag{6.10}$$

If $s_b \sim 1$ and $s_\tau \sim 1$ we see that there is no tension between the R_K data and the $\tau \to 3\mu$ data; in fact eq. (6.9) translates into a bound on the compositeness scale of the strange quark

$$s_s \geq 0.02\left(\frac{M_*/\text{TeV}}{g_*}\right)^{2/3}, \tag{6.11}$$

which is similar to the naive expectations for the left-handed strange quark compositeness $s_s \sim V_{ts}$.

Thus we can conclude that it is possible to fit R_K as well within the partial compositeness paradigm.

7 Summary and outlook

In this paper, we have studied various aspects of the R_D and R_{D^*} anomalies in depth. The main objective of our work has been to understand potential correlations of R_{D,D^*} to other $\Delta F = 1$ and $\Delta F = 2$ processes that give rise to constraints on the NP explanations, and thus allowing us to identify the desired properties of the underlying UV theory.

JHEP11(2018)187

After reviewing the possible roles of vector, axial-vector, scalar, pseudo-scalar and tensor operators in solving these anomalies (sections 2 and 3), we have investigated (section 4) how the linearly realised $SU(2) \times U(1)$ symmetry can give rise to correlations to other well measured $\Delta F = 1$ processes, e.g. $B \to K^* \nu\nu$, $B \to \rho\nu\nu$, $B \to \tau\nu$ and couplings like $Z\tau\tau$, $Z\nu\nu$ and $W\tau\nu$, posing serious difficulties in explaining R_{D,D^*}.

We then extend our analysis to composite Higgs paradigm with the partial compositeness mechanism to generate the fermion masses. In this case, because of an available power-counting rule, the $\Delta F = 2$ processes, namely K, B_d and B_s mixing measurements turn out to be extremely constraining. We show that generically the models with partial compositeness can offer an explanation of these anomalies only if the scale of compositeness is below 0.90 (0.64) TeV for scenarios with (without) leptoquarks. While the requirement of such a low scale is favoured by the electroweak hierarchy problem, it is problematic from direct searches, and also indirect electroweak precision measurements unless some additional cancellations are involved.

Finally, in section 6 we also comment on the possibility of explaining the other neutral current B-meson anomalies R_K and R_{K^*} in this framework.

As the charged current anomalies require a NP scale which is rather low ($\sim$ TeV), they might as well be the harbingers of new physics at the TeV scale. It is thus important to critically examine the models that can provide simultaneous solutions to different problems at the TeV scale. At this point, it seems that the manifestation of New Physics, if any, in the dynamics of flavour transitions is likely to be quite non-generic and subtle. Thus the interpretation of any NP signal would require a large amount of data with a high precision. It is encouraging that such a large amount of data are expected to come from both the LHCb and Belle-II in the near future, and hopefully, we are not far from an exciting discovery.

Acknowledgments

We thank Pritibhajan Byakti for collaboration in the initial stage of this work. We would also like to thank D. Marzocca and B. Gripaios for discussions, and Pouya Asadi and David Shih for pointing out a sign mistake to us. The research of DB was supported in part by the Israel Science Foundation (grant no. 780/17).

A Decay width of the B_c meson

The differential decay rate for the process $B_c^-(p) \to \tau^-(k_1) + \bar{\nu}_\tau(k_2)$ is given by

$$\frac{d\Gamma}{d\Omega} = \frac{1}{32\pi^2} \frac{|\mathbf{k_1}|}{m_{B_c}^2} \overline{|\mathcal{M}|^2}$$

where, $\mathbf{k_1}$ is the 3-momentum of the τ in the rest frame of the B_c meson, and

$$|\mathbf{k_1}| = \frac{m_{B_c}^2 - m_\tau^2}{2m_{B_c}} .$$

JHEP11(2018)187

The matrix element is given by,

$$i\mathcal{M} = \frac{2G_F V_{cb}}{\sqrt{2}}\Big[C^{cb\tau}_{\rm AL}\langle 0|\bar{c}\gamma^\mu\gamma_5 b|B_c(p)\rangle\bar{u}(k_1)(i\gamma_\mu P_L)v(k_2) + C^{cb\tau}_{\rm PL}\langle 0|\bar{c}\gamma_5 b|B_c(p)\rangle\bar{u}(k_1)(iP_L)v(k_2)$$
$$+C^{cb\tau}_{AR}\langle 0|\bar{c}\gamma^\mu\gamma_5 b|B_c(p)\rangle\bar{u}(k_1)(i\gamma_\mu P_R)v(k_2) + C^{cb\tau}_{PR}\langle 0|\bar{c}\gamma_5 b|B_c(p)\rangle\bar{u}(k_1)(iP_R)v(k_2)\Big]$$

(The operators $\mathcal{O}^{cb\ell\nu}_{\rm VL,VR}$, $\mathcal{O}^{cb\ell\nu}_{\rm SL,SR}$ and $\mathcal{O}^{cb\ell\nu}_{\rm TL,TR}$ do not contribute because the corresponding matrix elements, $\langle 0|\bar{c}\gamma^\mu b|B_c\rangle$, $\langle 0|\bar{c}b|B_c\rangle$ and $\langle 0|\bar{c}\sigma^{\mu\nu}b|B_c\rangle$ identically vanish)

$$= \frac{2G_F V_{cb}}{\sqrt{2}}\, i f_{B_c}\Big[C^{cb\tau}_{\rm AL}\, p^\mu\,\bar{u}(k_1)(i\gamma_\mu P_L)v(k_2) - C^{cb\tau}_{\rm PL}\frac{m^2_{B_c}}{m_b+m_c}\bar{u}(k_1)(iP_L)v(k_2)$$
$$+C^{cb\tau}_{AR}p^\mu\,\bar{u}(k_1)(i\gamma_\mu P_R)v(k_2) - C^{cb\tau}_{PR}\frac{m^2_{B_c}}{m_b+m_c}\bar{u}(k_1)(iP_R)v(k_2)\Big]$$

(In the above step, we have used $\langle 0|\bar{c}\gamma^\mu\gamma_5 b|B_c(p)\rangle = i f_{B_c}p^\mu$, and

$$\langle 0|\bar{c}\gamma_5 b|B_c(p)\rangle = -i f_{B_c}\frac{m^2_{B_c}}{m_b+m_c}\ )$$

$$= \frac{2G_F V_{cb}}{\sqrt{2}}\, i f_{B_c}\Big[C^{cb\tau}_{\rm AL}\, m_\tau\,\bar{u}(k_1)(iP_L)v(k_2) - C^{cb\tau}_{\rm PL}\frac{m^2_{B_c}}{m_b+m_c}\bar{u}(k_1)(iP_L)v(k_2)$$
$$+C^{cb\tau}_{AR}m_\tau\,\bar{u}(k_1)(iP_R)v(k_2) - C^{cb\tau}_{PR}\frac{m^2_{B_c}}{m_b+m_c}\bar{u}(k_1)(iP_R)v(k_2)\Big]$$

$$= \frac{2G_F V_{cb}}{\sqrt{2}}\, i m_\tau f_{B_c}\Big[\left(C^{cb\tau}_{\rm AL} - C^{cb\tau}_{\rm PL}\frac{m^2_{B_c}}{m_\tau(m_b+m_c)}\right)\bar{u}(k_1)(iP_L)v(k_2)$$
$$+\left(C^{cb\tau}_{AR} - C^{cb\tau}_{PR}\frac{m^2_{B_c}}{m_\tau(m_b+m_c)}\right)\bar{u}(k_1)(iP_R)v(k_2)\Big]$$

This gives,

$$\overline{|\mathcal{M}|^2} = \Big[2G_F^2|V_{cb}|^2\Big]\Big[m_\tau^2 f_{B_c}^2\Big]\Big[m_{B_c}^2\left(1-\frac{m_\tau^2}{m_{B_c}^2}\right)\Big]\times$$
$$\left(\left|C^{cb\tau}_{\rm AL} - \frac{m^2_{B_c}}{m_\tau(m_b+m_c)}C^{cb\tau}_{\rm PL}\right|^2 + \left|C^{cb\tau}_{AR} - \frac{m^2_{B_c}}{m_\tau(m_b+m_c)}C^{cb\tau}_{PR}\right|^2\right)$$

Thus, the partial decay rate is given by,

$$\Gamma_{B_c\to\tau\nu} = \frac{1}{16\,\pi\, m_{B_c}}\left(1-\frac{m_\tau^2}{m_{B_c}^2}\right)\overline{|\mathcal{M}|^2}$$
$$= \frac{1}{8\pi}G_F^2|V_{cb}|^2 f_{B_c}^2 m_\tau^2 m_{B_c}\left(1-\frac{m_\tau^2}{m_{B_c}^2}\right)^2\times$$
$$\left(\left|C^{cb\tau}_{\rm AL} - \frac{m^2_{B_c}}{m_\tau(m_b+m_c)}C^{cb\tau}_{\rm PL}\right|^2 + \left|C^{cb\tau}_{AR} - \frac{m^2_{B_c}}{m_\tau(m_b+m_c)}C^{cb\tau}_{PR}\right|^2\right)$$

JHEP11(2018)187

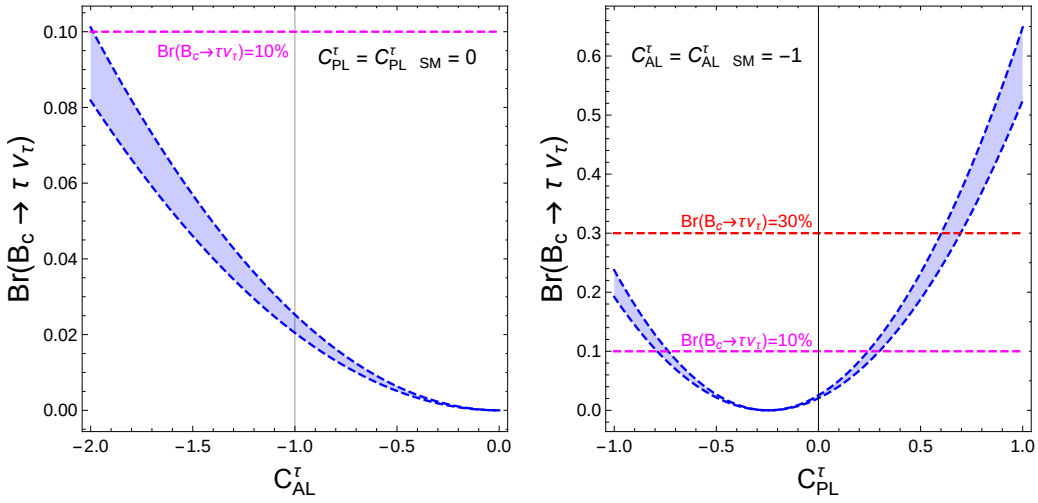

Figure 6. The $\mathrm{Br}(B_c \to \tau\,\nu_\tau)$ as a function of C^τ_{AL} and C^τ_{PL}. The upper bounds, 30% and 10% on this branching fraction from [53] and [54] respectively are also shown. The SM branching ratio is $\approx 2\%$. We have used $f_{B_c} = 0.434 \pm 0.015\,\mathrm{GeV}$ [111] in our calculation.

which gives, for the branching ratio,

$$\mathcal{B}(B_c^- \to \tau^- \bar{\nu}_\tau) = \frac{1}{8\pi} G_F^2 |V_{cb}|^2 f_{B_c}^2 m_\tau^2 m_{B_c} \tau_{B_c} \left(1 - \frac{m_\tau^2}{m_{B_c}^2}\right)^2 \times \left(\left| C_{\mathrm{AL}}^{cb\tau} - \frac{m_{B_c}^2}{m_\tau (m_b + m_c)} C_{\mathrm{PL}}^{cb\tau} \right|^2 + \left| C_{AR}^{cb\tau} - \frac{m_{B_c}^2}{m_\tau (m_b + m_c)} C_{PR}^{cb\tau} \right|^2 \right) \tag{A.1}$$

The variation of $\mathrm{Br}(B_c \to \tau\,\nu_\tau)$ as a function of C^τ_{AL} or C^τ_{PL} is shown in figure 6.

B Form factors for $B_c \to J/\psi$ and $B_c \to \eta_c$ decay processes

B.1 Vector and axial-vector form-factors

B.1.1 $B_c \to \eta_c$

The $B_c \to \eta_c$ matrix elements are parametrised in the same way as the $B \to D$ matrix elements, see for example section 4 of [51]. Unfortunately, only preliminary lattice results are available for $B_c \to \eta_c$ matrix elements [112]. In figure 7, we show the pQCD estimates of the F_+ and F_0 form-factors from [16]. The preliminary lattice results from [112] are also overlaid.

The functional form of F_0 and F_+ is given by

$$f = f_0 \exp\left(a\, q^2 + b\, (q^2)^2\right) \tag{B.1}$$

where f can be either F_0 or F_+. Then $f_0 = 0.48 \pm 0.06$, $a_{0(+)} = 0.037(0.055)$, $b_{0(+)} = 0.0007(0.0014)$.

$$\langle \eta_c(p_{\eta_c}, M_{\eta_c}) | \bar{c} \gamma^\mu b | \bar{B}(p_{B_c}, M_{B_c}) \rangle = F_+(q^2) \left[(p_{B_c} + p_{\eta_c})^\mu - \frac{M_{B_c}^2 - M_{\eta_c}^2}{q^2} q^\mu \right] + F_0(q^2) \frac{M_{B_c}^2 - M_{\eta_c}^2}{q^2} q^\mu \tag{B.2}$$

$$\langle \eta_c(p_{\eta_c}, M_{\eta_c}) | \bar{c} \gamma^\mu \gamma_5 b | \bar{B}(p_{B_c}, M_{B_c}) \rangle = 0 \tag{B.3}$$

JHEP11(2018)187

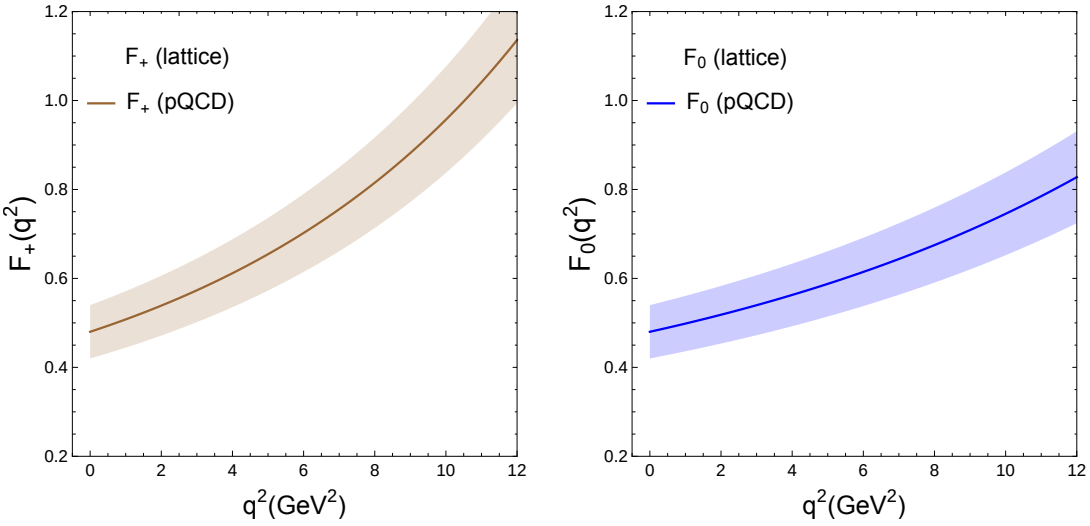

Figure 7. Form factors $F_0(q^2)^{B_c\to\eta_c}$ and $F_+(q^2)^{B_c\to\eta_c}$ from pQCD [16] and lattice [112].

B.1.2 $B_c \to J/\psi$

Similarly, parametrisation of the different $B_c \to J/\psi$ matrix elements are the same as those for $B \to D^*$ matrix elements, see again [51] for the notations. The pQCD estimates [16] for the $B_c \to J/\psi$ form-factors: V, A_0, A_1 and A_2, are shown in figure 8. Preliminary lattice results for V and A_1 from [112] are also shown.

B.2 Tensor form-factors

As no estimate of the tensor form-factors exists in the literature, we use the quark level equations of motion to relate them to the other form-factors. We show this explicitly below.

B.2.1 $B_c \to \eta_c$

The tensorial form factors are given by

$$\langle \eta_c(p_{\eta_c}, M_{\eta_c})|\bar{c}\, i\sigma^{\mu\nu} b|\bar{B}(p_{B_c}, M_{B_c})\rangle = (p^\mu_{B_c} p^\nu_{\eta_c} - p^\nu_{B_c} p^\mu_{\eta_c}) \frac{2F_T(q^2)}{M_{B_c} + M_{\eta_c}} \tag{B.4}$$

$$\langle \eta_c(p_{\eta_c}, M_{\eta_c})|\bar{c}\sigma^{\mu\nu}\gamma_5 b|\bar{B}(p_{B_c}, M_{B_c})\rangle = \varepsilon^{\mu\nu\rho\sigma} p_{B_c\rho} p_{\eta_c\sigma} \frac{2F_T(q^2)}{M_{B_c} + M_{\eta_c}} \tag{B.5}$$

Multiplying the l.h.s. of eq. (B.4) by q_μ and using $i\sigma^{\mu\nu} = \eta^{\mu\nu} - \gamma^\mu\gamma^\nu$ we get,

$$\begin{aligned} q_\mu \langle \eta_c|\bar{c} i\sigma^{\mu\nu} b|\bar{B}_c\rangle &= q^\nu \langle \eta_c|\bar{c}b|\bar{B}_c\rangle - \langle \eta_c|\bar{c}\not{q}\gamma^\nu b|\bar{B}_c\rangle \\ &= \langle \eta_c|\bar{c}b|\bar{B}_c\rangle q^\nu + (m_b + m_c)\langle \eta_c|\bar{c}\gamma^\nu b|\bar{B}_c\rangle - 2p_B^\nu \langle \eta_c|\bar{c}b|\bar{B}_c\rangle \\ &= -\langle \eta_c|\bar{c}b|\bar{B}_c\rangle (p_{B_c} + p_{\eta_c})^\nu + (m_b + m_c)\langle \eta_c|\bar{c}\gamma^\nu b|\bar{B}_c\rangle \\ &= -F_0 \frac{M^2_{B_c} - M^2_{\eta_c}}{m_b - m_c}(p_{B_c} + p_{\eta_c})^\nu \\ &\quad + (m_b + m_c)\left[F_+(p_{B_c} + p_{\eta_c})^\nu - (F_+ - F_0)\frac{M^2_{B_c} - M^2_{\eta_c}}{q^2} q^\nu\right] \end{aligned} \tag{B.6}$$

JHEP11(2018)187

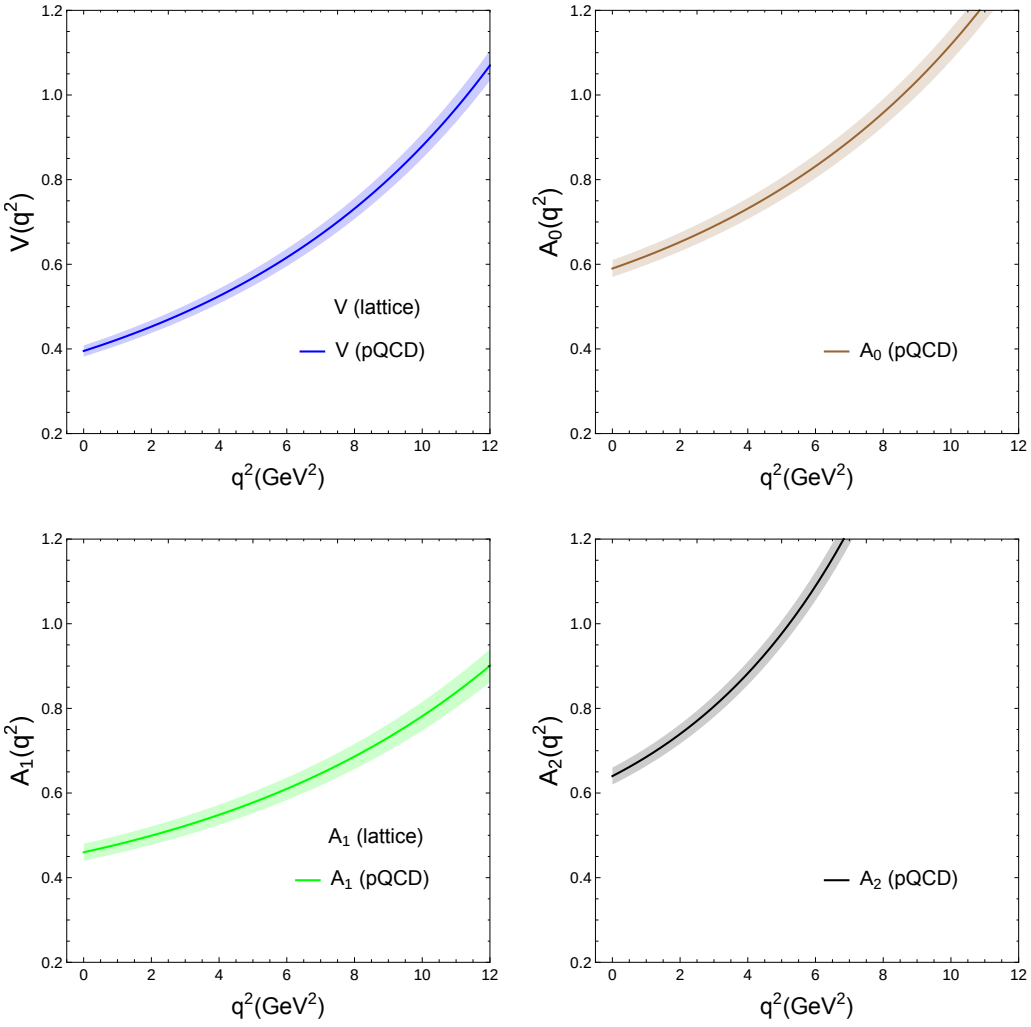

Figure 8. Form factors $V(q^2)^{B_c\to J/\psi}$, $A_0(q^2)^{B_c\to J/\psi}$, $A_1(q^2)^{B_c\to J/\psi}$ and $A_2(q^2)^{B_c\to J/\psi}$ from pQCD and lattice.

The l.h.s. of eq. (B.6), using the tensor form factor, is then

$$\left[(p_{B_c}-p_{\eta_c})^\nu\left(-\frac{M_{B_c}^2-M_{\eta_c}^2}{2}\right)+(p_{B_c}+p_{\eta_c})^\nu\left(\frac{M_{B_c}^2+M_{\eta_c}^2}{2}-p_{B_c}.p_{\eta_c}\right)\right]\frac{2F_T}{M_{B_c}+M_{\eta_c}} \tag{B.7}$$

Noting that $q=p_{B_c}-p_{\eta_c}$, we can equate the coefficients of q^ν on either side of eq. (B.6). This gives us the relation between the tensor and the vector form factors to be

$$-\frac{M_{B_c}^2-M_{\eta_c}^2}{M_{B_c}+M_{\eta_c}}F_T=-(m_b+m_c)\frac{M_{B_c}^2-M_{\eta_c}^2}{q^2}(F_+-F_0) \tag{B.8}$$

$$\implies F_T=(m_b+m_c)\frac{M_{B_c}+M_{\eta_c}}{q^2}(F_+-F_0) \tag{B.9}$$

JHEP11(2018)187

B.2.2 $B_c \to J/\psi$

The hadronic matrix elements for $\bar{B} \to V$ transition are parametrised by

$$\langle V(p_V,\epsilon,M_V)|\bar{c}\gamma_\mu b|\bar{B}(p_B,M_B)\rangle = i\varepsilon_{\mu\nu\rho\sigma}\epsilon^{\nu *}p_B^\rho p_V^\sigma \frac{2V(q^2)}{M_B+M_V} \tag{B.10}$$

$$\begin{aligned}\langle V(p_V,\epsilon,M_V)|\bar{c}\gamma_\mu\gamma_5 b|\bar{B}(p_B,M_B)\rangle =& 2M_V\frac{\epsilon^*.q}{q^2}q_\mu A_0(q^2)+(M_B+M_V)\left[\epsilon_\mu^*-\frac{\epsilon^*.q}{q^2}q_\mu\right]A_1(q^2)\\ &-\frac{\epsilon^*.q}{M_B+M_V}\left[(p_B+p_V)_\mu-\frac{M_B^2-M_V^2}{q^2}q_\mu\right]A_2(q^2)\end{aligned} \tag{B.11}$$

$$\langle V(p_V,\epsilon,M_V)|\bar{c}\gamma_5 b|\bar{B}(p_B,M_B)\rangle = -\epsilon^*.q\frac{2M_V}{m_b+m_c}A_0(q^2) \tag{B.12}$$

$$\begin{aligned}\langle V(p_V,\epsilon,M_V)|\bar{c}\ i\sigma_{\mu\nu} b|\bar{B}(p_B,M_B)\rangle =& -i\varepsilon_{\mu\nu\alpha\beta}\Bigg[-\epsilon^{\alpha *}(p_V+p_B)^\beta T_1(q^2)\\ &+\frac{M_B^2-M_V^2}{q^2}\epsilon^{*\alpha}q^\beta\left(T_1(q^2)-T_2(q^2)\right)\\ &+2\frac{\epsilon^*.q}{q^2}p_B^\alpha p_V^\beta\left(T_1(q^2)-T_2(q^2)-\frac{q^2}{M_B^2-M_{D^*}^2}T_3(q^2)\right)\Bigg]\end{aligned} \tag{B.13}$$

$$\langle V(p_V,\epsilon,M_V)|\bar{c}\ i\sigma_{\mu\nu}q^\nu b|\bar{B}(p_B,M_B)\rangle = -2i\varepsilon_{\mu\nu\rho\sigma}\epsilon^{*\nu}p_B^\rho p_V^\sigma T_1(q^2) \tag{B.14}$$

Using,

$$i\sigma_{\mu\nu} = \eta_{\mu\nu} - \gamma_\mu\gamma_\nu \tag{B.15}$$

the l.h.s. of eq. (B.14) yields,

$$\begin{aligned}\langle V\left(p_V,\epsilon,M_V\right)|\bar{c}\ i\sigma_{\mu\nu}q^\nu b|\bar{B}(p_B,M_B)\rangle &= \langle V\left(p_V,\epsilon,M_V\right)|\bar{c}\left(q_\mu-\gamma_\mu\ \not{q}\right)b|\bar{B}(p_B)\rangle\\ &= q_\mu\langle V\left(p_V,\epsilon,M_V\right)|\bar{c}b|\bar{B}(p_B,M_B)\rangle\\ &\quad-(m_b+m_c)\langle V\left(p_V,\epsilon,M_V\right)|\bar{c}\ \gamma_\mu b|\bar{B}(p_B,M_B)\rangle\end{aligned} \tag{B.16}$$

The first term vanishes, and after using eq. (B.10) and (B.14), leaves

$$-2i\varepsilon_{\mu\nu\rho\sigma}\epsilon^{*\nu}p_B^\rho p_V^\sigma T_1(q^2) = -(m_b+m_c)\times 2i\varepsilon_{\mu\nu\rho\sigma}\epsilon^{\nu *}p_B^\rho p_V^\sigma\frac{V(q^2)}{M_B+M_V}$$

which give us

$$T_1(q^2) = \frac{m_b+m_c}{M_B+M_V}V(q^2) \tag{B.17}$$

Consider the term $\langle V\left(p_V,\epsilon,M_V\right)|\bar{c}\ i\sigma_{\mu\nu}q^\nu\gamma_5 b|\bar{B}(p_B,M_B)\rangle$. Using

$$\sigma_{\mu\nu}\gamma_5 = \frac{i}{2}\varepsilon_{\mu\nu\rho\sigma}\sigma^{\rho\sigma} \qquad \text{(we use } \epsilon^{0123}=1\text{, which implied that } \epsilon_{0123}=-1\text{)}$$

we have

$$\langle V\left(p_V,\epsilon,M_V\right)|\bar{c}\ i\sigma_{\mu\nu}q^\nu\gamma_5 b|\bar{B}(p_B)\rangle = \frac{i}{2}\varepsilon_{\mu\nu\rho\sigma}\langle V\left(p_V,M_V\epsilon\right)|\bar{c}\ i\sigma^{\rho\sigma}q^\nu b|\bar{B}(p_B)\rangle$$

JHEP11(2018)187

Simplification of the r.h.s. using eq. (B.13), we get,

$$
\begin{aligned}
&= \frac{i}{2}\varepsilon_{\mu\nu\rho\sigma}q^{\nu}\left[-i\varepsilon^{\rho\sigma\alpha\beta}\left(-\epsilon^{*}_{\alpha}(p_{B_c}+p_{J/\psi})_{\beta}T_1+\frac{M^2_{B_c}-M^2_{J/\psi}}{q^2}\epsilon^{*}_{\alpha}q_{\beta}\,(T_1-T_2)\right.\right.\\
&\quad\left.\left.-\frac{\epsilon^{*}.q}{q^2}(p_{B_c}+p_{J/\psi})_{\alpha}(p_{B_c}-p_{J/\psi})_{\beta}\left(T_1-T_2-\frac{q^2}{M^2_{B_c}-M^2_{J/\psi}}T_3\right)\right)\right]\\
&= -\left(\delta^{\alpha}_{\mu}\delta^{\beta}_{\nu}-\delta^{\alpha}_{\nu}\delta^{\beta}_{\mu}\right)\left[-\epsilon^{*}_{\alpha}(p_{B_c}+p_{J/\psi})_{\beta}T_1+\frac{M^2_{B_c}-M^2_{J/\psi}}{q^2}\epsilon^{*}_{\alpha}q_{\beta}\,(T_1-T_2)\right.\\
&\quad\left.-\frac{\epsilon^{*}.q}{q^2}(p_{B_c}+p_{J/\psi})_{\alpha}q_{\beta}\left(T_1-T_2-\frac{q^2}{M^2_{B_c}-M^2_{J/\psi}}T_3\right)\right] \qquad \text{(B.18)}\\
&= \left[(p_{B_c}+p_{J/\psi}).q\;\epsilon^{*}_{\mu}-\epsilon^{*}.q(p_{B_c}+p_{J/\psi})_{\mu}\right]T_1-\left(M^2_{B_c}-M^2_{J/\psi}\right)\left(\epsilon^{*}_{\mu}-\frac{\epsilon^{*}.q}{q^2}q_{\mu}\right)(T_1-T_2)\\
&\quad+\epsilon^{*}.q\left[(p_{B_c}+p_{J/\psi})_{\mu}-\frac{(p_{B_c}+p_{J/\psi}).q}{q^2}q_{\mu}\right]\left(T_1-T_2-\frac{q^2}{M^2_{B_c}-M^2_{J/\psi}}T_3\right)\\
&= \epsilon^{*}_{\mu}\left[(M^2_{B_c}-M^2_{J/\psi})T_2\right]-\epsilon^{*}.q(p_{B_c}+p_{J/\psi})_{\mu}\left[T_2+\frac{q^2}{M^2_{B_c}-M^2_{J/\psi}}T_3\right]+\left(\frac{\epsilon^{*}.q}{q^2}q_{\mu}\right)\left[q^2\;T_3\right]
\end{aligned}
$$

The l.h.s. , simplified using the equation of motion is,

$$
\begin{aligned}
\langle J/\psi|\bar{c}\;i\sigma_{\mu\nu}q^{\nu}\gamma_5 b|\bar{B}_c\rangle &= (m_b-m_c)\langle J/\psi|\bar{c}\;\gamma_{\mu}\gamma_5 b|\bar{B}_c\rangle\\
&= (m_b-m_c)\left[2M_{J/\psi}\left(\frac{\epsilon^{*}.q}{q^2}q_{\mu}\right)A_0+(M_{B_c}+M_{J/\psi})\left(\epsilon^{*}_{\mu}-\frac{\epsilon^{*}.q}{q^2}q_{\mu}\right)A_1\right.\\
&\quad\left.-\frac{\epsilon^{*}.q}{M_{B_c}+M_{J/\psi}}\left((p_{B_c}+p_{J/\psi})_{\mu}-\frac{M^2_{B_c}-M^2_{J/\psi}}{q^2}q_{\mu}\right)A_2\right] \qquad \text{(B.19)}
\end{aligned}
$$

Comparing the coefficients of ϵ^{*}_{μ} from either side, we get

$$T_2 = \frac{m_b-m_c}{M_{B_c}-M_{J/\psi}}A_1 \qquad \text{(B.20)}$$

Comparing the coefficients of $\epsilon^{*}.q\;q_{\mu}/q^2$ from either side, we get

$$T_3 = -\left(\frac{m_b-m_c}{q^2}\right)\left(M_{B_c}(A_1-A_2)+M_{J/\psi}(A_1+A_2-2A_0)\right) \qquad \text{(B.21)}$$

The equations (B.17), (B.20) and (B.21) agree with those given in [113].

C Formulae for calculating branching ratios

The double differential branching fractions for the decays $B\to D\ell\nu_\ell$ and $B\to D^*\ell\nu_\ell$ can be written as

$$\frac{d^2\mathcal{B}^{D^{(*)}}_{\ell}}{dq^2\,d(\cos\theta)} = \mathcal{N}\,|p_{D^{(*)}}|\,\left(a^{D^{(*)}}_{\ell}+b^{D^{(*)}}_{\ell}\cos\theta+c^{D^{(*)}}_{\ell}\cos^2\theta\right). \qquad \text{(C.1)}$$

JHEP11(2018)187

The normalisation factor, $\mathcal{N}$ and the absolute value of the $D^{(*)}$-meson momentum, $|p_{D^{(*)}}|$ are given by,

$$\mathcal{N} = \frac{\tau_B\, G_F^2 |V_{cb}|^2 q^2}{256\pi^3 M_B^2} \left(1 - \frac{m_\ell^2}{q^2}\right)^2, \quad |p_{D^{(*)}}| = \frac{\sqrt{\lambda(M_B^2, M_{D^{(*)}}^2, q^2)}}{2M_B}, \tag{C.2}$$

where $\lambda(a,b,c) = a^2 + b^2 + c^2 - 2(ab + bc + ca)$. The angle θ is defined as the angle between the lepton and $D^{(*)}$-meson in the lepton-neutrino centre-of-mass frame, and q^2 is the invariant mass squared of the lepton-neutrino system.

C.1 Analytic formulas for $B \to D$ decay

The quantities a_ℓ^D, b_ℓ^D and c_ℓ^D for negative and positive helicity lepton are given by [51]:

Negative helicity lepton.

$$\begin{aligned}
a_\ell^D(-) &= \frac{8M_B^2|p_D|^2}{q^2} |\mathbf{C}_{\mathrm{VL}}^\ell|^2 \mathbf{F}_+^2 + m_\ell \left[\frac{32M_B^2|p_D|^2}{q^2\,(M_B+M_D)} \mathcal{R}\left(\mathbf{C}_{\mathbf{TL}}^\ell \mathbf{C}_{\mathrm{VL}}^{\ell *}\right) \mathbf{F}_+ \mathbf{F_T}\right] \\
&\quad + m_\ell^2 \left[\frac{32|p_D|^2 M_B^2}{q^2\,(M_B+M_D)^2} |\mathbf{C}_{\mathrm{TL}}^\ell|^2 \mathbf{F_T^2}\right] \\
b_\ell^D(-) &= 0 \\
c_\ell^D(-) &= -\frac{8M_B^2|p_D|^2}{q^2} |\mathbf{C}_{\mathrm{VL}}^\ell|^2 \mathbf{F}_+^2 - m_\ell \left[\frac{32|p_D|^2 M_B^2}{q^2\,(M_B+M_D)} \mathcal{R}\left(\mathbf{C}_{\mathrm{VL}}^\ell \mathbf{C}_{\mathrm{TL}}^\ell\right) \mathbf{F}_+ \mathbf{F_T}\right] \\
&\quad - m_\ell^2 \left[\frac{32|p_D|^2 M_B^2}{(M_B+M_D)^2\, q^2} |\mathbf{C}_{\mathrm{TL}}^\ell|^2 \mathbf{F_T^2}\right]
\end{aligned} \tag{C.3}$$

Positive helicity lepton.

$$\begin{aligned}
a_\ell^D(+) &= \frac{2\left(M_B^2 - M_D^2\right)^2}{(m_b - m_c)^2} |\mathbf{C}_{\mathrm{SL}}^\ell|^2 \mathbf{F_0^2} + m_\ell \left[\frac{4\left(M_B^2 - M_D^2\right)^2}{q^2 (m_b - m_c)} \mathcal{R}\left(\mathbf{C}_{\mathrm{SL}}^\ell \mathbf{C}_{\mathrm{VL}}^{\ell *}\right) \mathbf{F_0^2}\right] \\
&\quad + m_\ell^2 \left[\frac{2\left(M_B^2 - M_D^2\right)^2}{q^4} |\mathbf{C}_{\mathrm{VL}}^\ell|^2 \mathbf{F_0^2}\right] \\
b_\ell^D(+) &= \left[-16 M_B |p_D| \frac{M_B - M_D}{m_b - m_c} \mathcal{R}\left(\mathbf{C}_{\mathbf{SL}}^\ell \mathbf{C}_{\mathbf{TL}}^{\ell *}\right) \mathbf{F_0} \mathbf{F_T}\right] \\
&\quad - m_\ell \left[\frac{16|p_D|\,(M_B - M_D)\, M_B}{q^2} \mathcal{R}\left(\mathbf{C}_{\mathrm{VL}}^\ell \mathbf{C}_{\mathbf{TL}}^{\ell *}\right) \mathbf{F_0} \mathbf{F_T}\right. \\
&\qquad \left. + \frac{8|p_D| M_B \left(M_B^2 - M_D^2\right)}{q^2\,(m_b - m_c)} \mathcal{R}\left(\mathbf{C}_{\mathrm{SL}}^\ell \mathbf{C}_{\mathrm{VL}}^{\ell *}\right) \mathbf{F_0} \mathbf{F}_+\right] \\
&\quad - m_\ell^2 \left[\frac{8|p_D| M_B \left(M_B^2 - M_D^2\right)}{q^4} |\mathbf{C}_{\mathrm{VL}}^\ell|^2 \mathbf{F_0} \mathbf{F}_+\right] \\
c_\ell^D(+) &= \left[\frac{32|p_D|^2 M_B^2}{(M_B+M_D)^2} |\mathbf{C}_{\mathrm{TL}}^\ell|^2 \mathbf{F_T^2}\right] - \frac{32 M_B^2 |p_D|^2}{(M_B+M_D)\, q^2} \mathcal{R}\left(\mathbf{C}_{\mathrm{VL}}^\ell \mathbf{C}_{\mathrm{TL}}^{\ell *}\right) \mathbf{F}_+ \mathbf{F_T} \\
&\quad + m_\ell^2 \left[\frac{8|p_D|^2 M_B^2}{q^4} |\mathbf{C}_{\mathrm{VL}}^\ell|^2 \mathbf{F}_+^2\right]
\end{aligned} \tag{C.4}$$

JHEP11(2018)187

C.2 Semi-numerical formulas for R_D

We now provide semi-numerical formulae for the branching ratios and R_D in terms of the Wilson coefficients (WCs) (from now onwards, instead of using "$cb\ell\nu$" we will just use "ℓ" in the superscript of the operators and WCs):

$$\begin{aligned}\mathcal{B}(B\to D\tau\nu_\tau) = \Big(&6.9 + 13.9\ \mathbf{\Delta C^\tau_{VL}} + 11.9\ \mathbf{\Delta C^\tau_{SL}} + 3.5\ \mathbf{\Delta C^\tau_{TL}}\\ &+ 6.9\ \mathbf{(\Delta C^\tau_{VL})^2} + 9.4\ \mathbf{(\Delta C^\tau_{SL})^2} + 1.2\ \mathbf{(\Delta C^\tau_{TL})^2}\\ &+ 11.9\ \mathbf{\Delta C^\tau_{VL}\Delta C^\tau_{SL}} + 3.5\ \mathbf{\Delta C^\tau_{VL}\Delta C^\tau_{TL}}\Big)\times 10^{-3} \qquad \text{(C.5)}\\ \mathcal{B}(B\to D\ell_0\,\nu_{\ell_0}) = \Big(&23.3 + 46.6\ \mathbf{\Delta C^{\ell_0}_{VL}} + 2.0\ \mathbf{\Delta C^{\ell_0}_{SL}} + 1.0\ \mathbf{\Delta C^{\ell_0}_{TL}}\\ &+ 23.3\ \mathbf{(\Delta C^{\ell_0}_{VL})^2} + 33.5\ \mathbf{(\Delta C^{\ell_0}_{SL})^2} + 3.5\ \mathbf{(\Delta C^{\ell_0}_{TL})^2}\\ &+ 2.0\ \mathbf{\Delta C^{\ell_0}_{VL}\Delta C^{\ell_0}_{SL}} + 1.0\ \mathbf{\Delta C^{\ell_0}_{VL}\Delta C^{\ell_0}_{TL}}\Big)\times 10^{-3} \qquad \text{(C.6)}\end{aligned}$$

Here, ΔC^ℓ_i correspond to the NP WCs g^ℓ_i of eq. (2.1). The above formulas are based on the analytic expressions of the decay amplitudes given above which are based on ref. [51]. In order to obtain the various numerical coefficients, central values of the form-factors (see [51] for more details) and other parameters have been used.

If NP is assumed to exist only in the decay to τ leptons, one gets from the above formulas

$$\begin{aligned}R_D = &\,0.30 + 0.60\,\mathbf{\Delta C^\tau_{VL}} + 0.51\,\mathbf{\Delta C^\tau_{SL}} + 0.15\,\mathbf{\Delta C^\tau_{TL}}\\ &+ 0.30\,\mathbf{(\Delta C^\tau_{VL})^2} + 0.40\,\mathbf{(\Delta C^\tau_{SL})^2} + 0.05\,\mathbf{(\Delta C^\tau_{TL})^2}\\ &+ 0.51\,\mathbf{\Delta C^\tau_{VL}\Delta C^\tau_{SL}} + 0.15\,\mathbf{\Delta C^\tau_{VL}\Delta C^\tau_{TL}} \qquad \text{(C.7)}\end{aligned}$$

C.3 Analytic formulas for $B \to D^*$ decay

Negative helicity lepton.

$$\begin{aligned}a^{D^*}_\ell(-) = &\frac{8M_B^2\,|p_{D^*}|^2}{(M_B+M_{D^*})^2}\left|\mathbf{C^\ell_{VL}}\right|^2\mathbf{V^2} + \frac{(M_B+M_{D^*})^2\,(8M_{D^*}^2q^2+\lambda)}{2M_{D^*}^2q^2}\left|\mathbf{C^\ell_{AL}}\right|^2\mathbf{A_1^2}\\ &+\frac{8M_B^4|p_{D^*}|^4}{M_{D^*}^2\,(M_B+M_{D^*})^2\,q^2}\left|\mathbf{C^\ell_{AL}}\right|^2\mathbf{A_2^2} - \frac{4\,|p_{D^*}|^2\,M_B^2\,(M_B^2-M_{D^*}^2-q^2)}{M_{D^*}^2q^2}\left|\mathbf{C^\ell_{AL}}\right|^2\mathbf{A_1A_2}\\ &+m_\ell\left[\frac{32M_B^2\,|p_{D^*}|^2}{q^2\,(M_B+M_{D^*})}\mathcal{R}\left(\mathbf{C^\ell_{VL}C^{\ell*}_{TL}}\right)\mathbf{VT_1}\right.\\ &+\frac{8\,(M_B+M_{D^*})\left(2M_{D^*}^2\,(M_B^2-M_{D^*}^2)+M_B^2\,|p_{D^*}|^2\right)}{q^2M_{D^*}^2}\mathcal{R}\left(\mathbf{C^\ell_{AL}C^{\ell*}_{TL}}\right)\mathbf{A_1T_2}\\ &-\frac{8M_B^2\,(M_B^2-M_{D^*}^2-q^2)\,|p_{D^*}|^2}{q^2\,(M_B-M_{D^*})\,M_{D^*}^2}\mathcal{R}\left(\mathbf{C^\ell_{AL}C^{\ell*}_{TL}}\right)\mathbf{A_1T_3}\\ &-\frac{8M_B^2\,(M_B^2+3M_{D^*}^2-q^2)\,|p_{D^*}|^2}{q^2\,(M_B+M_{D^*})\,M_{D^*}^2}\mathcal{R}\left(\mathbf{C^\ell_{AL}C^{\ell*}_{TL}}\right)\mathbf{A_2T_2}\\ &\left.+\frac{32M_B^4|p_{D^*}|^4}{q^2M_{D^*}^2\,(M_B+M_{D^*})\,(M_B^2-M_{D^*}^2)}\mathcal{R}\left(\mathbf{C^\ell_{AL}C^{\ell*}_{TL}}\right)\mathbf{A_2T_3}\right]\\ &+m_\ell^2\left[\frac{32M_B^2\,|p_{D^*}|^2}{q^4}\left|\mathbf{C^\ell_{TL}}\right|^2\mathbf{T_1^2} + \frac{2\,(8M_{D^*}^2\,(2\,(M_B^2+M_{D^*}^2)-q^2)\,q^2+(4M_{D^*}^2+q^2)\,\lambda)}{q^4M_{D^*}^2}\left|\mathbf{C^\ell_{TL}}\right|^2\mathbf{T_2^2}\right.\\ &\left.+\frac{32M_B^4|p_{D^*}|^4}{q^2M_{D^*}^2\,(M_B^2-M_{D^*}^2)^2}\left|\mathbf{C^\ell_{TL}}\right|^2\mathbf{T_3^2} - \frac{16M_B^2\,|p_{D^*}|^2\,(M_B^2+3M_{D^*}^2-q^2)}{q^2M_{D^*}^2\,(M_B^2-M_{D^*}^2)}\left|\mathbf{C^\ell_{TL}}\right|^2\mathbf{T_2T_3}\right]\end{aligned}$$

JHEP11(2018)187

$$
\begin{aligned}
b_\ell^{D^*}(-) = & -16|p_{D^*}|M_B\mathcal{R}\left(\mathbf{C}_{\rm VL}^{\ell}\mathbf{C}_{\rm AL}^{\ell *}\right)\mathbf{V}\mathbf{A_1} - m_\ell\left[\frac{32M_B\left(M_B-M_{D^*}\right)|p_{D^*}|}{q^2}\mathcal{R}\left(\mathbf{C}_{\rm VL}^{\ell}\mathbf{C}_{\rm TL}^{\ell *}\right)\mathbf{V}\mathbf{T_2}\right. \\
& \left. + \frac{32M_B\left(M_B+M_{D^*}\right)|p_{D^*}|}{q^2}\mathcal{R}\left(\mathbf{C}_{\rm AL}^{\ell}\mathbf{C}_{\rm TL}^{\ell *}\right)\mathbf{A_1}\mathbf{T_1}\right] - m_\ell^2\left[\frac{64M_B\left(M_B^2-M_{D^*}^2\right)|p_{D^*}|}{q^4}\left|\mathbf{C}_{\rm TL}^{\ell}\right|^{\mathbf{2}}\mathbf{T_1}\mathbf{T_2}\right] \\
c_\ell^{D^*}(-) = & \frac{8|p_{D^*}|^2M_B^2}{\left(M_B+M_{D^*}\right)^2}\left|\mathbf{C}_{\rm VL}^{\ell}\right|^{\mathbf{2}}\mathbf{V^2} - \frac{\left(M_B+M_{D^*}\right)^2\lambda}{2M_{D^*}^2q^2}\left|\mathbf{C}_{\rm AL}^{\ell}\right|^{\mathbf{2}}\mathbf{A_1^2} - \frac{8|p_{D^*}|^4M_B^4}{\left(M_B+M_{D^*}\right)^2M_{D^*}^2q^2}\left|\mathbf{C}_{\rm AL}^{\ell}\right|^{\mathbf{2}}\mathbf{A_2^2} \\
& + \frac{4|p_{D^*}|^2M_B^2\left(M_B^2-M_{D^*}^2-q^2\right)}{M_{D^*}^2q^2}\left|\mathbf{C}_{\rm AL}^{\ell}\right|^{\mathbf{2}}\mathbf{A_1}\mathbf{A_2} \\
& + m_\ell\left[\frac{32M_B^2|p_{D^*}|^2}{q^2\left(M_B+M_{D^*}\right)}\mathcal{R}\left(\mathbf{C}_{\rm VL}^{\ell}\mathbf{C}_{\rm TL}^{\ell *}\right)\mathbf{V}\mathbf{T_1} - \frac{8M_B^2\left(M_B+M_{D^*}\right)|p_{D^*}|^2}{q^2M_{D^*}^2}\mathcal{R}\left(\mathbf{C}_{\rm AL}^{\ell}\mathbf{C}_{\rm TL}^{\ell *}\right)\mathbf{A_1}\mathbf{T_2}\right. \\
& + \frac{8M_B^2\left(M_B^2-M_{D^*}^2-q^2\right)|p_{D^*}|^2}{q^2M_{D^*}^2\left(M_B-M_{D^*}\right)}\mathcal{R}\left(\mathbf{C}_{\rm AL}^{\ell}\mathbf{C}_{\rm TL}^{\ell *}\right)\mathbf{A_1}\mathbf{T_3} \\
& + \frac{8M_B^2\left(M_B^2+3M_{D^*}^2-q^2\right)|p_{D^*}|^2}{q^2M_{D^*}^2\left(M_B+M_{D^*}\right)}\mathcal{R}\left(\mathbf{C}_{\rm AL}^{\ell}\mathbf{C}_{\rm TL}^{\ell *}\right)\mathbf{A_2}\mathbf{T_2} \\
& - \frac{32M_B^4|p_{D^*}|^4}{q^2M_{D^*}^2\left(M_B+M_{D^*}\right)\left(M_B^2-M_{D^*}^2\right)}\mathcal{R}\left(\mathbf{C}_{\rm AL}^{\ell}\mathbf{C}_{\rm TL}^{\ell *}\right)\mathbf{A_2}\mathbf{T_3} \\
& + m_\ell^2\left[\frac{32M_B^2|p_{D^*}|^2}{q^4}\left|\mathbf{C}_{\rm TL}^{\ell}\right|^{\mathbf{2}}\mathbf{T_1^2} + \frac{2\left(4M_{D^*}^2-q^2\right)\lambda}{M_{D^*}^2q^4}\left|\mathbf{C}_{\rm TL}^{\ell}\right|^{\mathbf{2}}\mathbf{T_2^2}\right. \\
& \left. - \frac{32M_B^4|p_{D^*}|^4}{q^2M_{D^*}^2\left(M_B^2-M_{D^*}^2\right)^2}\left|\mathbf{C}_{\rm TL}^{\ell}\right|^{\mathbf{2}}\mathbf{T_3^2} + \frac{16M_B^2|p_{D^*}|^2\left(M_B^2+3M_{D^*}^2-q^2\right)}{q^2M_{D^*}^2\left(M_B^2-M_{D^*}^2\right)}\left|\mathbf{C}_{\rm TL}^{\ell}\right|^{\mathbf{2}}\mathbf{T_2}\mathbf{T_3}\right] \qquad \text{(C.8)}
\end{aligned}
$$

Positive helicity lepton.

$$
\begin{aligned}
a_\ell^{D^*}(+) = & \frac{8|p_{D^*}|^2M_B^2}{\left(m_b+m_c\right)^2}\left|\mathbf{C}_{\rm PL}^{\ell}\right|^{\mathbf{2}}\mathbf{A_0^2} + \frac{32M_B^2|p_{D^*}|^2}{q^2}\left|\mathbf{C}_{\rm TL}^{\ell}\right|^{\mathbf{2}}\mathbf{T_1^2} + \frac{8\left(M_B^2-M_{D^*}^2\right)^2}{q^2}\left|\mathbf{C}_{\rm TL}^{\ell}\right|^{\mathbf{2}}\mathbf{T_2^2} \\
& - m_\ell\left[\frac{16|p_{D^*}|^2M_B^2}{\left(m_b+m_c\right)q^2}\mathcal{R}\left(\mathbf{C}_{\rm AL}^{\ell}\mathbf{C}_{\rm PL}^{\ell *}\right)\mathbf{A_0^2} - \frac{32M_B^2|p_{D^*}|^2}{q^2\left(M_B+M_{D^*}\right)}\mathcal{R}\left(\mathbf{C}_{\rm VL}^{\ell}\mathbf{C}_{\rm TL}^{\ell *}\right)\mathbf{V}\mathbf{T_1}\right. \\
& \left. - \frac{8(M_B+M_{D^*})\left(M_B^2-M_{D^*}^2\right)}{q^2}\mathcal{R}\left(\mathbf{C}_{\rm AL}^{\ell}\mathbf{C}_{\rm TL}^{\ell *}\right)\mathbf{A_1}\mathbf{T_2}\right] \\
& + m_\ell^2\left[\frac{8|p_{D^*}|^2M_B^2}{q^4}\left|\mathbf{C}_{\rm AL}^{\ell}\right|^{\mathbf{2}}\mathbf{A_0^2} + \frac{8|p_{D^*}|^2M_B^2}{\left(M_B+M_{D^*}\right)^2q^2}\left|\mathbf{C}_{\rm VL}^{\ell}\right|^{\mathbf{2}}\mathbf{V^2} + \frac{2\left(M_B+M_{D^*}\right)^2}{q^2}\left|\mathbf{C}_{\rm AL}^{\ell}\right|^{\mathbf{2}}\mathbf{A_1^2}\right] \\
b_\ell^{D^*}(+) = & \frac{8M_B\left(M_B^2+3M_{D^*}^2-q^2\right)|p_{D^*}|}{\left(m_b+m_c\right)M_{D^*}}\mathcal{R}\left(\mathbf{C}_{\rm PL}^{\ell}\mathbf{C}_{\rm TL}^{\ell *}\right)\mathbf{A_0}\mathbf{T_2} \\
& - \frac{32M_B^3|p_{D^*}|^3}{\left(m_b+m_c\right)M_{D^*}\left(M_B^2-M_{D^*}^2\right)}\mathcal{R}\left(\mathbf{C}_{\rm PL}^{\ell}\mathbf{C}_{\rm TL}^{\ell *}\right)\mathbf{A_0}\mathbf{T_3} \\
& + m_\ell\left[\frac{4|p_{D^*}|M_B\left(M_B+M_{D^*}\right)\left(M_B^2-M_{D^*}^2-q^2\right)}{M_{D^*}\left(m_b+m_c\right)q^2}\mathcal{R}\left(\mathbf{C}_{\rm AL}^{\ell}\mathbf{C}_{\rm PL}^{\ell *}\right)\mathbf{A_0}\mathbf{A_1}\right. \\
& - \frac{16}{\left(m_b+m_c\right)}\frac{|p_{D^*}|^3M_B^3}{\left(M_B+M_{D^*}\right)M_{D^*}q^2}\mathcal{R}\left(\mathbf{C}_{\rm AL}^{\ell}\mathbf{C}_{\rm PL}^{\ell *}\right)\mathbf{A_0}\mathbf{A_2} \\
& \left. - \frac{8M_B\left(M_B^2+3M_{D^*}^2-q^2\right)|p_{D^*}|}{M_{D^*}q^2}\mathcal{R}\left(\mathbf{C}_{\rm AL}^{\ell}\mathbf{C}_{\rm TL}^{\ell *}\right)\mathbf{A_0}\mathbf{T_2} + \frac{32M_B^3|p_{D^*}|^3}{q^2M_{D^*}\left(M_B^2-M_{D^*}^2\right)}\mathcal{R}\left(\mathbf{C}_{\rm AL}^{\ell}\mathbf{C}_{\rm TL}^{\ell *}\right)\mathbf{A_0}\mathbf{T_3}\right] \\
& + m_\ell^2\left[-\frac{4|p_{D^*}|M_B\left(M_B+M_{D^*}\right)}{M_{D^*}q^4}\left(M_B^2-M_{D^*}^2-q^2\right)\left|\mathbf{C}_{\rm AL}^{\ell}\right|^{\mathbf{2}}\mathbf{A_0}\mathbf{A_1} + \frac{16|p_{D^*}|^3M_B^3}{\left(M_B+M_{D^*}\right)M_{D^*}q^4}\left|\mathbf{C}_{\rm AL}^{\ell}\right|^{\mathbf{2}}\mathbf{A_0}\mathbf{A_2}\right] \\
c_\ell^{D^*}(+) = & -\frac{32M_B^2|p_{D^*}|^2}{q^2}\left|\mathbf{C}_{\rm TL}^{\ell}\right|^{\mathbf{2}}\mathbf{T_1^2} - \frac{2\left(4M_{D^*}^2-q^2\right)\lambda}{M_{D^*}^2q^2}\left|\mathbf{C}_{\rm TL}^{\ell}\right|^{\mathbf{2}}\mathbf{T_2^2} \\
& + \frac{32M_B^4|p_{D^*}|^4}{M_{D^*}^2\left(M_B^2-M_{D^*}^2\right)^2}\left|\mathbf{C}_{\rm TL}^{\ell}\right|^{\mathbf{2}}\mathbf{T_3^2} - \frac{16M_B^2|p_{D^*}|^2\left(M_B^2+3M_{D^*}^2-q^2\right)}{M_{D^*}^2\left(M_B^2-M_{D^*}^2\right)}\left|\mathbf{C}_{\rm TL}^{\ell}\right|^{\mathbf{2}}\mathbf{T_2}\mathbf{T_3} \\
& - m_\ell\left[\frac{32M_B^2|p_{D^*}|^2}{q^2\left(M_B+M_{D^*}\right)}\mathcal{R}\left(\mathbf{C}_{\rm VL}^{\ell}\mathbf{C}_{\rm TL}^{\ell *}\right)\mathbf{V}\mathbf{T_1} - \frac{8M_B^2\left(M_B+M_{D^*}\right)|p_{D^*}|^2}{q^2M_{D^*}^2}\mathcal{R}\left(\mathbf{C}_{\rm AL}^{\ell}\mathbf{C}_{\rm TL}^{\ell *}\right)\mathbf{A_1}\mathbf{T_2}\right.
\end{aligned}
$$

JHEP11(2018)187

$$
\begin{aligned}
&+\frac{8M_B^2\left(M_B^2-M_{D^*}^2-q^2\right)|p_{D^*}|^2}{q^2M_{D^*}^2\left(M_B-M_{D^*}\right)}\mathcal{R}\left(\mathbf{C}_{\mathrm{AL}}^{\ell}\mathbf{C}_{\mathrm{TL}}^{\ell*}\right)\mathbf{A_1T_3}+\frac{8M_B^2\left(M_B^2+3M_{D^*}^2-q^2\right)|p_{D^*}|^2}{q^2M_{D^*}^2\left(M_B+M_{D^*}\right)}\mathcal{R}\left(\mathbf{C}_{\mathrm{AL}}^{\ell}\mathbf{C}_{\mathrm{TL}}^{\ell*}\right)\mathbf{A_2T_2}\\
&-\frac{32M_B^4|p_{D^*}|^4}{q^2M_{D^*}^2\left(M_B+M_{D^*}\right)\left(M_B^2-M_{D^*}^2\right)}\mathcal{R}\left(\mathbf{C}_{\mathrm{AL}}^{\ell}\mathbf{C}_{\mathrm{TL}}^{\ell*}\right)\mathbf{A_2T_3}\\
&+m_\ell^2\left[-\frac{8\,|p_{D^*}|^2M_B^2}{\left(M_B+M_{D^*}\right)^2q^2}\left|\mathbf{C}_{\mathrm{VL}}^{\ell}\right|^{\mathbf{2}}\mathbf{V^2}+\frac{\left(M_B+M_{D^*}\right)^2\lambda}{2M_{D^*}^2q^4}\left|\mathbf{C}_{\mathrm{AL}}^{\ell}\right|^{\mathbf{2}}\mathbf{A_1^2}\right.\\
&\left.+\frac{8|p_{D^*}|^4M_B^4}{M_{D^*}^2\left(M_B+M_{D^*}\right)^2q^4}\left|\mathbf{C}_{\mathrm{AL}}^{\ell}\right|^{\mathbf{2}}\mathbf{A_2^2}-\frac{4\,|p_{D^*}|^2M_B^2}{M_{D^*}^2q^4}\left(M_B^2-M_{D^*}^2-q^2\right)\left|\mathbf{C}_{\mathrm{AL}}^{\ell}\right|^{\mathbf{2}}\mathbf{A_1A_2}\right]
\end{aligned}
\tag{C.9}
$$

C.4 Semi-numerical formulas for R_{D^*}

$$
\begin{aligned}
\mathcal{B}\left(B\to D^*\tau\nu_\tau\right)=&\Big(13.8+1.6\ \mathbf{\Delta C}_{\mathrm{VL}}^{\tau}-26.1\ \mathbf{\Delta C}_{\mathrm{AL}}^{\tau}+1.6\ \mathbf{\Delta C}_{\mathrm{PL}}^{\tau}\\
&-28.8\ \mathbf{\Delta C}_{\mathrm{TL}}^{\tau}+0.8\ \left(\mathbf{\Delta C}_{\mathrm{VL}}^{\tau}\right)^2+13.0\ \left(\mathbf{\Delta C}_{\mathrm{AL}}^{\tau}\right)^2\\
&+0.6\ \left(\mathbf{\Delta C}_{\mathrm{PL}}^{\tau}\right)^2+42.1\ \left(\mathbf{\Delta C}_{\mathrm{TL}}^{\tau}\right)^2+5.4\ \mathbf{\Delta C}_{\mathrm{VL}}^{\tau}\mathbf{\Delta C}_{\mathrm{TL}}^{\tau}\\
&-1.6\ \mathbf{\Delta C}_{\mathrm{AL}}^{\tau}\mathbf{\Delta C}_{\mathrm{PL}}^{\tau}+34.2\ \mathbf{\Delta C}_{\mathrm{AL}}^{\tau}\mathbf{\Delta C}_{\mathrm{TL}}^{\tau}\Big)\times10^{-3}\\
\mathcal{B}\left(B\to D^*\ell_0\nu_{\ell_0}\right)=&\Big(54.9+11.9\ \mathbf{\Delta C}_{\mathrm{VL}}^{\ell_0}-151.5\ \mathbf{\Delta C}_{\mathrm{AL}}^{\ell_0}+0.5\ \mathbf{\Delta C}_{\mathrm{PL}}^{\ell_0}\\
&-6.8\ \mathbf{\Delta C}_{\mathrm{TL}}^{\ell_0}+3.8\ \left(\mathbf{\Delta C}_{\mathrm{VL}}^{\ell_0}\right)^2+51.1\ \left(\mathbf{\Delta C}_{\mathrm{AL}}^{\ell_0}\right)^2\\
&+3.3\ \left(\mathbf{\Delta C}_{\mathrm{PL}}^{\ell_0}\right)^2+163.4\ \left(\mathbf{\Delta C}_{\mathrm{TL}}^{\ell_0}\right)^2+1.9\ \mathbf{\Delta C}_{\mathrm{VL}}^{\ell_0}\mathbf{\Delta C}_{\mathrm{TL}}^{\ell_0}\\
&-0.5\ \mathbf{\Delta C}_{\mathrm{AL}}^{\ell_0}\mathbf{\Delta C}_{\mathrm{PL}}^{\ell_0}+6.6\ \mathbf{\Delta C}_{\mathrm{AL}}^{\ell_0}\mathbf{\Delta C}_{\mathrm{TL}}^{\ell_0}\Big)\times10^{-3}\\
R_{D^*}=&\,0.25+0.03\ \mathbf{\Delta C}_{\mathrm{VL}}^{\tau}-0.48\ \mathbf{\Delta C}_{\mathrm{AL}}^{\tau}+0.03\ \mathbf{\Delta C}_{\mathrm{PL}}^{\tau}-0.52\ \mathbf{\Delta C}_{\mathrm{TL}}^{\tau}\\
&+0.01\ \left(\mathbf{\Delta C}_{\mathrm{VL}}^{\tau}\right)^2+0.24\ \left(\mathbf{\Delta C}_{\mathrm{AL}}^{\tau}\right)^2+0.01\ \left(\mathbf{\Delta C}_{\mathrm{PL}}^{\tau}\right)^2+0.77\ \left(\mathbf{\Delta C}_{\mathrm{TL}}^{\tau}\right)^2\\
&+0.10\ \mathbf{\Delta C}_{\mathrm{VL}}^{\tau}\mathbf{\Delta C}_{\mathrm{TL}}^{\tau}-0.03\ \mathbf{\Delta C}_{\mathrm{AL}}^{\tau}\mathbf{\Delta C}_{\mathrm{PL}}^{\tau}+0.62\ \mathbf{\Delta C}_{\mathrm{AL}}^{\tau}\mathbf{\Delta C}_{\mathrm{TL}}^{\tau}
\end{aligned}
$$

C.5 Semi-numerical formulas for R_{η_c}

$$
\begin{aligned}
\mathcal{B}\left(B_c\to\eta_c\tau\nu_\tau\right)=&\Big(1.4+2.9\ \mathbf{\Delta C}_{\mathrm{VL}}^{\tau}+2.5\ \mathbf{\Delta C}_{\mathrm{SL}}^{\tau}+0.6\ \mathbf{\Delta C}_{\mathrm{TL}}^{\tau}\\
&+1.4\ \left(\mathbf{\Delta C}_{\mathrm{VL}}^{\tau}\right)^{\mathbf{2}}+1.9\ \left(\mathbf{\Delta C}_{\mathrm{SL}}^{\tau}\right)^{\mathbf{2}}+0.2\ \left(\mathbf{\Delta C}_{\mathrm{TL}}^{\tau}\right)^{\mathbf{2}}\\
&+2.5\ \mathbf{\Delta C}_{\mathrm{VL}}^{\tau}\mathbf{\Delta C}_{\mathrm{SL}}^{\tau}+0.6\ \mathbf{\Delta C}_{\mathrm{VL}}^{\tau}\mathbf{\Delta C}_{\mathrm{TL}}^{\tau}\Big)\times10^{-3}
\end{aligned}
\tag{C.10}
$$

$$
\begin{aligned}
\mathcal{B}\left(B_c\to\eta_c\ell_0\,\nu_{\ell_0}\right)=&\Big(4.6+9.3\ \mathbf{\Delta C}_{\mathrm{VL}}^{\ell_0}+0.4\ \mathbf{\Delta C}_{\mathrm{SL}}^{\ell_0}+0.2\ \mathbf{\Delta C}_{\mathrm{TL}}^{\ell_0}\\
&+4.6\ \left(\mathbf{\Delta C}_{\mathrm{VL}}^{\ell_0}\right)^{\mathbf{2}}+7.0\ \left(\mathbf{\Delta C}_{\mathrm{SL}}^{\ell_0}\right)^{\mathbf{2}}+0.4\ \left(\mathbf{\Delta C}_{\mathrm{TL}}^{\ell_0}\right)^{\mathbf{2}}\\
&+0.4\ \mathbf{\Delta C}_{\mathrm{VL}}^{\ell_0}\mathbf{\Delta C}_{\mathrm{SL}}^{\ell_0}+0.2\ \mathbf{\Delta C}_{\mathrm{VL}}^{\ell_0}\mathbf{\Delta C}_{\mathrm{TL}}^{\ell_0}\Big)\times10^{-3}
\end{aligned}
\tag{C.11}
$$

$$
\begin{aligned}
R_{\eta_c}=&\,0.30+0.62\ \mathbf{\Delta C}_{\mathrm{VL}}^{\tau}+0.53\ \mathbf{\Delta C}_{\mathrm{SL}}^{\tau}+0.13\ \mathbf{\Delta C}_{\mathrm{TL}}^{\tau}\\
&+0.30\ \left(\mathbf{\Delta C}_{\mathrm{VL}}^{\tau}\right)^2+0.41\ \left(\mathbf{\Delta C}_{\mathrm{SL}}^{\tau}\right)^2+0.04\ \left(\mathbf{\Delta C}_{\mathrm{TL}}^{\tau}\right)^2\\
&+0.53\ \mathbf{\Delta C}_{\mathrm{VL}}^{\tau}\mathbf{\Delta C}_{\mathrm{SL}}^{\tau}+0.13\ \mathbf{\Delta C}_{\mathrm{VL}}^{\tau}\mathbf{\Delta C}_{\mathrm{TL}}^{\tau}\,.
\end{aligned}
\tag{C.12}
$$

JHEP11(2018)187

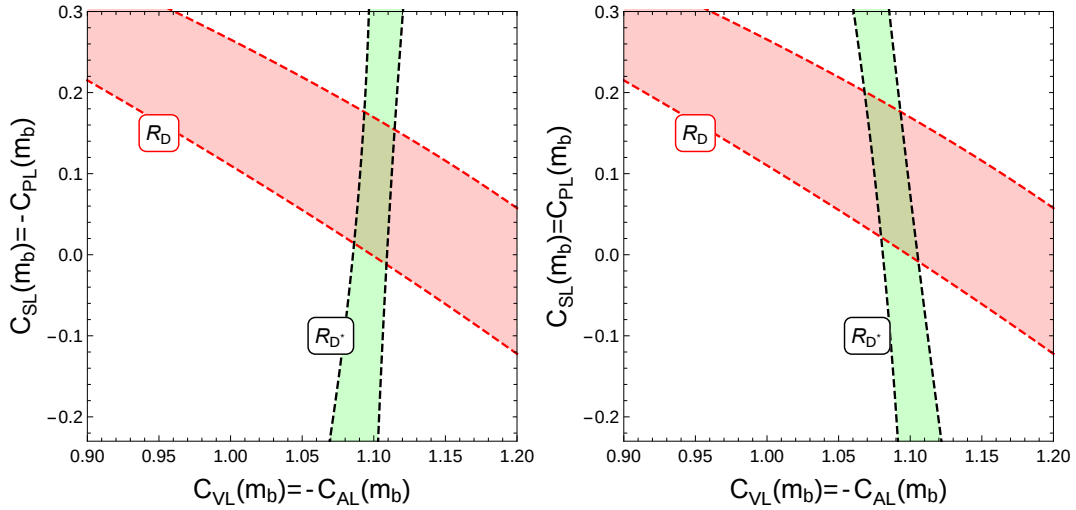

Figure 9. The red and green shaded regions correspond to the values of $C^\tau_{\rm VL}$ $(= -C^\tau_{\rm AL})$ and $C^\tau_{\rm SL}$ $(= -C^\tau_{\rm PL}$ for the left panel and $= C^\tau_{\rm PL}$ for the right panel) that satisfy the experimental measurement of R_D and R_{D^*} within 1σ respectively.

C.6 Semi-numerical formulas for $R_{J/\psi}$

$$\begin{aligned}\mathcal{B}(B_c \to J/\psi\ \tau\nu_\tau) = \Big(&3.1 + 0.1\ \Delta\mathbf{C}^\tau_{\rm VL} - 6.2\ \Delta\mathbf{C}^\tau_{\rm AL} + 0.4\ \Delta\mathbf{C}^\tau_{\rm PL}\\ &- 7.7\ \Delta\mathbf{C}^\tau_{\rm TL} + 3.1\ (\Delta\mathbf{C}^\tau_{\rm AL})^2\\ &+ 0.2\ (\Delta\mathbf{C}^\tau_{\rm PL})^2 + 8.2\ \Delta\mathbf{C}^\tau_{\rm TL}{}^2 + 0.3\ \Delta\mathbf{C}^\tau_{\rm VL}\Delta\mathbf{C}^\tau_{\rm TL}\\ &- 0.4\ \Delta\mathbf{C}^\tau_{\rm AL}\Delta\mathbf{C}^\tau_{\rm PL} + 8.0\ \Delta\mathbf{C}^\tau_{\rm AL}\Delta\mathbf{C}^\tau_{\rm TL}\Big)\times 10^{-3}\end{aligned} \tag{C.13}$$

$$\begin{aligned}\mathcal{B}(B_c \to J/\psi\ \ell_0\nu_{\ell_0}) = \Big(&10.8 + 0.7\ \Delta\mathbf{C}^{\ell_0}_{\rm VL} - 34.2\ \Delta\mathbf{C}^{\ell_0}_{\rm AL} + 0.2\ \Delta\mathbf{C}^{\ell_0}_{\rm PL}\\ &- 1.8\ \Delta\mathbf{C}^{\ell_0}_{\rm TL} + 0.2\ \left(\Delta\mathbf{C}^{\ell_0}_{\rm VL}\right)^2 + 10.6\ \left(\Delta\mathbf{C}^{\ell_0}_{\rm AL}\right)^2\\ &+ 1.0\ \left(\Delta\mathbf{C}^{\ell_0}_{\rm PL}\right)^2 + 36.5\ \left(\Delta\mathbf{C}^{\ell_0}_{\rm TL}\right)^2 + 0.1\ \Delta\mathbf{C}^{\ell_0}_{\rm VL}\Delta\mathbf{C}^{\ell_0}_{\rm TL}\\ &- 0.2\ \Delta\mathbf{C}^{\ell_0}_{\rm AL}\Delta\mathbf{C}^{\ell_0}_{\rm PL} + 0.6\ \Delta\mathbf{C}^{\ell_0}_{\rm AL}\Delta\mathbf{C}^{\ell_0}_{\rm TL}\Big)\times 10^{-3}\end{aligned} \tag{C.14}$$

$$\begin{aligned}R_{J/\psi} = &\ 0.29 + 0.01\ \Delta\mathbf{C}^\tau_{\rm VL} - 0.57\ \Delta\mathbf{C}^\tau_{\rm AL} + 0.04\ \Delta\mathbf{C}^\tau_{\rm PL} - 0.71\ \Delta\mathbf{C}^\tau_{\rm TL}\\ &+ 0.29\ (\Delta\mathbf{C}^\tau_{\rm AL})^2 + 0.02\ (\Delta\mathbf{C}^\tau_{\rm PL})^2 + 0.76\ (\Delta\mathbf{C}^\tau_{\rm TL})^2\\ &+ 0.03\ \Delta\mathbf{C}^\tau_{\rm VL}\Delta\mathbf{C}^\tau_{\rm TL} - 0.04\ \Delta\mathbf{C}^\tau_{\rm AL}\Delta\mathbf{C}^\tau_{\rm PL} + 0.74\ \Delta\mathbf{C}^\tau_{\rm AL}\Delta\mathbf{C}^\tau_{\rm TL}\,.\end{aligned} \tag{C.15}$$

C.7 Combination of vector and scalar operators

In this appendix, we briefly comment on the scenario where both vector and scalar operators are present (see, for example [114] for a model). In figure 9, we show the allowed regions in the $C^\tau_{\rm VL}$-$C^\tau_{\rm SL}$ plane assuming $C^\tau_{\rm VL} = -C^\tau_{\rm AL}$ and $C^\tau_{\rm SL} = \pm C^\tau_{\rm PL}$.

It can be seen that the overlap of the red and green regions (that corresponds to the simultaneous solution of R_D and R_{D^*}) touches the $C^\tau_{\rm SL} = \pm C^\tau_{\rm PL} = 0$ point. Thus, a

JHEP11(2018)187

combination of the vector and scalar operators extends the solution with only the vector operator discussed in section 3.1. Interestingly, if the red shaded region shrinks in the future due to more precise measurement of R_D (without affecting the current central value much), the combination of scalar and vector operators may lead to a better fit than with only vector operators.

D From the gauge to the mass eigenstates

$\boldsymbol{[C_{lq}^{(3)}]'_{p'r's't'}\left(\bar{l}'_{p'}\gamma_\mu\sigma^I l'_{r'}\right)\left(\bar{q}'_{s'}\gamma^\mu\sigma^I q'_{t'}\right)}$**.** Using eq. (4.12) and the definitions from eq. (4.14), we get,

$$
\begin{aligned}
&\sum_{p',r',s',t'}\left[[C_{lq}^{(3)}]'_{p'r's't'}\left(\bar{l}'_{p'}\gamma_\mu\sigma^I l'_{r'}\right)\left(\bar{q}'_{s'}\gamma^\mu\sigma^I q'_{t'}\right)\right]\\
&=\sum_{p,r,s,t}\Bigg[\sum_{p',r',s',t'}[C_{lq}^{(3)}]'_{p'r's't'}\Big[(V_L^\nu)^\dagger_{pp'}(V_L^\nu)_{r'r}(V_L^u)^\dagger_{ss'}(V_L^u)_{t't}\left(\bar{\nu}_p\gamma^\mu P_L\nu_r\right)\left(\bar{u}_s\gamma_\mu P_L u_t\right)\\
&\qquad+(V_L^e)^\dagger_{pp'}(V_L^e)_{r'r}(V_L^d)^\dagger_{ss'}(V_L^d)_{t't}\left(\bar{e}_p\gamma^\mu P_L e_r\right)\left(\bar{d}_s\gamma_\mu P_L d_t\right)\\
&\qquad-(V_L^e)^\dagger_{pp'}(V_L^e)_{r'r}(V_L^u)^\dagger_{ss'}(V_L^u)_{t't}\left(\bar{e}_p\gamma^\mu P_L e_r\right)\left(\bar{u}_s\gamma_\mu P_L u_t\right)\\
&\qquad-(V_L^\nu)^\dagger_{pp'}(V_L^\nu)_{r'r}(V_L^d)^\dagger_{ss'}(V_L^d)_{t't}\left(\bar{\nu}_p\gamma^\mu P_L\nu_r\right)\left(\bar{d}_s\gamma_\mu P_L d_t\right)\\
&\qquad+2(V_L^\nu)^\dagger_{pp'}(V_L^e)_{r'r}(V_L^d)^\dagger_{ss'}(V_L^u)_{t't}\left(\bar{\nu}_p\gamma^\mu P_L e_r\right)\left(\bar{d}_s\gamma_\mu P_L u_t\right)\\
&\qquad+2(V_L^e)^\dagger_{pp'}(V_L^\nu)_{r'r}(V_L^u)^\dagger_{ss'}(V_L^d)_{t't}\left(\bar{e}_p\gamma^\mu P_L\nu_r\right)\left(\bar{u}_s\gamma_\mu P_L d_t\right)\Big]\Bigg]\\
&=\sum_{p,r,s,t}\Big[[\tilde{C}_{lq}^{(3)\nu\nu uu}]_{prst}\left(\bar{\nu}_p\gamma^\mu P_L\nu_r\right)\left(\bar{u}_s\gamma_\mu P_L u_t\right)+[\tilde{C}_{lq}^{(3)eedd}]_{prst}\left(\bar{e}_p\gamma^\mu P_L e_r\right)\left(\bar{d}_s\gamma_\mu P_L d_t\right)\\
&\quad-[\tilde{C}_{lq}^{(3)eeuu}]_{prst}\left(\bar{e}_p\gamma^\mu P_L e_r\right)\left(\bar{u}_s\gamma_\mu P_L u_t\right)-[\tilde{C}_{lq}^{(3)\nu\nu dd}]_{prst}\left(\bar{\nu}_p\gamma^\mu P_L\nu_r\right)\left(\bar{d}_s\gamma_\mu P_L d_t\right)\\
&\quad+2[\tilde{C}_{lq}^{(3)\nu edu}]_{prst}\left(\bar{\nu}_p\gamma^\mu P_L e_r\right)\left(\bar{d}_s\gamma_\mu P_L u_t\right)+2[\tilde{C}_{lq}^{(3)e\nu ud}]_{prst}\left(\bar{e}_p\gamma^\mu P_L\nu_r\right)\left(\bar{u}_s\gamma_\mu P_L d_t\right)\Big],
\end{aligned}
\tag{D.1}
$$

where

$$
\begin{aligned}
&\sum_{p',r',s',t'}[C_{lq}^{(3)}]'_{p'r's't'}(V_L^\nu)^\dagger_{pp'}(V_L^\nu)_{r'r}(V_L^u)^\dagger_{ss'}(V_L^u)_{t't}\equiv[\tilde{C}_{lq}^{(3)\nu\nu uu}]_{prst}\\
&\sum_{p',r',s',t'}[C_{lq}^{(3)}]'_{p'r's't'}(V_L^e)^\dagger_{pp'}(V_L^e)_{r'r}(V_L^d)^\dagger_{ss'}(V_L^d)_{t't}\equiv[\tilde{C}_{lq}^{(3)eedd}]_{prst}\\
&\sum_{p',r',s',t'}[C_{lq}^{(3)}]'_{p'r's't'}(V_L^e)^\dagger_{pp'}(V_L^e)_{r'r}(V_L^u)^\dagger_{ss'}(V_L^u)_{t't}\equiv[\tilde{C}_{lq}^{(3)eeuu}]_{prst}\\
&\sum_{p',r',s',t'}[C_{lq}^{(3)}]'_{p'r's't'}(V_L^\nu)^\dagger_{pp'}(V_L^\nu)_{r'r}(V_L^d)^\dagger_{ss'}(V_L^d)_{t't}\equiv[\tilde{C}_{lq}^{(3)\nu\nu dd}]_{prst}\\
&\sum_{p',r',s',t'}[C_{lq}^{(3)}]'_{p'r's't'}(V_L^\nu)^\dagger_{pp'}(V_L^e)_{r'r}(V_L^d)^\dagger_{ss'}(V_L^u)_{t't}\equiv[\tilde{C}_{lq}^{(3)\nu edu}]_{prst}\\
&\sum_{p',r',s',t'}[C_{lq}^{(3)}]'_{p'r's't'}(V_L^e)^\dagger_{pp'}(V_L^\nu)_{r'r}(V_L^u)^\dagger_{ss'}(V_L^d)_{t't}\equiv[\tilde{C}_{lq}^{(3)e\nu ud}]_{prst}
\end{aligned}
\tag{D.2}
$$

JHEP11(2018)187

$[\boldsymbol{C}^{(3)}_{\boldsymbol{\phi l}}]'_{\boldsymbol{p'r'}}\left(\boldsymbol{\phi^\dagger i\overleftrightarrow{D}^I_\mu\phi}\right)\left(\boldsymbol{\bar{l}'_{p'}\,\sigma^I\gamma^\mu\,l'_{r'}}\right)$.

$$
\begin{aligned}
&\sum_{p',r'}[C^{(3)}_{\phi l}]'_{p'r'}\left(\phi^\dagger i\overleftrightarrow{D}^I_\mu\phi\right)\left(\bar{l}'_{p'}\,\sigma^I\gamma^\mu\,l'_{r'}\right)\\
&\quad=\left(v^2+2vh+h^2\right)\sum_{p,r}\Bigg[\sum_{p',r'}[C^{(3)}_{\phi l}]'_{p'r'}\Bigg[-\frac{1}{2}\frac{g_2}{\cos\theta_W}(V^\nu_L)^\dagger_{pp'}(V^\nu_L)_{r'r}Z_\mu\left(\overline{\nu}_p\gamma^\mu P_L\nu_r\right)\\
&\qquad+\frac{1}{2}\frac{g_2}{\cos\theta_W}(V^e_L)^\dagger_{pp'}(V^e_L)_{r'r}Z_\mu\left(\overline{e}_p\gamma^\mu P_L e_r\right)-\frac{g_2}{\sqrt{2}}(V^\nu_L)^\dagger_{pp'}(V^e_L)_{r'r}W^+_\mu\left(\overline{\nu}_p\gamma^\mu P_L e_r\right)\\
&\qquad-\frac{g_2}{\sqrt{2}}(V^e_L)^\dagger_{pp'}(V^\nu_L)_{r'r}W^-_\mu\left(\overline{e}_p\gamma^\mu P_L\nu_r\right)\Bigg]\Bigg]\\
&\quad=\left(v^2+2vh+h^2\right)\sum_{p,r}\Bigg[-\frac{1}{2}\frac{g_2}{\cos\theta_W}[\tilde{C}^{(3)\nu\nu}_{\phi l}]_{pr}Z_\mu\left(\overline{\nu}_p\gamma^\mu P_L\nu_r\right)\\
&\qquad+\frac{1}{2}\frac{g_2}{\cos\theta_W}[\tilde{C}^{(3)ee}_{\phi l}]_{pr}Z_\mu\left(\overline{e}_p\gamma^\mu P_L e_r\right)-\frac{g_2}{\sqrt{2}}[\tilde{C}^{(3)\nu e}_{\phi l}]_{pr}W^+_\mu\left(\overline{\nu}_p\gamma^\mu P_L e_r\right)\\
&\qquad-\frac{g_2}{\sqrt{2}}[\tilde{C}^{(3)e\nu}_{\phi l}]_{pr}W^-_\mu\left(\overline{e}_p\gamma^\mu P_L\nu_r\right)\Bigg],
\end{aligned}
\tag{D.3}
$$

where

$$
\begin{aligned}
\sum_{p',r'}[C^{(3)}_{\phi l}]'_{p'r'}(V^\nu_L)^\dagger_{pp'}(V^\nu_L)_{r'r}&=[\tilde{C}^{(3)\nu\nu}_{\phi l}]_{pr}\\
\sum_{p',r'}[C^{(3)}_{\phi l}]'_{p'r'}(V^e_L)^\dagger_{pp'}(V^e_L)_{r'r}&=[\tilde{C}^{(3)ee}_{\phi l}]_{pr}\\
\sum_{p',r'}[C^{(3)}_{\phi l}]'_{p'r'}(V^\nu_L)^\dagger_{pp'}(V^e_L)_{r'r}&=[\tilde{C}^{(3)\nu e}_{\phi l}]_{pr}\\
\sum_{p',r'}[C^{(3)}_{\phi l}]'_{p'r'}(V^e_L)^\dagger_{pp'}(V^\nu_L)_{r'r}&=[\tilde{C}^{(3)e\nu}_{\phi l}]_{pr}
\end{aligned}
\tag{D.4}
$$

$[\boldsymbol{C_{ledq}}]'_{\boldsymbol{p'r's't'}}\left(\boldsymbol{\bar{l}'^j_{p'}e'_{r'}}\right)\left(\boldsymbol{\bar{d}'_{s'}q'^j_{t'}}\right)$.

$$
\begin{aligned}
&\sum_{p',r',s',t'}[C_{ledq}]'_{p'r's't'}\left(\bar{l}'^j_{p'}e'_{r'}\right)\left(\bar{d}'_{s'}q'^j_{t'}\right)\\
&\quad=\sum_{p,r,s,t}\Bigg[\sum_{p',r',s',t'}[C_{ledq}]'_{p'r's't'}\Bigg[(V^\nu_L)^\dagger_{pp'}(V^e_R)_{r'r}(V^d_R)^\dagger_{ss'}(V^u_L)_{t't}\left(\bar{\nu}_pP_Re_r\right)\left(\bar{d}_sP_Lu_t\right)\\
&\qquad+(V^e_L)^\dagger_{pp'}(V^e_R)_{r'r}(V^d_R)^\dagger_{ss'}(V^d_L)_{t't}\left(\bar{e}_pP_Re_r\right)\left(\bar{d}_sP_Ld_t\right)\Bigg]\Bigg]\\
&\quad=\sum_{p,r,s,t}\Bigg[[\tilde{C}^{\nu edu}_{ledq}]_{prst}\left(\bar{\nu}_pP_Re_r\right)\left(\bar{d}_sP_Lu_t\right)+[\tilde{C}^{eedd}_{ledq}]_{prst}\left(\bar{e}_pP_Re_r\right)\left(\bar{d}_sP_Ld_t\right)\Bigg],
\end{aligned}
\tag{D.5}
$$

JHEP11(2018)187

where

$$\sum_{p',r',s',t'} [C_{ledq}]'_{p'r's't'} (V_L^\nu)^\dagger_{pp'} (V_R^e)_{r'r} (V_R^d)^\dagger_{ss'} (V_L^u)_{t't} = [\tilde{C}^{\nu edu}_{ledq}]_{prst}$$
$$\sum_{p',r',s',t'} [C_{ledq}]'_{p'r's't'} (V_L^e)^\dagger_{pp'} (V_R^e)_{r'r} (V_R^d)^\dagger_{ss'} (V_L^d)_{t't} = [\tilde{C}^{eedd}_{ledq}]_{prst} \tag{D.6}$$

$\boldsymbol{[C^{(1)}_{lequ}]'_{p'r's't'} \left(\bar{l}'^j_{p'} e'_{r'}\right) \epsilon_{jk} \left(\bar{q}'^k_{s'} u'_{t'}\right).}$

$$\begin{aligned}
&\sum_{p',r',s',t'} [C^{(1)}_{lequ}]'_{p'r's't'} \left(\bar{l}'^j_{p'} e'_{r'}\right) \epsilon_{jk} \left(\bar{q}'^k_{s'} u'_{t'}\right) \\
&= \sum_{p,r,s,t} \Bigg[\sum_{p',r',s',t'} [C^{(1)}_{lequ}]'_{p'r's't'} \Bigg[(V_L^\nu)^\dagger_{pp'} (V_R^e)_{r'r} (V_L^d)^\dagger_{ss'} (V_R^u)_{t't} \left(\bar{\nu}_p P_R e_r\right) \left(\bar{d}_s P_R u_t\right) \\
&\quad - (V_L^e)^\dagger_{pp'} (V_R^e)_{r'r} (V_L^u)^\dagger_{ss'} (V_R^u)_{t't} \left(\bar{e}_p P_R e_r\right) \left(\bar{u}_s P_R u_t\right) \Bigg] \Bigg] \\
&= \sum_{p,r,s,t} \left[[\tilde{C}^{(1)\nu edu}_{lequ}]_{prst} \left(\bar{\nu}_p P_R e_r\right) \left(\bar{d}_s P_R u_t\right) - [\tilde{C}^{(1)eedu}_{lequ}]_{prst} \left(\bar{e}_p P_R e_r\right) \left(\bar{u}_s P_R u_t\right) \right],
\end{aligned} \tag{D.7}$$

where

$$\sum_{p',r',s',t'} [C^{(1)}_{lequ}]'_{p'r's't'} (V_L^\nu)^\dagger_{pp'} (V_R^e)_{r'r} (V_L^d)^\dagger_{ss'} (V_R^u)_{t't} = [\tilde{C}^{(1)\nu edu}_{lequ}]_{prst}$$
$$\sum_{p',r',s',t'} [C^{(1)}_{lequ}]'_{p'r's't'} (V_L^e)^\dagger_{pp'} (V_R^e)_{r'r} (V_L^u)^\dagger_{ss'} (V_R^u)_{t't} = [\tilde{C}^{(1)eedu}_{lequ}]_{prst} \tag{D.8}$$

Thus,

$$\Delta C^{cb\tau\nu_3}_{\mathrm{SL}} = \frac{1}{2} \frac{\Lambda^2_{\mathrm{SM}}}{\Lambda^2} \left([\tilde{C}^{\nu edu}_{ledq}]_{3332} + [\tilde{C}^{(1)\nu edu}_{lequ}]_{3332} \right)^*, \tag{D.9}$$

$$\Delta C^{cb\tau\nu_3}_{\mathrm{PL}} = \frac{1}{2} \frac{\Lambda^2_{\mathrm{SM}}}{\Lambda^2} \left([\tilde{C}^{\nu edu}_{ledq}]_{3332} - [\tilde{C}^{(1)\nu edu}_{lequ}]_{3332} \right)^*. \tag{D.10}$$

$\boldsymbol{[C^{(3)}_{lequ}]'_{p'r's't'} \left(\bar{l}'^j_{p'} \sigma^{\mu\nu} e'_{r'}\right) \epsilon_{jk} \left(\bar{q}'^k_{s'} \sigma_{\mu\nu} u'_{t'}\right).}$

$$\begin{aligned}
&\sum_{p',r',s',t'} [C^{(3)}_{lequ}]'_{p'r's't'} \left(\bar{l}'^j_{p'} \sigma^{\mu\nu} e'_{r'}\right) \epsilon_{jk} \left(\bar{q}'^k_{s'} \sigma_{\mu\nu} u'_{t'}\right) \\
&= \sum_{p,r,s,t} \Bigg[\sum_{p',r',s',t'} [C^{(3)}_{lequ}]'_{p'r's't'} \Bigg[(V_L^\nu)^\dagger_{pp'} (V_R^e)_{r'r} (V_L^d)^\dagger_{ss'} (V_R^u)_{t't} \left(\bar{\nu}_p \sigma^{\mu\nu} P_R e_r\right) \left(\bar{d}_s \sigma_{\mu\nu} P_R u_t\right) \\
&\quad - (V_L^e)^\dagger_{pp'} (V_R^e)_{r'r} (V_L^u)^\dagger_{ss'} (V_R^u)_{t't} \left(\bar{e}_p \sigma^{\mu\nu} P_R e_r\right) \left(\bar{u}_s \sigma_{\mu\nu} P_R u_t\right) \Bigg] \Bigg] \\
&= \sum_{p,r,s,t} \left[[\tilde{C}^{(3)\nu edu}_{lequ}]_{prst} \left(\bar{\nu}_p \sigma^{\mu\nu} P_R e_r\right) \left(\bar{d}_s \sigma_{\mu\nu} P_R u_t\right) - [\tilde{C}^{(3)eedu}_{lequ}]_{prst} \left(\bar{e}_p \sigma^{\mu\nu} P_R e_r\right) \left(\bar{u}_s \sigma_{\mu\nu} P_R u_t\right) \right],
\end{aligned} \tag{D.11}$$

JHEP11(2018)187

where

$$\sum_{p',r',s',t'} [C^{(3)}_{lequ}]'_{p'r's't'} (V_L^{\nu})^{\dagger}_{pp'} (V_R^{e})_{r'r} (V_L^{d})^{\dagger}_{ss'} (V_R^{u})_{t't} = [\tilde{C}^{(3)\nu edu}_{lequ}]_{prst}$$
$$\sum_{p',r',s',t'} [C^{(3)}_{lequ}]'_{p'r's't'} (V_L^{e})^{\dagger}_{pp'} (V_R^{e})_{r'r} (V_L^{u})^{\dagger}_{ss'} (V_R^{u})_{t't} = [\tilde{C}^{(3)eedu}_{lequ}]_{prst} \tag{D.12}$$

Thus,

$$\Delta C^{cb\tau\nu_3}_{\rm TL} = \frac{1}{2}\frac{\Lambda^2_{\rm SM}}{\Lambda^2} \left([\tilde{C}^{(3)\nu edu}_{lequ}]_{3332}\right)^* . \tag{D.13}$$

E Mixing of $[C^{(3,1)}_{lq}]'$ and $[C^{(3,1)}_{\phi l}]'$

The β-functions of $[C^{(3)}_{\phi l}]'_{33}$ and $[C^{(3)}_{lq}]'_{3333}$ can be approximately written as (assuming that no other couplings are generated at the matching scale Λ) [52, 115]

$$16\pi^2 \frac{d}{d\log\mu}[C^{(3)}_{\phi l}]'_{33} = \left(-5g_2^2 + 6y_t^2 + 6y_b^2 + 4y_\tau^2\right)[C^{(3)}_{\phi l}]'_{33} + 3y_\tau^2 [C^{(1)}_{\phi l}]'_{33} + \left(2g_2^2 - 6y_b^2 - 6y_t^2\right)[C^{(3)}_{lq}]'_{3333} \tag{E.1}$$

$$16\pi^2 \frac{d}{d\log\mu}[C^{(1)}_{\phi l}]'_{33} = \left(\frac{1}{3}g_1^2 + 6y_t^2 + 6y_b^2 + 6y_\tau^2\right)[C^{(1)}_{\phi l}]'_{33} + 9y_\tau^2 [C^{(3)}_{\phi l}]'_{33} + \left(\frac{2}{3}g_1^2 - 6y_b^2 + 6y_t^2\right)[C^{(1)}_{lq}]'_{3333} \tag{E.2}$$

This gives

$$[C^{(3)}_{\phi l}]'_{33}(m_t) \simeq 0.027\,[C^{(3)}_{lq}]'_{3333}(\Lambda)\,\log(\Lambda/m_t)\,, \tag{E.3}$$
$$[C^{(1)}_{\phi l}]'_{33}(m_t) \simeq -0.034\,[C^{(1)}_{lq}]'_{3333}(\Lambda)\,\log(\Lambda/m_t)\,. \tag{E.4}$$

Thus, we get

$$\begin{aligned}\Delta g_L^{\tau} &\simeq \frac{1}{2}\left([C^{(3)}_{\phi l}]'_{33}(m_t) + [C^{(3)}_{\phi l}]'^{*}_{33}(m_t) + [C^{(1)}_{\phi l}]'_{33}(m_t) + [C^{(1)}_{\phi l}]'^{*}_{33}(m_t)\right)\frac{v^2}{\Lambda^2} \\ &\simeq \left(0.0014\,([C^{(3)}_{lq}]'_{3333} + [C^{(3)}_{lq}]'^{*}_{3333}) - 0.0018\,([C^{(1)}_{lq}]'_{3333} + [C^{(1)}_{lq}]'^{*}_{3333})\right) \\ &\quad \times \left(\frac{\rm TeV}{\Lambda}\right)^2 (1 + 0.6\log(\Lambda/{\rm TeV}))\end{aligned} \tag{E.5}$$

$$\begin{aligned}\Delta g_L^{\nu} &\simeq \frac{1}{2}\left(-[C^{(3)}_{\phi l}]'_{33}(m_t) - [C^{(3)}_{\phi l}]'^{*}_{33}(m_t) + [C^{(1)}_{\phi l}]'_{33}(m_t) + [C^{(1)}_{\phi l}]'^{*}_{33}(m_t)\right)\frac{v^2}{\Lambda^2} \\ &\simeq -\left(0.0014\,([C^{(3)}_{lq}]'_{3333} + [C^{(3)}_{lq}]'^{*}_{3333}) + 0.0018\,([C^{(1)}_{lq}]'_{3333} + [C^{(1)}_{lq}]'^{*}_{3333})\right) \\ &\quad \times \left(\frac{\rm TeV}{\Lambda}\right)^2 (1 + 0.6\log(\Lambda/{\rm TeV}))\end{aligned} \tag{E.6}$$

$$\begin{aligned}\Delta g_W^{\tau} &\simeq -\left([C^{(3)}_{\phi l}]'_{33}(m_t) + [C^{(3)}_{\phi l}]'^{*}_{33}(m_t)\right)\frac{v^2}{\Lambda^2} \\ &\simeq -0.0028\left([C^{(3)}_{lq}]'_{3333} + [C^{(3)}_{lq}]'^{*}_{3333}\right)\left(\frac{\rm TeV}{\Lambda}\right)^2 (1 + 0.6\log(\Lambda/{\rm TeV}))\end{aligned} \tag{E.7}$$

JHEP11(2018)187

Using $|\Delta g_L^\tau| \lesssim 6\times 10^{-4}$, and in the absence of $[C_{lq}^{(1)}]'_{3333}$, we get

$$\left|[C_{lq}^{(3)}]'_{3333} + [C_{lq}^{(3)}]'^{*}_{3333}\right| \lesssim \frac{0.43}{(1+0.6\log(\Lambda/\text{TeV}))}\left(\frac{\Lambda}{\text{TeV}}\right)^2 \tag{E.8}$$

In the presence of both $[C_{lq}^{(1)}]'_{3333}$ and $[C_{lq}^{(3)}]'_{3333}$, combining all the constraints on Δg_W^τ, Δg_L^τ and $|\Delta g_L^\nu| < 1.2\times 10^{-3}$ we get

$$\begin{aligned}
&\left|[C_{lq}^{(1)}]'_{3333}+[C_{lq}^{(1)}]'^{*}_{3333}\right| \lesssim \frac{0.5}{(1+0.6\log(\Lambda/\text{TeV}))}\left(\frac{\Lambda}{\text{TeV}}\right)^2 \\
&\frac{-0.63}{(1+0.6\log(\Lambda/\text{TeV}))}\left(\frac{\Lambda}{\text{TeV}}\right)^2 \lesssim [C_{lq}^{(3)}]'_{3333}+[C_{lq}^{(3)}]'^{*}_{3333} \lesssim \frac{0.14}{(1+0.6\log(\Lambda/\text{TeV}))}\left(\frac{\Lambda}{\text{TeV}}\right)^2 .
\end{aligned} \tag{E.9}$$

F Constraints from Z interactions with fermions

One of the advantages of the MCHM5 model is that it can provide protection for some of the g_Z^τ, g_Z^b, g_Z^ν couplings. Indeed, discrete P_{LR} symmetry [116] protects g_Z^τ, however it cannot protect $(g_Z^\nu, g_Z^\tau, g_W^\tau)$ at the same time. Indeed let us consider the leptonic part of the lagrangian in eq. (5.10) and allow the splitting of the mixing parameters defined in the eq. (5.12):

$$\begin{aligned}
\mathcal{L} = {} & i\overline{\tilde{\mathcal{O}}}_{l_1}\left(\not{D}+i\not{E}\right)\tilde{\mathcal{O}}_{l_1} + i\overline{\tilde{\mathcal{O}}}_{l_2}\left(\not{D}+i\not{E}\right)\mathcal{O}_{l_2} + \left(ic_1\overline{\tilde{\mathcal{O}}}^i_{l_1}\not{d}_i\tilde{\mathcal{O}}_N + ic_2\overline{\tilde{\mathcal{O}}}^i_{l_2}\not{d}_i\tilde{\mathcal{O}}_e + h.c.\right) \\
& - m_4^{(1)}\overline{\tilde{\mathcal{O}}}_{l_1}\tilde{\mathcal{O}}_{l_1} - m_4^{(2)}\overline{\tilde{\mathcal{O}}}_{l_2}\tilde{\mathcal{O}}_{l_2} - m_1^{(e)}\overline{\tilde{\mathcal{O}}}_e\tilde{\mathcal{O}}_e - m_1^{(N)}\overline{\tilde{\mathcal{O}}}_N\tilde{\mathcal{O}}_N \\
& + \lambda_l^{(4)}\bar{\tilde{l}}_L U(h)_{Ii}\mathcal{O}_{l_1} + \lambda_l^{(1)}\bar{\tilde{l}}_L U(h)_{I5}\mathcal{O}_N + \tilde{\lambda}_l^{(4)}\bar{\tilde{l}}_L U(h)_{Ii}\mathcal{O}_{l_2} + \tilde{\lambda}_l^{(1)}\bar{\tilde{l}}_L U(h)_{I5}\mathcal{O}_e\,.
\end{aligned} \tag{F.1}$$

Then the modifications to g_Z^τ, g_Z^ν can be read-off from the refs. [99, 117], where analogous discussion was applied to the top quark, so that

$$\begin{aligned}
\delta g_Z^\tau &= -\frac{v^2}{4f^2}\frac{M_*^2\left[\left(\tilde{\lambda}_l^{(4)}m_1^{(e)}\right)^2 + \left(\tilde{\lambda}_l^{(1)}m_4^{(2)}\right)^2 - 2\sqrt{2}c_2\tilde{\lambda}_l^{(4)}\tilde{\lambda}_l^{(1)}m_1^{(e)}m_4^{(2)}\right]}{\left(m_1^{(e)}\right)^2\left(\left(m_4^{(2)}\right)^2 + \left(\tilde{\lambda}_l^{(4)}M_*\right)^2\right)}, \\
\delta g_Z^\nu &= -\frac{v^2}{4f^2}\frac{M_*^2\left[\left(\lambda_l^{(4)}m_1^{(N)}\right)^2 + \left(\lambda_l^{(1)}m_4^{(1)}\right)^2 - 2\sqrt{2}c_1\lambda_l^{(4)}\lambda_l^{(1)}m_1^{(N)}m_4^{(2)}\right]}{\left(m_1^{(N)}\right)^2\left(\left(m_4^{(1)}\right)^2 + \left(\lambda_l^{(4)}M_*\right)^2\right)}.
\end{aligned} \tag{F.2}$$

We can see that P_{LR} symmetry forces the δg_Z^τ to depend only on $\tilde{\lambda}_l^{(1,4)}$ and δg_Z^ν on $\lambda_l^{(1,4)}$. Since the bound on g_Z^τ is a bit stronger, it is natural to assume that $\lambda_l > \tilde{\lambda}_l$ and the contribution to $R_{D,D*}$ is dominated by λ_l. Note that this coupling does not enter the leading expression of the τ mass which scales as

$$m_\tau \propto \lambda_e\tilde{\lambda}_l^{(1,4)}\,. \tag{F.3}$$

Then in order to pass the constraints from g_Z^ν we will have to tune additionally the parameter c_1 as was suggested in [24].

JHEP11(2018)187

References

[1] S. Aoki et al., *Review of lattice results concerning low-energy particle physics*, *Eur. Phys. J.* **C 77** (2017) 112 [arXiv:1607.00299] [INSPIRE].

[2] HPQCD collaboration, H. Na, C.M. Bouchard, G.P. Lepage, C. Monahan and J. Shigemitsu, *$B \to Dl\nu$ form factors at nonzero recoil and extraction of $|V_{cb}|$*, *Phys. Rev.* **D 92** (2015) 054510 [*Erratum ibid.* **D 93** (2016) 119906] [arXiv:1505.03925] [INSPIRE].

[3] HFLAV collaboration, Y. Amhis et al., *Averages of b-hadron, c-hadron and τ-lepton properties as of summer 2016*, *Eur. Phys. J.* **C 77** (2017) 895 [arXiv:1612.07233] [INSPIRE].

[4] D. Bigi and P. Gambino, *Revisiting $B \to D\ell\nu$*, *Phys. Rev.* **D 94** (2016) 094008 [arXiv:1606.08030] [INSPIRE].

[5] S. Fajfer, J.F. Kamenik and I. Nisandzic, *On the $B \to D^* \tau \bar{\nu}_\tau$ Sensitivity to New Physics*, *Phys. Rev.* **D 85** (2012) 094025 [arXiv:1203.2654] [INSPIRE].

[6] D. Bigi, P. Gambino and S. Schacht, *$R(D^*)$, $|V_{cb}|$ and the Heavy Quark Symmetry relations between form factors*, *JHEP* **11** (2017) 061 [arXiv:1707.09509] [INSPIRE].

[7] Belle collaboration, S. Hirose et al., *Measurement of the τ lepton polarization and $R(D^*)$ in the decay $\bar{B} \to D^* \tau^- \bar{\nu}_\tau$*, *Phys. Rev. Lett.* **118** (2017) 211801 [arXiv:1612.00529] [INSPIRE].

[8] Belle collaboration, S. Hirose et al., *Measurement of the τ lepton polarization and $R(D^*)$ in the decay $\bar{B} \to D^* \tau^- \bar{\nu}_\tau$ with one-prong hadronic τ decays at Belle*, *Phys. Rev.* **D 97** (2018) 012004 [arXiv:1709.00129] [INSPIRE].

[9] LHCb collaboration, *Measurement of the ratio of branching fractions $\mathcal{B}(B_c^+ \to J/\psi \tau^+ \nu_\tau)/\mathcal{B}(B_c^+ \to J/\psi \mu^+ \nu_\mu)$*, *Phys. Rev. Lett.* **120** (2018) 121801 [arXiv:1711.05623] [INSPIRE].

[10] BaBar collaboration, J.P. Lees et al., *Evidence for an excess of $\bar{B} \to D^{(*)} \tau^- \bar{\nu}_\tau$ decays*, *Phys. Rev. Lett.* **109** (2012) 101802 [arXiv:1205.5442] [INSPIRE].

[11] BaBar collaboration, J.P. Lees et al., *Measurement of an Excess of $\bar{B} \to D^{(*)} \tau^- \bar{\nu}_\tau$ Decays and Implications for Charged Higgs Bosons*, *Phys. Rev.* **D 88** (2013) 072012 [arXiv:1303.0571] [INSPIRE].

[12] Belle collaboration, M. Huschle et al., *Measurement of the branching ratio of $\bar{B} \to D^{(*)} \tau^- \bar{\nu}_\tau$ relative to $\bar{B} \to D^{(*)} \ell^- \bar{\nu}_\ell$ decays with hadronic tagging at Belle*, *Phys. Rev.* **D 92** (2015) 072014 [arXiv:1507.03233] [INSPIRE].

[13] LHCb collaboration, *Measurement of the ratio of branching fractions $\mathcal{B}(\bar{B}^0 \to D^{*+} \tau^- \bar{\nu}_\tau)/\mathcal{B}(\bar{B}^0 \to D^{*+} \mu^- \bar{\nu}_\mu)$*, *Phys. Rev. Lett.* **115** (2015) 111803 [*Erratum ibid.* **115** (2015) 159901] [arXiv:1506.08614] [INSPIRE].

[14] Belle collaboration, Y. Sato et al., *Measurement of the branching ratio of $\bar{B}^0 \to D^{*+} \tau^- \bar{\nu}_\tau$ relative to $\bar{B}^0 \to D^{*+} \ell^- \bar{\nu}_\ell$ decays with a semileptonic tagging method*, *Phys. Rev.* **D 94** (2016) 072007 [arXiv:1607.07923] [INSPIRE].

JHEP11(2018)187

[15] A. Raphaël, $R(D^*)$ *status: overview and prospects*, Talk given at *FPCP Conference*, Prague, 5 June 2017, [https://indico.cern.ch/event/586719/contributions/2531261/attachments/1470695/2275576/2_fpcp_talk_wormser.pdf].

[16] W.-F. Wang, Y.-Y. Fan and Z.-J. Xiao, *Semileptonic decays* $B_c \to (\eta_c, J/\Psi) l\nu$ *in the perturbative QCD approach*, *Chin. Phys.* **C 37** (2013) 093102 [arXiv:1212.5903] [INSPIRE].

[17] R. Barbieri, G. Isidori, A. Pattori and F. Senia, *Anomalies in B-decays and* U(2) *flavour symmetry*, *Eur. Phys. J.* **C 76** (2016) 67 [arXiv:1512.01560] [INSPIRE].

[18] B. Gripaios, M. Nardecchia and S.A. Renner, *Composite leptoquarks and anomalies in B-meson decays*, *JHEP* **05** (2015) 006 [arXiv:1412.1791] [INSPIRE].

[19] C. Niehoff, P. Stangl and D.M. Straub, *Direct and indirect signals of natural composite Higgs models*, *JHEP* **01** (2016) 119 [arXiv:1508.00569] [INSPIRE].

[20] R. Barbieri, C.W. Murphy and F. Senia, *B-decay Anomalies in a Composite Leptoquark Model*, *Eur. Phys. J.* **C 77** (2017) 8 [arXiv:1611.04930] [INSPIRE].

[21] C. Niehoff, P. Stangl and D.M. Straub, *Electroweak symmetry breaking and collider signatures in the next-to-minimal composite Higgs model*, *JHEP* **04** (2017) 117 [arXiv:1611.09356] [INSPIRE].

[22] E. Megias, G. Panico, O. Pujolàs and M. Quirós, *A Natural origin for the LHCb anomalies*, *JHEP* **09** (2016) 118 [arXiv:1608.02362] [INSPIRE].

[23] D. Buttazzo, A. Greljo, G. Isidori and D. Marzocca, *Toward a coherent solution of diphoton and flavor anomalies*, *JHEP* **08** (2016) 035 [arXiv:1604.03940] [INSPIRE].

[24] R. Barbieri and A. Tesi, *B-decay anomalies in Pati-Salam* SU(4), *Eur. Phys. J.* **C 78** (2018) 193 [arXiv:1712.06844] [INSPIRE].

[25] G. D'Ambrosio and A.M. Iyer, *Flavour issues in warped custodial models: B anomalies and rare K decays*, *Eur. Phys. J.* **C 78** (2018) 448 [arXiv:1712.08122] [INSPIRE].

[26] F. Sannino, P. Stangl, D.M. Straub and A.E. Thomsen, *Flavor Physics and Flavor Anomalies in Minimal Fundamental Partial Compositeness*, *Phys. Rev.* **D 97** (2018) 115046 [arXiv:1712.07646] [INSPIRE].

[27] A. Carmona and F. Goertz, *Recent* $\boldsymbol{B}$ *Physics Anomalies - a First Hint for Compositeness?*, arXiv:1712.02536 [INSPIRE].

[28] D. Marzocca, *Addressing the B-physics anomalies in a fundamental Composite Higgs Model*, *JHEP* **07** (2018) 121 [arXiv:1803.10972] [INSPIRE].

[29] P. Asadi, M.R. Buckley and D. Shih, *It's all right(-handed neutrinos): a new* W' *model for the* $R_{D^{(*)}}$ *anomaly*, *JHEP* **09** (2018) 010 [arXiv:1804.04135] [INSPIRE].

[30] A. Greljo, D.J. Robinson, B. Shakya and J. Zupan, $R(D^{(*)})$ *from* W' *and right-handed neutrinos*, *JHEP* **09** (2018) 169 [arXiv:1804.04642] [INSPIRE].

[31] A. Datta, M. Duraisamy and D. Ghosh, *Diagnosing New Physics in* $b \to c\tau\nu_\tau$ *decays in the light of the recent BaBar result*, *Phys. Rev.* **D 86** (2012) 034027 [arXiv:1206.3760] [INSPIRE].

[32] M. Tanaka and R. Watanabe, *New physics in the weak interaction of* $\bar{B} \to D^{(*)}\tau\bar{\nu}$, *Phys. Rev.* **D 87** (2013) 034028 [arXiv:1212.1878] [INSPIRE].

[33] D. Choudhury, D.K. Ghosh and A. Kundu, *B decay anomalies in an effective theory*, *Phys. Rev.* **D 86** (2012) 114037 [arXiv:1210.5076] [INSPIRE].

JHEP11(2018)187

[34] Y. Sakaki, M. Tanaka, A. Tayduganov and R. Watanabe, *Testing leptoquark models in $\bar{B} \to D^{(*)}\tau\bar{\nu}$*, *Phys. Rev.* **D 88** (2013) 094012 [arXiv:1309.0301] [INSPIRE].

[35] B. Bhattacharya, A. Datta, D. London and S. Shivashankara, *Simultaneous Explanation of the R_K and $R(D^{(*)})$ Puzzles*, *Phys. Lett.* **B 742** (2015) 370 [arXiv:1412.7164] [INSPIRE].

[36] O. Catà and M. Jung, *Signatures of a nonstandard Higgs boson from flavor physics*, *Phys. Rev.* **D 92** (2015) 055018 [arXiv:1505.05804] [INSPIRE].

[37] M. Freytsis, Z. Ligeti and J.T. Ruderman, *Flavor models for $\bar{B} \to D^{(*)}\tau\bar{\nu}$*, *Phys. Rev.* **D 92** (2015) 054018 [arXiv:1506.08896] [INSPIRE].

[38] D. Choudhury, A. Kundu, S. Nandi and S.K. Patra, *Unified resolution of the $R(D)$ and $R(D^*)$ anomalies and the lepton flavor violating decay $h \to \mu\tau$*, *Phys. Rev.* **D 95** (2017) 035021 [arXiv:1612.03517] [INSPIRE].

[39] A. Celis, M. Jung, X.-Q. Li and A. Pich, *Scalar contributions to $b \to c(u)\tau\nu$ transitions*, *Phys. Lett.* **B 771** (2017) 168 [arXiv:1612.07757] [INSPIRE].

[40] D. Choudhury, A. Kundu, R. Mandal and R. Sinha, *Minimal unified resolution to $R_{K^{(*)}}$ and $R(D^{(*)})$ anomalies with lepton mixing*, *Phys. Rev. Lett.* **119** (2017) 151801 [arXiv:1706.08437] [INSPIRE].

[41] A. Crivellin, D. Müller and T. Ota, *Simultaneous explanation of $R(D^{(*)})$ and $b \to s\mu^+\mu^-$: the last scalar leptoquarks standing*, *JHEP* **09** (2017) 040 [arXiv:1703.09226] [INSPIRE].

[42] P. Colangelo and F. De Fazio, *Scrutinizing $\overline{B} \to D^*(D\pi)\ell^-\overline{\nu}_\ell$ and $\overline{B} \to D^*(D\gamma)\ell^-\overline{\nu}_\ell$ in search of new physics footprints*, *JHEP* **06** (2018) 082 [arXiv:1801.10468] [INSPIRE].

[43] MILC collaboration, J.A. Bailey et al., *$B \to D\ell\nu$ form factors at nonzero recoil and $|V_{cb}|$ from $2+1$-flavor lattice QCD*, *Phys. Rev.* **D 92** (2015) 034506 [arXiv:1503.07237] [INSPIRE].

[44] D. Melikhov and B. Stech, *Weak form-factors for heavy meson decays: An Update*, *Phys. Rev.* **D 62** (2000) 014006 [hep-ph/0001113] [INSPIRE].

[45] M. Atoui, D. Becirevic, V. Morénas and F. Sanfilippo, *Lattice QCD study of $B_s \to D_s\ell\bar{\nu}_\ell$ decay near zero recoil*, PoS(LATTICE2013)384 (2014) [arXiv:1311.5071] [INSPIRE].

[46] I. Caprini, L. Lellouch and M. Neubert, *Dispersive bounds on the shape of $\bar{B} \to D^{(*)}$ lepton anti-neutrino form-factors*, *Nucl. Phys.* **B 530** (1998) 153 [hep-ph/9712417] [INSPIRE].

[47] Heavy Flavor Averaging Group (HFAG) collaboration, Y. Amhis et al., *Averages of b-hadron, c-hadron and τ-lepton properties as of summer 2014*, arXiv:1412.7515 [INSPIRE].

[48] Fermilab Lattice and MILC collaborations, J.A. Bailey et al., *Update of $|V_{cb}|$ from the $\bar{B} \to D^*\ell\bar{\nu}$ form factor at zero recoil with three-flavor lattice QCD*, *Phys. Rev.* **D 89** (2014) 114504 [arXiv:1403.0635] [INSPIRE].

[49] F.U. Bernlochner, Z. Ligeti, M. Papucci and D.J. Robinson, *Combined analysis of semileptonic B decays to D and D^*: $R(D^{(*)})$, $|V_{cb}|$ and new physics*, *Phys. Rev.* **D 95** (2017) 115008 [*Erratum ibid.* **D 97** (2018) 059902] [arXiv:1703.05330] [INSPIRE].

[50] M. Jung and D.M. Straub, *Constraining new physics in $b \to c\ell\nu$ transitions*, arXiv:1801.01112 [INSPIRE].

[51] D. Bardhan, P. Byakti and D. Ghosh, *A closer look at the R_D and R_{D^*} anomalies*, *JHEP* **01** (2017) 125 [arXiv:1610.03038] [INSPIRE].

JHEP11(2018)187

[52] R. Alonso, E.E. Jenkins, A.V. Manohar and M. Trott, *Renormalization Group Evolution of the Standard Model Dimension Six Operators III: Gauge Coupling Dependence and Phenomenology*, *JHEP* **04** (2014) 159 [arXiv:1312.2014] [INSPIRE].

[53] R. Alonso, B. Grinstein and J. Martin Camalich, *Lifetime of B_c^- Constrains Explanations for Anomalies in $B \to D^{(*)}\tau\nu$*, *Phys. Rev. Lett.* **118** (2017) 081802 [arXiv:1611.06676] [INSPIRE].

[54] A.G. Akeroyd and C.-H. Chen, *Constraint on the branching ratio of $B_c \to \tau\bar{\nu}$ from LEP1 and consequences for $R(D^{(*)})$ anomaly*, *Phys. Rev.* **D 96** (2017) 075011 [arXiv:1708.04072] [INSPIRE].

[55] I. Doršner, S. Fajfer, N. Košnik and I. Nišandžić, *Minimally flavored colored scalar in $\bar{B} \to D^{(*)}\tau\bar{\nu}$ and the mass matrices constraints*, *JHEP* **11** (2013) 084 [arXiv:1306.6493] [INSPIRE].

[56] D. Bečirević, I. Doršner, S. Fajfer, N. Košnik, D.A. Faroughy and O. Sumensari, *Scalar leptoquarks from grand unified theories to accommodate the B-physics anomalies*, *Phys. Rev.* **D 98** (2018) 055003 [arXiv:1806.05689] [INSPIRE].

[57] U. Nierste, S. Trine and S. Westhoff, *Charged-Higgs effects in a new $B \to D$ tau nu differential decay distribution*, *Phys. Rev.* **D 78** (2008) 015006 [arXiv:0801.4938] [INSPIRE].

[58] M. Duraisamy and A. Datta, *The Full $B \to D^*\tau^-\bar{\nu}_\tau$ Angular Distribution and CP-violating Triple Products*, *JHEP* **09** (2013) 059 [arXiv:1302.7031] [INSPIRE].

[59] Z. Ligeti, M. Papucci and D.J. Robinson, *New Physics in the Visible Final States of $B \to D^{(*)}\tau\nu$*, *JHEP* **01** (2017) 083 [arXiv:1610.02045] [INSPIRE].

[60] R. Alonso, A. Kobach and J. Martin Camalich, *New physics in the kinematic distributions of $\bar{B} \to D^{(*)}\tau^-(\to \ell^-\bar{\nu}_\ell\nu_\tau)\bar{\nu}_\tau$*, *Phys. Rev.* **D 94** (2016) 094021 [arXiv:1602.07671] [INSPIRE].

[61] A.K. Alok, D. Kumar, S. Kumbhakar and S.U. Sankar, *D^* polarization as a probe to discriminate new physics in $\bar{B} \to D^*\tau\bar{\nu}$*, *Phys. Rev.* **D 95** (2017) 115038 [arXiv:1606.03164] [INSPIRE].

[62] B. Grzadkowski, M. Iskrzynski, M. Misiak and J. Rosiek, *Dimension-Six Terms in the Standard Model Lagrangian*, *JHEP* **10** (2010) 085 [arXiv:1008.4884] [INSPIRE].

[63] ALEPH, DELPHI, L3, OPAL collaborations and LEP Electroweak Working Group, *A Combination of preliminary electroweak measurements and constraints on the standard model*, hep-ex/0511027 [INSPIRE].

[64] ALEPH, DELPHI, L3, OPAL, SLD collaborations, LEP Electroweak Working Group, SLD Electroweak Group and SLD Heavy Flavour Group, *Precision electroweak measurements on the Z resonance*, *Phys. Rept.* **427** (2006) 257 [hep-ex/0509008] [INSPIRE].

[65] A. Pich, *Precision Tau Physics*, *Prog. Part. Nucl. Phys.* **75** (2014) 41 [arXiv:1310.7922] [INSPIRE].

[66] BELLE collaboration, J. Grygier et al., *Search for $\boldsymbol{B \to h\nu\bar{\nu}}$ decays with semileptonic tagging at Belle*, *Phys. Rev.* **D 96** (2017) 091101 [arXiv:1702.03224] [INSPIRE].

[67] A.J. Buras, J. Girrbach-Noe, C. Niehoff and D.M. Straub, *$B \to K^{(*)}\nu\bar{\nu}$ decays in the Standard Model and beyond*, *JHEP* **02** (2015) 184 [arXiv:1409.4557] [INSPIRE].

JHEP11(2018)187

[68] C. Hambrock, A. Khodjamirian and A. Rusov, *Hadronic effects and observables in $B \to \pi\ell^+\ell^-$ decay at large recoil*, *Phys. Rev.* **D 92** (2015) 074020 [arXiv:1506.07760] [INSPIRE].

[69] BELLE II collaboration, E. Manoni, *Studies of missing energy decays of B meson at Belle II*, PoS(EPS-HEP2017)226 (2017).

[70] B. Capdevila, A. Crivellin, S. Descotes-Genon, L. Hofer and J. Matias, *Searching for New Physics with $b \to s\tau^+\tau^-$ processes*, *Phys. Rev. Lett.* **120** (2018) 181802 [arXiv:1712.01919] [INSPIRE].

[71] D.A. Faroughy, A. Greljo and J.F. Kamenik, *Confronting lepton flavor universality violation in B decays with high-p_T tau lepton searches at LHC*, *Phys. Lett.* **B 764** (2017) 126 [arXiv:1609.07138] [INSPIRE].

[72] F. Feruglio, P. Paradisi and A. Pattori, *Revisiting Lepton Flavor Universality in B Decays*, *Phys. Rev. Lett.* **118** (2017) 011801 [arXiv:1606.00524] [INSPIRE].

[73] D. Buttazzo, A. Greljo, G. Isidori and D. Marzocca, *B-physics anomalies: a guide to combined explanations*, *JHEP* **11** (2017) 044 [arXiv:1706.07808] [INSPIRE].

[74] F. Feruglio, P. Paradisi and A. Pattori, *On the Importance of Electroweak Corrections for B Anomalies*, *JHEP* **09** (2017) 061 [arXiv:1705.00929] [INSPIRE].

[75] C. Bobeth and U. Haisch, *New Physics in Γ_{12}^s: $(\bar{s}b)(\bar{\tau}\tau)$ Operators*, *Acta Phys. Polon.* **B 44** (2013) 127 [arXiv:1109.1826] [INSPIRE].

[76] A. Dighe and D. Ghosh, *How large can the branching ratio of $B_s \to \tau^+\tau^-$ be?*, *Phys. Rev.* **D 86** (2012) 054023 [arXiv:1207.1324] [INSPIRE].

[77] D.B. Kaplan and H. Georgi, SU(2) × U(1) *Breaking by Vacuum Misalignment*, *Phys. Lett.* **B 136** (1984) 183 [INSPIRE].

[78] D.B. Kaplan, *Flavor at SSC energies: A New mechanism for dynamically generated fermion masses*, *Nucl. Phys.* **B 365** (1991) 259 [INSPIRE].

[79] R. Contino, Y. Nomura and A. Pomarol, *Higgs as a holographic pseudoGoldstone boson*, *Nucl. Phys.* **B 671** (2003) 148 [hep-ph/0306259] [INSPIRE].

[80] R. Contino, *The Higgs as a Composite Nambu-Goldstone Boson*, in *Physics of the large and the small, TASI 09, proceedings of the Theoretical Advanced Study Institute in Elementary Particle Physics*, Boulder, Colorado, U.S.A., 1–26 June 2009, pp. 235–306 (2011) [DOI:10.1142/9789814327183_0005] [arXiv:1005.4269] [INSPIRE].

[81] G. Panico and A. Wulzer, *The Composite Nambu-Goldstone Higgs*, *Lect. Notes Phys.* **913** (2016) 1 [arXiv:1506.01961] [INSPIRE].

[82] R. Contino, T. Kramer, M. Son and R. Sundrum, *Warped/composite phenomenology simplified*, *JHEP* **05** (2007) 074 [hep-ph/0612180] [INSPIRE].

[83] S.R. Coleman, J. Wess and B. Zumino, *Structure of phenomenological Lagrangians. 1.*, *Phys. Rev.* **177** (1969) 2239 [INSPIRE].

[84] C.G. Callan Jr., S.R. Coleman, J. Wess and B. Zumino, *Structure of phenomenological Lagrangians. 2.*, *Phys. Rev.* **177** (1969) 2247 [INSPIRE].

[85] R. Contino, D. Marzocca, D. Pappadopulo and R. Rattazzi, *On the effect of resonances in composite Higgs phenomenology*, *JHEP* **10** (2011) 081 [arXiv:1109.1570] [INSPIRE].

JHEP11(2018)187

[86] G. Ecker, J. Gasser, H. Leutwyler, A. Pich and E. de Rafael, *Chiral Lagrangians for Massive Spin 1 Fields*, *Phys. Lett.* **B 223** (1989) 425 [INSPIRE].

[87] UTFIT collaboration, M. Bona et al., *Model-independent constraints on $\Delta F = 2$ operators and the scale of new physics*, *JHEP* **03** (2008) 049 [arXiv:0707.0636] [INSPIRE].

[88] ETM collaboration, N. Carrasco et al., *B-physics from $N_f = 2$ tmQCD: the Standard Model and beyond*, *JHEP* **03** (2014) 016 [arXiv:1308.1851] [INSPIRE].

[89] C. Csáki, A. Falkowski and A. Weiler, *The Flavor of the Composite Pseudo-Goldstone Higgs*, *JHEP* **09** (2008) 008 [arXiv:0804.1954] [INSPIRE].

[90] K. Agashe, A. Azatov and L. Zhu, *Flavor Violation Tests of Warped/Composite SM in the Two-Site Approach*, *Phys. Rev.* **D 79** (2009) 056006 [arXiv:0810.1016] [INSPIRE].

[91] R. Barbieri, G. Isidori, J. Jones-Perez, P. Lodone and D.M. Straub, U(2) *and Minimal Flavour Violation in Supersymmetry*, *Eur. Phys. J.* **C 71** (2011) 1725 [arXiv:1105.2296] [INSPIRE].

[92] R. Barbieri, D. Buttazzo, F. Sala, D.M. Straub and A. Tesi, *A 125 GeV composite Higgs boson versus flavour and electroweak precision tests*, *JHEP* **05** (2013) 069 [arXiv:1211.5085] [INSPIRE].

[93] CMS collaboration, *Search for vector-like T and B quark pairs in final states with leptons at $\sqrt{s} = 13$ TeV*, *JHEP* **08** (2018) 177 [arXiv:1805.04758] [INSPIRE].

[94] ATLAS collaboration, *Combination of the searches for pair-produced vector-like partners of the third-generation quarks at $\sqrt{s} = 13$ TeV with the ATLAS detector*, arXiv:1808.02343 [INSPIRE].

[95] M. Ciuchini, E. Franco, S. Mishima and L. Silvestrini, *Electroweak Precision Observables, New Physics and the Nature of a 126 GeV Higgs Boson*, *JHEP* **08** (2013) 106 [arXiv:1306.4644] [INSPIRE].

[96] GFITTER GROUP collaboration, M. Baak et al., *The global electroweak fit at NNLO and prospects for the LHC and ILC*, *Eur. Phys. J.* **C 74** (2014) 3046 [arXiv:1407.3792] [INSPIRE].

[97] J. de Blas et al., *Electroweak precision observables and Higgs-boson signal strengths in the Standard Model and beyond: present and future*, *JHEP* **12** (2016) 135 [arXiv:1608.01509] [INSPIRE].

[98] A. Azatov, R. Contino, A. Di Iura and J. Galloway, *New Prospects for Higgs Compositeness in $h \to Z\gamma$*, *Phys. Rev.* **D 88** (2013) 075019 [arXiv:1308.2676] [INSPIRE].

[99] C. Grojean, O. Matsedonskyi and G. Panico, *Light top partners and precision physics*, *JHEP* **10** (2013) 160 [arXiv:1306.4655] [INSPIRE].

[100] D. Ghosh, M. Salvarezza and F. Senia, *Extending the Analysis of Electroweak Precision Constraints in Composite Higgs Models*, *Nucl. Phys.* **B 914** (2017) 346 [arXiv:1511.08235] [INSPIRE].

[101] M. Redi and A. Weiler, *Flavor and CP Invariant Composite Higgs Models*, *JHEP* **11** (2011) 108 [arXiv:1106.6357] [INSPIRE].

[102] M. Chala and M. Spannowsky, *Behavior of composite resonances breaking lepton flavor universality*, *Phys. Rev.* **D 98** (2018) 035010 [arXiv:1803.02364] [INSPIRE].

JHEP11(2018)187

[103] G. D'Amico et al., *Flavour anomalies after the R_{K^*} measurement*, *JHEP* **09** (2017) 010 [arXiv:1704.05438] [INSPIRE].

[104] B. Capdevila, A. Crivellin, S. Descotes-Genon, J. Matias and J. Virto, *Patterns of New Physics in $b \to s\ell^+\ell^-$ transitions in the light of recent data*, *JHEP* **01** (2018) 093 [arXiv:1704.05340] [INSPIRE].

[105] M. Ciuchini et al., *On Flavourful Easter eggs for New Physics hunger and Lepton Flavour Universality violation*, *Eur. Phys. J.* **C 77** (2017) 688 [arXiv:1704.05447] [INSPIRE].

[106] L.-S. Geng, B. Grinstein, S. Jäger, J. Martin Camalich, X.-L. Ren and R.-X. Shi, *Towards the discovery of new physics with lepton-universality ratios of $b \to s\ell\ell$ decays*, *Phys. Rev.* **D 96** (2017) 093006 [arXiv:1704.05446] [INSPIRE].

[107] W. Altmannshofer, P. Stangl and D.M. Straub, *Interpreting Hints for Lepton Flavor Universality Violation*, *Phys. Rev.* **D 96** (2017) 055008 [arXiv:1704.05435] [INSPIRE].

[108] D. Ghosh, *Explaining the R_K and R_{K^*} anomalies*, *Eur. Phys. J.* **C 77** (2017) 694 [arXiv:1704.06240] [INSPIRE].

[109] D. Bardhan, P. Byakti and D. Ghosh, *Role of Tensor operators in R_K and R_{K^*}*, *Phys. Lett.* **B 773** (2017) 505 [arXiv:1705.09305] [INSPIRE].

[110] Particle Data Group collaboration, C. Patrignani et al., *Review of Particle Physics*, *Chin. Phys.* **C 40** (2016) 100001 [INSPIRE].

[111] HPQCD collaboration, B. Colquhoun et al., *B-meson decay constants: a more complete picture from full lattice QCD*, *Phys. Rev.* **D 91** (2015) 114509 [arXiv:1503.05762] [INSPIRE].

[112] HPQCD collaboration, B. Colquhoun, C. Davies, J. Koponen, A. Lytle and C. McNeile, *B_c decays from highly improved staggered quarks and NRQCD*, PoS(LATTICE2016)281 (2016) [arXiv:1611.01987] [INSPIRE].

[113] R. Watanabe, *New Physics effect on $B_c \to J/\psi\tau\bar{\nu}$ in relation to the $R_{D^{(*)}}$ anomaly*, *Phys. Lett.* **B 776** (2018) 5 [arXiv:1709.08644] [INSPIRE].

[114] M. Bordone, C. Cornella, J. Fuentes-Martin and G. Isidori, *A three-site gauge model for flavor hierarchies and flavor anomalies*, *Phys. Lett.* **B 779** (2018) 317 [arXiv:1712.01368] [INSPIRE].

[115] E.E. Jenkins, A.V. Manohar and M. Trott, *Renormalization Group Evolution of the Standard Model Dimension Six Operators II: Yukawa Dependence*, *JHEP* **01** (2014) 035 [arXiv:1310.4838] [INSPIRE].

[116] K. Agashe, R. Contino, L. Da Rold and A. Pomarol, *A Custodial symmetry for $Zb\bar{b}$*, *Phys. Lett.* **B 641** (2006) 62 [hep-ph/0605341] [INSPIRE].

[117] A. Azatov, C. Grojean, A. Paul and E. Salvioni, *Resolving gluon fusion loops at current and future hadron colliders*, *JHEP* **09** (2016) 123 [arXiv:1608.00977] [INSPIRE].

JHEP11(2018)187